Automatic Design for Manufacturing in Power Electronics Based on Power Converter Arrays

Andre Andreta

Communauté
UNIVERSITÉ Grenoble Alpes

THÈSE

Pour obtenir le grade de

DOCTEUR DE LA COMMUNAUTE UNIVERSITE GRENOBLE ALPES

Spécialité : **Génie Electrique**

Arrêté ministériel : 25 mai 2016

Présentée par

André Gutierrez ANDRETA

Thèse dirigée par **Yves LEMBEYE** et
Co-dirigée par **Jean-Christophe CREBIER** et
Luiz Fernando Lavado Villa

préparée au sein du **Laboratoire de Génie Electrique de Grenoble (G2ELab)**
dans le cadre de **l'École Doctorale Electronique, Electrotechnique, Automatique et Traitement du Signal (EEATS)**

Automatic Design for Manufacturing in Power Electronics Based on Power Converter Arrays

Thèse soutenue publiquement le **12 novembre 2019**
devant le jury composé de :

M. François COSTA
Professeur à l'ENS Cachan (SATIE), Président du Jury
M. Eric LABOURE
Professeur à Université Paris Sud (GEEPS), Rapporteur
M. Bruno ALLARD
Professeur à l'INSA de Lyon, (Ampère), Rapporteur
M. Sergio BUSQUETS MONGE
Associate Professor à l'Universitat Politecnica de Catalunya,Examinateur
M. Yves LEMBEYE
Professeur à l'Université Grenoble Alpes (G2Elab), Directeur de thèse
M. Jean Christophe CREBIER
Directeur de Recherches (G2Elab), Co-directeur de thèse
M. Luiz Fernando Lavado Villa
Maitre de Conférences à l'Université de Toulouse (LAAS), Co-encadrant

Abstract

This work presents an automatic design method for power electronic converters "Automatic Design for manufacturing" (ADFM). The method proposes to build power converter arrays (PCAs), by assembling standard-cells. The technique is highly inspired by the microelectronics industry, power electronics building blocks, and multicell converters. The power conversion stage of a PCA consists of several conversion standard cells (CSCs) connected in series and/or parallel.

One of the primary basis for the proper functioning of the ADFM method is the use of models for predicting the behaviour of the possible assemblies of standard cells. This thesis establishes this base following a three-step procedure: defining a plan of experiments to choose the relevant measurements that bring the most information of the PCAs; building a test bench capable of performing automatic measurements and finally studying statistical modelling methods to perform accurate predictions.

Experimental tests in nine different converters are performed, totalizing over 210 hours of tests. Predictions of efficiency and converter temperature made by the models are compared with real measurements to validate their accuracy. Finally, the models are employed for two main tasks: to assure that a given PCA in a given operating point has a safe operation; and to benchmark PCAs that perform similar power conversion.

Résumé

Ce travail présente une méthode de conception et de fabrication automatique de convertisseurs de puissance appelée « Automatic Design for manufacturing » (ADFM). La méthode consiste en concevoir des « *Power Converter Arrays* » (PCA) via l'assemblage de cellules standards. La technique est inspirée de l'industrie de la microélectronique, des PEBB (*Power Electronic Building Blocks*) et des convertisseurs multicellulaires. La partie de puissance d'un PCA est formé par plusieurs Cellules Standards de Conversion (CSC) connectées en série ou/et en parallèle en entrée comme en sortie.

Afin de prédire le comportement de tous les assemblages possibles de CSC, cette démarche s'appuie sur des modèles statistiques eux-mêmes déterminés par des caractérisations électrothermiques de convertisseurs tests. Cette thèse va établir les bases de cette modélisation en trois étapes : la définition d'un plan d'expérience ; la construction d'un banc d'essais pour réaliser des mesures automatiques, et finalement, l'étude des modèles statistiques permettant de réaliser prédictions précises.

9 convertisseurs ont ainsi été réalisés et caractérisés, totalisant plus de 210 heures de tests afin de réaliser toutes les étapes allant de la caractérisation aux prédictions de l'efficacité et de la température d'un convertisseur. Finalement, afin de valider cette nouvelle méthode, deux cas pratiques ont été traités. Le premier vise à comparer les résultats estimés avec ceux réellement atteints par un PCA, le second s'attache à montrer les perspectives d'une telle approche en comparant les performances estimées de plusieurs PCAs pour un profil de mission donné.

Acknowledgements

In the year of 2015, I was travelling in France, doing voluntary jobs. After six months, I got a bit lost and had no clue what to do next. I knew I had a solid background after spending seven years in university, studying electrical engineering, but I didn't know how to use it. On July 2nd, I took a train from Montpelier to Toulouse at 09h58 and, big coincidence or not, in the same train, in the same carriage, I saw a familiar face, a colleague that I hadn't seen in six years. This train changed the path of the following years of my life, and maybe a bit of his life as well. Fast-forward 5 years, I finish my PhD in Université Grenoble Alpes as the first student supervised by my old colleague.

First, I would like to thank all members of the jury committee that read carefully this work, proposed improvements and made a very productive discussion during the defence day: M. Bruno Allard, M. Eric Labouré, M. François Costa and M. Sergio Busquets.

The ideas involving this work evolved a lot during the three years, and I am very satisfied by the result. This was only possible because I had three amazing supervisors always by my side. Jean Christophe Crébier and Yves Lembeye are great researchers that have worked together for a long time and supervised several excellent works before me. I am very grateful to have spent these years working with them, their passion for their work motivated me a lot to reach my objectives. The effort they put into this work is immeasurable.

Especially in my thesis, I had the pleasure to have one more supervisor, the colleague in the train, M. Luiz Fernando Lavado Villa. His contributions were immense for this work, either over hours and hours in the telephone, or in his trips to Grenoble, or hosting me in Toulouse. Thanks to his contributions, not only scientifically, but also his writing skills made this work much better organized.

I also want to thank the Region Rhône Alpes Auvergne for its funding through project Mamaatech, Convention FEDER N°RA0020041.

The three years I spent in the G2ELab I met a lot of very interesting people that made my daily life very pleasant. First, I would like to thank my friends from power electronic team: Andressa Nakahata, Arthur Kazuti, Aurelien Maréchal, Beatriz de Luca, Blazej Czerniewski, Damien Sal y Rosas, Davy Colin, Fadel Bikinga, Gaetan Perez, Joe Glass, Leo Sterna, Lucas Souza, Luciano Alves, Luis Alves Rodrigues, Maximin Blanc, Melissa Castillo, Mor Sokhna Diop, Nasredinne Kesbia, Nicolas Botter, Nisith Bhowmick, Pawel Derkacz, Soleiman Galeishi, Tamiris Grossl Bade and Van Sang Nguyen. Also, the professors form PE team Yvan Avenas, Jean-Paul Ferrieux, David Frey, Pierre-Olivier Jennin, Pierre Lefranc and Jean-Luc Schanen.

Several people helped a lot in the accomplishment of this work. For the practical experiments, I would like to thank the engineers from the lab: Benoit Sarrazin, Alexis Derbey, Christophe Pollet and Florien Dumas. The stagières that

worked with me: Paul Audin, Silvain Marache, Rachid Hmamou and Othmane Aouassar. All the “service technique” and “service administrative” from the G2ELab that make the laboratory run as smoothly as possible.

My life in Grenoble was very exciting these three years, first I would like to thank my girlfriend, Sophie Ortiz, that helped me a lot to finish this work, either in discussions about data science or in several weekends spent in cafés around the city centre writing this thesis. Then, all my friends that shared the apartment I live: Elsa Liegeois, Thibaut Dufour, Clemence Chédru, Gabriel Dieny and Pacco Baily. Also my friend from the 3SR laboratory, always partners for climbing or beer: Olga Stamati, Cyrille Couture and Alessandro Tengattini

Gladly, before starting my PhD I spent one year living in Valence, in the ‘Valence Atelier Libre’ with Jay Hudnall and many other friends. This was a year of ‘introduction à la culture française’. I travelled all around France teaching people how to build homemade wind turbines, learning French and trying to put into practice my knowledge in power electronics. Despite that, the life in the atelier in Valence, was something incredible. I met many interesting people, ready to share their knowledge in many different fields. It is hard to measure how much I learned that year.

Finally, I would like to thank people from *Brasil*, my professors and friends from the power electronics laboratory INEP in Florianópolis. It is where I got a solid formation in power electronics that opened many doors for me. My friends from Amparo, that every year I go back are always ready for a party. My family, Pedro, José and Barbara, always there to support me in each decision, without their support I would not have gotten this far.

"We cannot choose our external circumstances, but we can always choose how we respond to them"

Epictetus

Contents

List of Abbreviations

DK	Design kit
ASPEC	Application Specified Power Electronics Converter
SC	Standard Cell
DAB	Dual Active Bridge
CSC	Conversion Standard Cell
TSC	Terminal Standard Cell
MSC	Measurement Standard Cell
FSC	Filtering Standard Cell
PSC	Power Connection Standard Cell
CoSC	Control Standard Cell
CAD	Computer-aided design
GM	G2ELab-Maatel (Technology Platform)
ISOP	Input series output parallel
IPOS	Input parallel output series
IPOP	Input parallel output parallel
ISOS	Input series output series
CPR	CSC Power Ratio
IR	Infra-red
DV	Voltage Difference
Vi	Input Voltage
Io	Output Current
Vo	Output voltage
Ta	Ambient Temperature
h	Heat coefficient
nline	Number of lines
ncol	Number of columns
nboard	Number of boards
Tc	Converter Temperature
OVAT	One variable at a time
CMU	Central Management Unit
GPR	Gaussian Process Regression
SOA	Safe Operating Area

Introduction

Modern society is undergoing a steady process of electrification due to the ubiquity of smartphones, the emerge of electrical mobility and the penetration of cheap renewable energies at close proximity to users. Common to all of these trends is the use of power electronics devices, which are omnipresent from the cell phone charger in the coat pocket to the electric car battery charger in the garage.

Despite the imminent central role of power electronics in modern life, the design and manufacturing processes of power electronics converters is extremely time consuming and expensive. In microelectronics, a field that historically emerged and developed in parallel with power electronics, scientist and engineers have put together their contributions and developed automated design methods that triggered a race to integrate billions of components into single devices, streamlining development and bringing unheard-of technology to the fingertips of consumers in a matter of decades. In contrast, power electronics developed the equivalent of a highly skilled watchmaker community, with extremely competent multi-disciplinary design teams working in technology silos. As a consequence, power electronics never evolved its equivalent of Moore's Law to reign in both costs and development time of its solutions.

The scientific community did try to simplify and to improve the design, manufacturing and industrialisation processes of power electronics converters in the past few decades. Methods such as Power electronic building blocks (PEBB) and multicell converters (MCC) are two of the most well-known examples. Both propose to simplify the design of power converters by using pre-designed blocks to create a converter, improving reliability, performance and speeding up the design process. However, converters built from these methods represent a very small percentage of the existing power electronics market. Which begs the question: why did these methods fail to galvanise the power electronics industry and trigger its own Moore law?

This work proposes to answer this question by associating base concepts from both PEBB and MCC together with principles of the microelectronics industry, to create a new design method in power electronics. This new method is called Automated Design for Manufacture (ADFM).

The core of the Automated Design for Manufacture method is to totally rethink what is a power converter and how to create one. A converter is no longer an exquisite piece of multidisciplinary engineering. Instead, it is the straight forward assembly of well-known and reliable standardised elements. ADFM proposes the use of a sort of virtual prototyping, to estimate if a certain assembly of standard elements is a suitable solution to the set of specifications in a matter of minutes and export performance-guaranteed manufacturing files instantly if it is. The result is the creation of a Power Converter Array.

In ADFM, Power Converter Arrays (PCAs) are composed by the physical assembly and electrical interconnection of standard cells. These standard cells are built from real components that can be configured to achieve a certain set of specifications in terms of efficiency, thermal behaviour and EMI management, among others. These standard cells can be regrouped into a comprehensive whole called a Technology Platform.

A mature Technology Platform (TP) is the key to the virtual prototyping of PCAs, making the TP a centrepiece of the ADFM methodology. Maturity translates as the thorough characterisation and minute description of each standard cell (and possibly PCAs) after these have undergone a process of industrial-grade development yielding stable versions.

The data of a mature TP is used to create models that can precisely interpolate the electrical and thermal behaviours of any mature PCA under any point of operation. The same models can also extrapolate, within a set confidence interval, the behaviour of new or exotic PCAs for which there is no data at all. PCA behaviour results, interpolated or extrapolated, can then be cross-checked with a set of safe operating conditions, providing the designer with extremely helpful hindsight on the PCA without building a single prototype. This makes mature TP behavioural models, and their associated data, the key to the success of the ADFM methodology. The objective of this thesis is to create these models.

To achieve its objective, this thesis will focus on the study of two important behaviours of a power electronic converter: conversion efficiency and converter operating temperature. These behaviours will be interpolated or extrapolated by statistical models trained from a large dataset acquired through a thoroughly designed set of experiments using a highly precise and fully automated test bench.

Organisation of the Thesis

Chapter 1 is dedicated to formalise the ADFM methodology. The ADFM method is presented, first in a more abstract way, illustrating how microelectronics practices could be used in power electronics. Then, it is explained in more detail, describing every step of the design of a PCA. A practical example is presented to illustrate the ADFM method, starting from a set of specifications going up to the efficiency and thermal behaviour measurements of a PCA. The PCA is built in the context of the Mamaatec project, financed by the Rhone Alpes Region. This chapter ends by addressing some core issues of creating models from statistical data.

Chapter 2 evaluates how many measurements/experiences/prototypes are required in order to get enough data to interpret the behaviour of the PCAs of a given TP. The evaluation takes into account practices of design of experiments (DOE), which consists of maximising the amount of information that can be obtained for a given amount of experimental effort. The chapter analyses how each variable affects the efficiency and the temperature of the converter and in the end comes up with an experimental plan.

Chapter 3 describes the test bench used in this work. This test bench is fully automated and designed to control all input variables of a PCA and measure all of its output variables.

Chapter 4 focuses on the models themselves. It briefly introduces statistical modelling, detailing several methods to fit models. The most promising method is selected and is used to fit several models to predict the efficiency and the operating temperature of the PCAs. Models are cross-compared, and the best are selected based on their accuracy in both interpolation and extrapolation of the efficiency and thermal behaviours.

Finally, **Chapter 5** emulates virtual prototyping by revisiting the example from chapter 1 and using the models from chapter 4. Three PCAs are validated against their safe operating conditions and their performance are virtually evaluated using a battery charge mission profile.

1 The Multicell converter design method

The history of power electronics (PE) can be traced back to the beginning of the XX century, where converters made with mercury-arc valve were built as the rectifier for the DC distribution line in Schenectady, New York, 1905 [1]. By the 1930s, it was introduced phase-controlled rectifiers as the 3 MW rectifier built for the New York City subway and the cycloconverter for the German railways [2]. The first "electronics revolution" is defined by the invention of the p-n-p-n Si transistor in 1956 at Bell Laboratories [3] and the introduction of the thyristor to the commercial market by GE [4].

From that time to now, power electronics became each year more and more present in modern life. Nowadays PE converters are present in energy generation and harvesting, such as in solar or wind power plants, in transmission, with converters at each HVDC line terminals, in consumption, with domestic electronics, supplies for home appliances, in electric or more electric transportation, with cars, buses, trains, airplanes, and ships, among several other applications. The European Center for Power Electronics (ECPE) estimates that, in 2019, 40 % of worldwide used energy is provided by power electronic converters [5].

The design process of a PE converter usually begins by a set of specifications that are imposed to the converter, such as voltage and current levels, the function to be performed, expected dynamic behaviour, the mission profile and also the converter operating conditions such as the operating temperature range. Other requirements are usually considered, sometimes with a proposed limit such as efficiency, power quality, power density, price and complexity. Also, in many applications, PE converters are subject to compliance with standards such as radiated and conducted EMI, but also mechanical and safety regulations. Each of those requirements are influencing the numerous choices that the designer has to make during the design process. The choices the designer has to make starts with the circuit topology, the values and rating of the components, the modulation scheme, the control strategy and the switching frequency. Then come decisions about which components to use and how to implement them, the technology of switches and the design of the magnetic components. Later the designer has to deal with the physical arrangements of the converter, the positions of the components, the way they are interconnected, cooled down and protected. Housing, cooling techniques and packaging must be defined according to operating and implementation conditions. Typically at this moment, a prototype can be constructed to verify if the specifications are achieved and if the performances are adequate to the desired levels. If the specifications are not achieved, or if the performances are below expectations, the designer has to take some steps back and modify some of the decisions. If the converter fulfils all requirements, it must pass through an industrialisation process.

Industrialisation process is carried out to optimise the component selections and sourcing from cost and availability point of views. Also, the manufacturing complexity is checked and the PE converter may be modified to ease component assembly or to enable fab-testing. Also, the PE converter reliability is tested throughout a set of accelerated ageing to verify that it complies with specifications over a minimum period of time. The converter is then entirely

checked for standard and regulations it must comply with before being shipped out to the assembly line for production. Finally, once this process is completed, and only then, can a price for the PE converter be set, its power density estimated, its efficiency verified and its reliability factors estimated.

The design process of a PE converter, as shown above, is a very complex and pluri-disciplinarily task. Several tools were developed to help the design process, such as: Circuit and control simulation, thermal and fluidic simulation, finite element modelling and electromagnetic interference analysis tools. However, it is still a task that requires many hours of work from various specialists in different fields. As a result, the whole design process of a brand-new converter is a very costly endeavour. To help solve this cost and time issue, Design Automation in Power Electronics emerged recently as a research field on its own, which is considered today as a hot research topic.

During the past years, some concepts were developed in a tentative to simplify/speed up the design process. Far from targeting automated design in power electronics, the literature has instead focused on aggregating CAD tools and methodologies. Among several research activities, it can be mentioned the System Integration initiative at CPES [6] and in France, the H2T-Tech consortium, led by Alstom in the early years of 2000 [7]. Despite these initiatives, PE converters remain highly heterogeneous from the material, the design and the manufacturing point of views. The extreme lack of standardisation in PE has ruined the efforts engaged toward automated design. In parallel to this high level and conceptual research activity, some interesting approaches have been developed toward the standardisation.

The Power Electronics Building Block (PEBB) concept, introduced in the late 90s', formalised the idea of improving reliability and reducing the costs using standard building blocks in the design of power electronics converters [8]–[13]. It proposed a method to build power converters faster, sparing engineering time and still achieving high-performance levels in terms of power density, efficiency and reliability [14], [15]. The PEBB methodology also led to other advantages such as speeding up technology development [16], scaling up converters voltage and current capabilities, creating plug and play devices [11] and becoming key pieces in a smart-grid [15].

PEBB based converters became standard for high voltage and high-power applications. It can be found in wind farms [18], ships propulsion systems [19], and power systems applications [20]. Figure 1.1 presents a high power converter from ABB, based on the PEBB concept. The PEBB approach brings several advantages to these solutions, such as scalability, capability to handle high voltage, reparability, reliability. However, the ideas of automation in the design of power converters and the similarity to microelectronics, that were stated in the first publications about the subject [21], are less present in the actual state of the art of the PEBB approach. The most notorious low and medium power applications of this standardised subsystem approach are the power modules and IPEM (Integrated Power Electronics Modules) [22], [23].

Figure 1.1 a) ABB ACS600: a 9 MW full power converter for large wind turbines based on PEBB concept. Source: Adapted from [24] b) A PEBB - One phase leg of a three-level VSI, 10 kV. Source: Adapted from [25].

Another approach that gives inspiration to automated design of power electronic converters comes from multi-cell converter topologies and architectures. The term multicell was first employed in the 90s' in [22] and [23] to designate what today is called a flying capacitor converter. The technique, at that time, was primarily focused on achieving high voltage power conversion and became used in several high power applications [28]. Today it is also implemented in low voltage applications, achieving high levels of efficiency and power density [29], [30].

At the beginning of the 2000s', the expression "multicell converter" was also referring to any converter topology composed by multiple conversion cells [31]. At this time, thanks to the improvement on low voltage MOSFETs performance and on integrated gate driver stages, the focus of multicell converters was not to create high voltage converters but to take profit of the benefits of the multicell proprieties to design more performant converters.

The most relevant benefits of the multicell approach (in both of the meanings) are: the distribution and reduction of switching and conduction losses among cell switches, the improvement of the harmonic spectrum by the interleaved operation and the spread of voltage and current ratings on the cells [32], [33]. In this way, multicell converters are capable of obtaining higher efficiency and better power densities than single-cell converters in several applications [34], [35]. Two examples of multicell converters are presented in Figure 1.2.

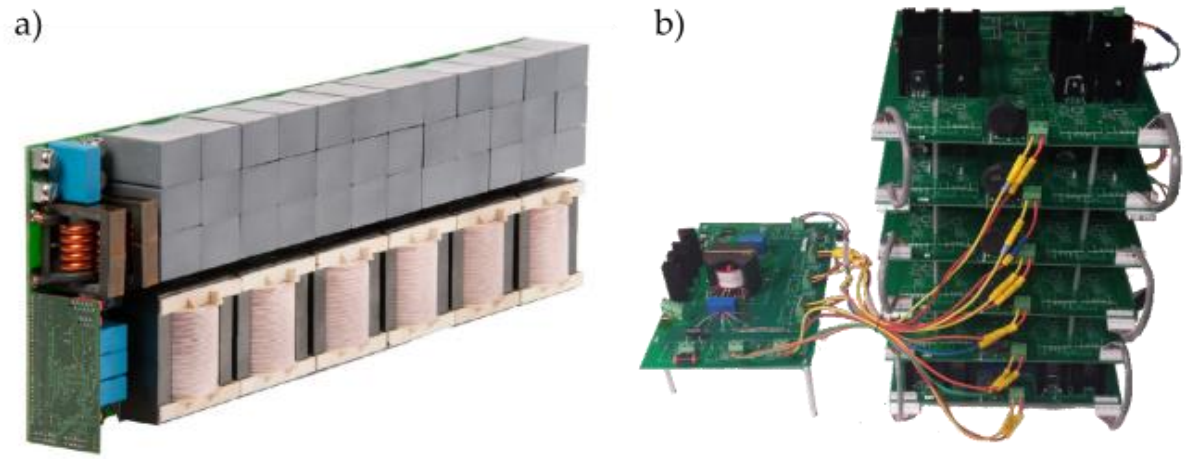

Figure 1.2 Examples of multicell converters. a) 3.3 kW Six fold-interleaved TCM rectifier. Source: adapted from [35]. b) 1 kW Cascaded multicell inverter. Source: adapted from [36].

At the time of writing this thesis, the Power Electronics Magazine March 2019 edition introduced, as the main topic, the automation in power electronics. The main article presents the latest works in CAD for power electronics with the coupling between optimisation tools and automatic design tools [37]. Several research groups around the world propose different solutions to obtain a more automatic design process. For example, in [38], tools are proposed for helping the designer taking decisions such as: the converter topology, the magnetic elements, the switching frequency. In the end, the designer can obtain an optimal solution with reduced modelling and simulation efforts.

Similarly, [39] presents tools for helping the designer to find the optimal topology for a converter specification and the exact components that should be used. In [40], it is presented a tool for automatic design of power modules.

These design methods are focused on helping the designer to make good/optimal choices during the converter design and to speed up the design process. However, none of them proposes to go from some converter specification to a final product by an automatic procedure. One factor that is very hard to take into account is the industrialisation process and normative compliance. Also, these design methods are based on theoretical models, which by their nature, are either limited in terms of precision due to averaging or prohibitive in terms of computation time due to variable coupling and complexity. In either case, these theoretical models require a series of experimental tests to validate the converter design, costing time and resources in the process.

Today Computer Aided Design still fight against the lack of standardisation in Power Electronics. There are so many possible solutions to be explored, so many components that can be used to perform almost the same job and the whole field is so much heterogeneous that it remains difficult to take into account all the necessary parameters and variables that should be considered to carry on a full and complete design to manufacture. This is precisely the starting point of the present research activity: **contribute to introduce standardisation with the objective to automate design to manufacture in Power Electronics**.

In order to achieve a more automatic and more reliable design process, this work presents the **Power Converter Array (PCA) design method**.

The main concept of PCA is to rely on the maturation of the conversion subsystem that is designed and optimised to be associated in large numbers to answer any specification from the same and standardised conversion cell. This method was first proposed in [41], supported mainly by applying the microelectronics industry ideas to power electronics. In [42], efforts were made to optimise the conversion cell. Later, [43] proposed to apply the idea of PCAs into a programmable converter. Several efficient solutions were achieved, with real case applications such as [44], proposing PCA for photovoltaic inverters and [45] applying PCAs to perform a battery management system. More recently, thanks to industrial partnership with MAATEL Company, more standardised conversion cells and more industrialised manufacturing and assembling processes were developed paving the road towards automated design for PE converter manufacturing.

This work builds on this matured view of the capabilities of the PCA design method. Allied with a strong industrial background developed in [46], the converters used and implemented in this work are more relevant to real case applications. The results obtained can be benchmarked with converters made by the traditional industrial approaches.

To better grasp the contributions represented by the design method proposed in this work, a brief overview of the state-of-the-art in the Power Electronics Industry is proposed below. It will be followed by a description of the method proposed in this work, from a conceptual framework (section 1.3) to the technical details (1.4 and 1.5). Finally, this chapter ends by stating the objectives of this thesis and its contributions to the proposed method.

1.1 Short review of the PE industry state

In the past 10 years, several advances were made in power electronics industry. First, the most relevant change is the increased adoption of wide bandgap devices in power converters. At the beginning of the 2000s, the emergence of Silicon Carbide (SiC) and Gallium Nitrate (GaN) active power devices promised to usher in a new era of ever-more efficient PE converters. The use of SiC took some time, but now it has become commonplace in industrial products [47]. GaN devices took less time to achieve a reliable level, thanks to progress in the wafer sourcing for blue LED. However, the market adoption was slower than expected due to system-level factors that restrict practical switching speeds and negate the performance advantages in GaN-based converters [48].

Huge improvements in integration could be seen in the past years. A good example of converters integration can be seen in the Google little box challenge (LBC) that took place in 2015. Highly integrated converters were created, pushing the limits of power density beyond the expectations [49]–[51]. However, these highly integrated solutions are still far from becoming off-the-shelf products. The cause of that is mainly the design effort to achieve these projects, with extreme innovative concepts are far from passing into real-world industrialization processes due to component sourcing, cost, design for manufacturing, and

reliability. LBC showed that it is possible to achieve these highly integrated solutions, but it also showed how much the design process in power electronics can be complex and expensive. Some groups reported that the design process took a group of specialists dedicated one year to achieve the final solution [52]. Even more, going through the industrialisation process, reliability tests and normative tests would require an extra and significant time and funding investment, especially in these cases were many new subsystem designs have been pushed to their limits.

From the LBC example, it is clear that integrated solutions, with high efficiency, high power density are hampered by the significant amount of costs related to the design process and the long period of design for manufacturing making the time-to-market and its commercialisation quite unrealistic to the present industry.

In terms of technology, a good example of what can be seen on the market of solar inverters for household applications provides an interesting comparison. In recent years one of the most sold solar inverter is the SMA Sunny Boy 5000TL. It has a nominal power of 5000 W, weights 26 kg with a volume of 47 L. The resulting power densities are about 0.2kW/kg and 0.1 kW/L. This inverter is presented in Figure 1.3Figure 1.3. In contrast, it can be seen the 2 kW inverter made by the group at University of Illinois submitted to the LBC, achieving 13 kW/L. Of course, this is not a fair comparison because the converter from the University of Illinois would still have to pass through several reliability tests, and the final cost of the converter is very hard to estimate as it depends on several industrialisation factors. However, it can be seen that today, the manufactured / mass production of power electronic converters have huge room for improvement but development costs are a barrier to highly integrated solutions.

Figure 1.3 Left: SMA Sunny Boy 5000TL, 5 kW, the most sold solar inverter in 2018. Right: Google little box challenge finalist 2 kW inverter from University of Illinois Pilawa research group. Source: Adapted from [52].

The ECPE position paper [5] states that one of the major weakness in power electronics industry in Europe is the slow transfer of innovations into products, or even failing to transfer.

The traditional design process of a power converter is certainly one of the reasons for this fact. The industry requires a very fast pace for new converters to be designed and produced. It seems that there is a missing link between converter design and the industrialisation process. Engineers often keep their converter design conservative to achieve faster results and avoid to cause extra complexity in the industrialisation process. In such a case, new designs are based on predesigned and qualified subsystems, lowering the qualification barrier of the new product but also lowering the opportunity to introduce new components or new results that would translate to many issues related to industrialisation. Innovations are entering the PE mass market from niche applications first where volume and cost per Watt enable or even require risky innovation.

The approach proposed by G2Elab Power Electronics team based on Automated Design for Manufacture (ADFM) tries to provide an answer to this challenge. The presentation of the PCA design method in the following section put in evidence how the methodology intends to provide an alternative to achieve a faster design, industrialisation and manufacturing processes.

1.2 Principles of the Power Converter Array Methodology

The core ideas behind the Power Converter Array (PCA) methodology comes from transposing the microelectronic digital integrated circuit design and manufacturing flow to power electronics. It is this flow that allowed the microelectronics industry to create extremely complex devices, containing billions of transistors while providing very high levels of reliability, constrained costs, managed complexity, simplified modularity, far-reaching system integration, waste management and overall production efficiency. Despite the potential, it is important to note that microelectronics and power electronics do present several major differences.

The first and most important difference between microelectronics and power electronics is functional. Microelectronics handles binary levels or small signals and tends ever to reduce its voltage and current ratings to achieve better performances. Power electronics handles power and energy, with large currents, large voltages and tends to address more and more smart grid or connected-to-grid applications. While a billion transistors can be integrated on a single square centimetre die in microelectronics, the same die surface hosts a single power transistor. This power transistor will be used to switch currents of hundreds of Amperes under a thousand Volts, and this component will only be a small part of a mega-Watt-range power converter.

The second difference between microelectronics and power electronics is technological. The design of an integrated circuit is based on a more homogeneous set of materials such as semiconductor (Silicon in most cases), conductors (aluminium or copper), and dielectric materials (silicon oxide or nitride), all handled and implemented through collective processes. In contrast, a power converter has a much more heterogeneous nature, relying on different

technologies of components, different types of materials and various assembly approaches and interconnection technologies.
Despite the differences between microelectronics and power electronics, the design methods used in the microelectronics industry do have an enormous potential to influence the design methods of power electronics converters. This method can be divided into four aspects, namely, the use of the standard cell methodology, the technology platform, the automated design environment and experimental data-driven models. Each aspect will be covered in detail in this section. While the challenges of transposing these aspects are immense, they are matched in kind by the equally immense benefits such as cost reduction, reliability increase, complexity management, automated design and scalability.

1.2.1 The use of the standard cell methodology in microelectronics

The design of integrated circuits and more especially digital circuits, relies on a set of standard cells (SC) that are thoroughly known and minutely described, accompanied by a high-level language that automatically drives the synthesis of complex architectures. This automated design also called the synthesis tool, does not run traditional time-domain simulations. It carries on the design with a high level of abstraction, based on a limited set of critical parameters, well representative of the behaviour of the standard cells, for example the propagation time from the input of the cell to its output. In such a way, it is possible to design integrated circuits just by knowing the standard cells functions and key parameters and assembling them with a high level of abstraction.
A designer of digital integrated circuits does not need to know how the standard cells are made, neither the way they are designed. The synthesis tool handles all necessary data made available in what is called the design kit (DK) to produce a schematic, a layout and the files needed to run behavioural simulations without requiring electric time-domain simulations.
The designer workflow starts with the high-level language and describes the circuit functionalities. Once this is done, the designer selects the inputs of the synthesis tool in terms of performance, speed, power consumption, cost and/or surface restrictions. The tool automatically yields the schematic and the full layout of the desired digital function. This is only possible because the synthesis tool hosts a set of databases describing the technology, the characteristics of the components and subsystems available to build the digital circuit. Among them, several “standard cells” are available and thoroughly described.
The abstraction level existing in microelectronics design is present in several other domains, such as in computer science. For example, someone using a software to draw an image does not need to have any knowledge in the programming of the software, nor how the program is converted in binary, nor how the transistors and capacitors inside the processor will be used when he or she performs an action in the software. These technological actions, illustrated in Figure.1.4, are completely transparent to the software end-user.
In the case of microelectronics, this abstraction level is only possible because its design concept relies on a completely standardised and fixed technology whose parameters can no longer be

tuned or changed once the technology has been optimised. This seemingly big restriction is a very important advantage. It allows the technology to be matured and described at its best performance level, becoming extremely reliable in many aspects. This approach guarantees that characteristics and performances of the Application Specific Integrated Circuits (ASIC) which will be produced using this fixed technology correspond to a satisfying degree of error to the performances predicted during the design process. As a result, a significant part of the industrialization process is addressed at the fixed technology level. The designer can then operate at a high abstraction level and remain confident that by following the design rules, the ASIC can be manufactured and it will work as expected, despite its complexity.

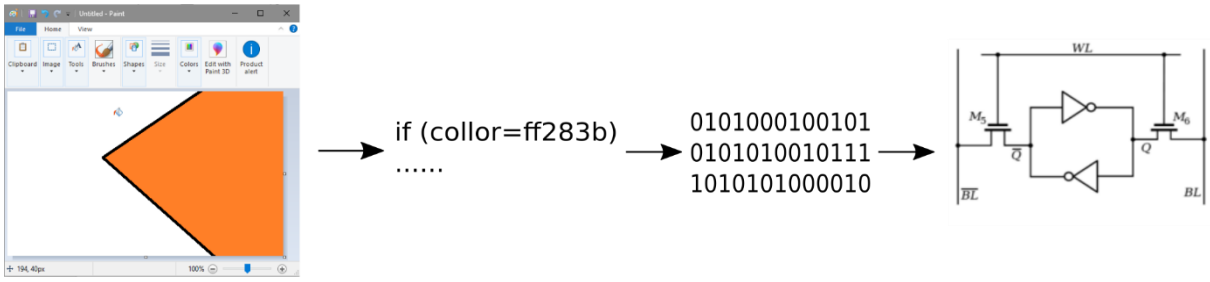

Figure 1.4 Decoupled actions that occur in a computer while using a software.

1.2.2 The use of Standard Cell Methodology in power electronics

In microelectronics and in computer science, there are three main concepts that have enabled automated design for manufacture, extreme complexity and good performances. The first one is segmentation, where a designer does not need to know everything about the process that will bring the design to a final product. The second one is abstraction, where the designer and the CAD tool does not handle all the details and parameters of the design. The last one is related to the technology framework that needs to be set in order to develop a technology and to link it with a design environment. For power electronics to achieve Automated Design for Manufacture, it must also address all these concepts.

The literature in power electronics provides two key concepts which can be used to address segmentation, abstraction and technology framework — first, the Power Electronics Building Block (PEBB) concept of modularity [53]. The PEBB divides typical functions of a power converter (measurement, control or power conversion) in building blocks and set up converters by assembling and interconnecting these blocks. Second, the Multi-Cell Converter (MCC) concept of scalability. In MCC topologies, a converter is built from standardised cells which are designed focused on scalability, which virtually enables any higher power ratings using off-the-shelf components. When combined, these two concepts yield a very solid formalism equivalent to the standard cell methodology from microelectronics.

The formalism for Automated Design for Manufacture (ADFM) in power electronics proposed in this work splits the design of a power converter into two concurrent aspects: the Converter Standard Cell (CSC) and the Power Converter Array (PCA). It is based on the CSC and the

PCA that an ADFM algorithm is capable of creating power converters based on a set of specifications from a designer.
The Converter Standard Cell (CSC) is an elementary building block based on a certain technology platform. This comprises its topology, switching components materials, driver references, PCB design, and so on. Once optimized for certain characteristics and performance, the CSC can be used as a basis for a designer to create a power converter with full segmentation.
The Power Converter Array (PCA) is the final converter which is built from the association of all standard cells relevant to a given set of specifications. It comprises a large set of standard cells, the CSC being one of them. PCA is the key to abstraction since it allows the designer to focus on the function of the power converter without worrying with details on the converter design, such as designing the switching cell or selecting its components.
The Automated Design For Manufacture (ADFM) algorithm links, among other standard cells, the CSC and the PCA together. To achieve this, the ADFM must have access to a thorough characterisation and minute description of each and every standard cell in order to automatically find solutions to a certain set of specifications via its optimisation algorithm. The ADFM requires a technology framework. This standard framework spans from the hardware implementation all the way to the software depiction of the standard cells, effectively enabling automated design.
A technology platform is the practical implementation of this formalism.

1.2.3 Technology platforms in microelectronics

A technology platform is the practical implementation of segmentation, abstraction and technology framework required by an ADFM algorithm. As such, the technology platform is highly influenced by the nature and details of technology being used and the application fields for which PCA will be designed and implemented.
In the case of digital microelectronics, the technology of standard cells is almost exclusively composed of CMOS transistors arranged in various architectures to produce logic functions. This very convenient technology-based enables the optimisation of these standard cells, and its few variants in order to constantly improve their performances.
The technology platform in digital microelectronics is thus a combination between technology base and a set of standard cells together with interconnection options. The whole manufacturing environment is totally transparent to the designer. Consequently, some microelectronics companies are specialized in manufacturing, offering open design platform through which designers can create whatever products they need to manufacture. These technology platforms are now very commonplace in microelectronics, but they are the result of a long and expensive maturation process of the entire microelectronics industry.

1.2.4 Technology platforms in power electronics

The creation of a transposition in power electronics requires a technology basis from which almost any Application Specified Power Electronics Converter (ASPEC) can be built. The

choice of the technology basis implies deciding upon a wide range of factors, such as the switching technology, the active and passive component technologies, the voltage rating, the current rating and the power rating, the interconnection and assembly technologies as well as cooling and shielding ones. As a result and similarly to microelectronics, several technology platforms may be required to cover the wide range of ASPEC converter market. Research contributions should focus, in this context, in defining and setting up technology frameworks that are coherent and complementary in order to offer solutions to numerous specifications.
For each technology platform, families of conversion standard cells (CSCs) must be designed, qualified and matured in order to reach satisfactory performance levels within specified budget constraints. Other essential standard cells are designed, matured and qualified in order to create a complete toolbox for designing and implementing a PCA. In such a way, interconnection, instrumentation, control, protection, filter and other standard cells are created sharing the same technology platform. When fully developed, the technology platform get to a point where no more modification is allowed in its SCs so they can be characterised, represented and modelled. The information yielded by this characterisation process feeds the database upon which the ADFM algorithm will operate.
This PhD work focuses on one specific technology platform and seeks to contribute to the characterisation, representation and modelling of one specific technology basis.

1.2.5 Automated design environments in microelectronics

The automated design environment in microelectronics is implemented via the computer-aided design (CAD) tools. CAD tools are extremely sophisticated and are able to handle designs of very high complexity.
The high levels of abstraction used in CAD tools mean that functions are no longer described as circuits but as programs. Through the use of these abstraction levels, CAD tools take the design seamlessly from the program up to the manufacturing files. During this process, the CAD tool supports the designer with design guidance, taking care of design rules, design checks, extraction, verification, statistical comparisons and more.
Design optimisation is also provided by some CAD tools. All the designer needs is to define the optimisation criteria and to compare, evaluate and select the best options. This optimisation process is carried out without conventional time-domain simulations, a feature that provides high speed to the overall optimisation process.
The standardization of the technology basis is the key to achieve such high levels of abstraction. By reducing the very complex physical problem of creating a microelectronics circuit to a limited number of parameters, the microelectronics industry has largely simplified the design effort of new products and open up the opportunity to design extremely complex systems and products. The results are CAD tools that allow the possibility to integrate billions of transistors able to implement hundreds of paralleled processors and auxiliary systems, all in one single chip of about 1cm² or less. Not only does the final design is guaranteed to work, it is also optimized for speed, power consumption, losses distribution and heat generation,

size optimisation, cost optimisation and whatever other characteristic deemed relevant by the designer.
Modern microelectronics product design has become an art largely due to automated design environments.

1.2.6 Automated design environments in power electronics

An automated design environment relies on a CAD tool that can allow a designer to operate at a high level of abstraction, to seamlessly go from programming to manufacturing while providing the designer with full support throughout the entire process. This CAD tool relies on the use of a highly standardised, thoroughly characterised and minutely described technology basis.
Three challenges stand on the way to create such a tool for power electronics design: formalism, technology basis choice and modelling methodology.
The challenge of formalism was addressed in a previous section through the Power Converter Array (PCA) approach. It combines the modularity concept from power electronics building blocks (PEBB) and the scalability concept from multicell converters to provide the formalism linking segmentation, abstraction and technology framework.
The challenge of choosing the technology basis was briefly addressed in the previous section. Since the power electronics industry has a very wide range of converter ratings, there is no technology basis that is as universal as CMOS for microelectronics. This means that the same CAD tool may have to handle a wider range of technology basis in order to address a wide range of specifications. Without the possibility of creating a unique and standardised technology basis, the burden falls upon the characterisation and description process to represent widely different technologies in a unified way that dispenses the use of time-domain simulations.
The final challenge is the modelling methodology. Since a CAD tool requires abstract models that are time-domain free for fast computing, this work proposes its associated modelling methodology to be completely data-driven and based on experimentation.
Experimental data-driven modelling is the key to thoroughly characterise and minutely describe the wide range of technology bases in power electronics, which will, in turn, enable power electronics automated design environments.

1.2.7 Experimental-data-based modelling in microelectronics

Microelectronics use experimental data-driven modelling to characterise thoroughly and minutely describe its technology bases. These models are used by the automated design environment together with a set of design rules that, if followed, guarantee the manufacturing of the device very close to design expectations.
Experimental data-driven modelling starts with each standard cell being subject to several experiments. Data representing their critical characteristics such as its physical dimensions, power consumption, propagation delays and critical parasitic effects are extracted with respect

to operating conditions such as clock frequency or junction temperature. Experiments are usually very complex and accurate, being conducted in specialized equipment. The data provides information about design parameters that contribute to the reliability of the component itself, which can later be used to optimize the automatic synthesis of other components.

Experimental data-driven models are based on the data collected and have varying levels of interpretability. Some very useful variables may be easily accessible to the designer, but not all physical variables will be, which is not necessary due to segmentation. Because experimental data-driven model parameters are based on real data, they dispense the use of theoretical models and long time-domain simulations to represent the behaviour of the technology basis. The design analysis can then focus on the assembly and interconnection of the standard cells. The impact of the interconnection in the design can be estimated via simple theoretical models.

Experimental data-driven models enabled the representation of microelectronics circuits without time-domain simulations. These models can be considered as one of the main reasons how microelectronic product design achieved such reliable levels seen today.

1.2.8 Experimental-data-based models in power electronics

Experimental data driven models in power electronics mostly focus on component characterisation. Applying experimentally driven models to the PCA approach implies creating models based on the behaviour the converter standard cell (CSC), other standard cells and their interconnections. Unlike in microelectronics where the impact of interconnections can be easily estimated using theoretical modes, interconnecting CSCs in a PCA may have a substantial impact on the overall behaviour of the system, from temperature to electromagnetic compatibility. Thus, two challenges emerge when using experimentally data-driven modelling for PCA: data volume and modelling technique.

The issue of data volume derives from the fact that interconnections cannot be simply modelled by theoretical models as in microelectronics. This makes it a necessity to actually build and experimentally characterise an extensive range of prototypes with different interconnections.

The issue of modelling technique focuses on finding the appropriate model that can, at the same time, provide a precise representation of the prototypes, which were characterised, and a reliable prediction of the prototypes, which were not characterised.

Table 1.1 resumes the key aspects of each principle presented in this section.

Table 1.1 Key aspects of each principle

Aspect of the methodology	Microelectronics	Power Electronics
The standard cell	Restricted number of standard cells with minor deviations	Identify how to divide the main functions of a converter in a family of standard cells
Technology platform	Standardised and matured process lines for CMOS cells with 2D interconnection	Multiple cells with 3D interconnection to be standardised
Automated Design Platform	Consolidated CAD industry using mature data-driven models	Enormous potential, but lacks abstraction levels to avoid time-domain simulations
Experimental-data-driven models	Models exist for the standard cell but not needed for interconnections	Models needed for the standard cells and interconnections

1.3 The PCA ADFM methodology

To explain in details how the methodology works, it is first presented an overview of the whole concept, and then it is presented details of each part of the design process.

1.3.1 Overview of the methodology

The PCA ADFM methodology proposes to introduce the concepts of the microelectronics industry presented in the past section into the design and production of a power electronics converter. The whole concept of the PCA methodology can be divided into three pillars:

- The design environment with a suite of tools for synthesis, layout, verification and extraction.
- The technology platform (TP) and its manufacturing processes together with its thoroughly characterised and minutely described families of standard cells ready to be assembled and interconnected.
- The design kit with all data and models related to the TP, which will be used to describe, design and predict any ASPEC behaviour.

Figure 1.5 illustrates the three pillars in what consists of the design process that goes from the converter specifications to the produced converter.
The process starts with a converter specification loaded as part of the input to the design environment. A pre-selection is carried out to identify which technology platforms are most suited to answer the converter specification needs.
The design environment then initiates the automated design using ADFM algorithms, which find the best solutions to configure and to assemble the various standard cells necessary to fulfil the specifications. An ADFM algorithm operates using design rules and model parameters, also called design parameters. These rules describe exactly how families of standard-cells behave and how they should be implemented for each technology platform

selected initially. These models and design rules must be available in the Model Database prior to initiating the design process.

Several solutions are synthesized and displayed to the power electronics designer who can then interactively refine different design specifications. These converter specifications may be electrical (type of conversion, input/output voltage, current and power ranges, efficiency), mechanical (width, length or height limits), norm compliance, thermal (minimum and maximum ambient temperature operation), economical (cost, number of parts per year). Once a suitable solution is selected, manufacturing files are produced, and a final check is performed.

The manufacturing files are then sent to a manufacturing plant where the technology platform has been previously qualified for manufacturing. As all components, subsystems and interconnect options are already known and selected, supply chain, process steps are all sets and rapid prototyping can be delivered. A final check of prototypes is usually required before entering in volume production.

The steps described above are all carried out with high celerity, from the specifications of the desired PE converter to the delivery of the first products. This increased gain in time is only possible because most of the design and industrialisation stages have been carried out prior during the technology platform set up.

Economically speaking, this approach relies on an offset between *lowering the development costs* of a product and *rising the capital expenditure* of developing a technology basis. In practice, a company that provides a PCA ADFM service that shortens the time-to-market of its clients' products will hope to have a strong return on investment on its original capital expenditure associated with the development of its technology basis.

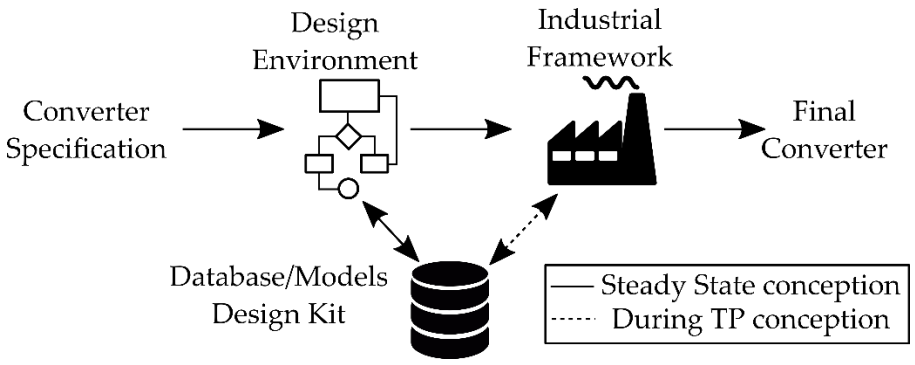

Figure 1.5 General concept of the PCA ADFM process.

From a power electronics perspective, the PCA ADFM approach proposes an offset between efficiency and development time. While the classic power converter approach may provide a very efficient ASPEC, it will come at the cost of a longer development time. In comparison, the PCA ADFM approach will probably provide a less efficient ASPEC, but at a much faster development time. This is particularly important when a company wishes to create a new product or revisit its current designs. Once the Technology Platform is developed and implemented, the models/rules are in place, and the algorithm is set, the time gain in going

from converter specifications to a final converter should payoff its lower ratings when compared with other design process.

1.3.2 Details on the PCA ADFM methodology

A power electronic converter can be divided into groups of components or sub-functions that perform specific functions.

- The power conversion sub-functions contain the active power switches with their associated drivers and auxiliary components as well as the passive storage elements.
- The isolated peripheral sub-functions contain voltage and/or current measurement devices and auxiliary power supplies.
- The control sub-function contains the digital controllers and their peripherals required to generate the driving signals to the power stages.
- Auxiliary power sub-function contain all other auxiliary components in the converter such as EMI filters, protections and cooling devices.

All these groups of functions are represented in Figure 1.6.

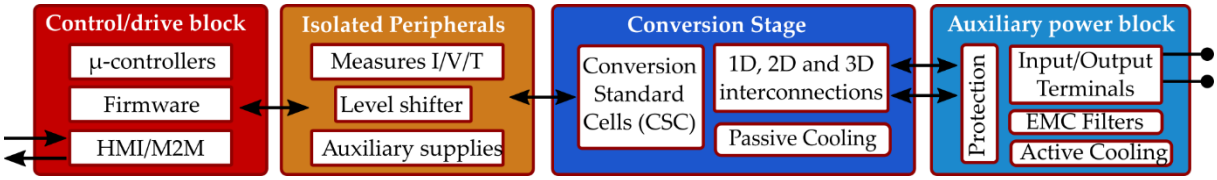

Figure 1.6 Categories of sub-functions that must exist to implement a power converter.

The PCA methodology relies on creating families of standard cells (SCs) to perform each of the functions necessary to implement and operate an ASPEC. These families of standard cells are developed within a technology framework, which follows a rigorous maturation process that guarantees optimal performances and industrialisation readiness. Within a certain family, each standard cell is designed to be compatible with its sisters' categories, from the functional, the physical, the electrical and the technological point of views, as is illustrated in Figure 1.7. Once thoroughly characterised, minutely described and technologically matured, the family of SCs is no longer modified. This guarantees the consistency needed to feed their information to the design tools and their reusability in the manufacturing process [46]. Table 1.2 presents the main SCs necessary to design a PCA, together with a short description of their main purpose.

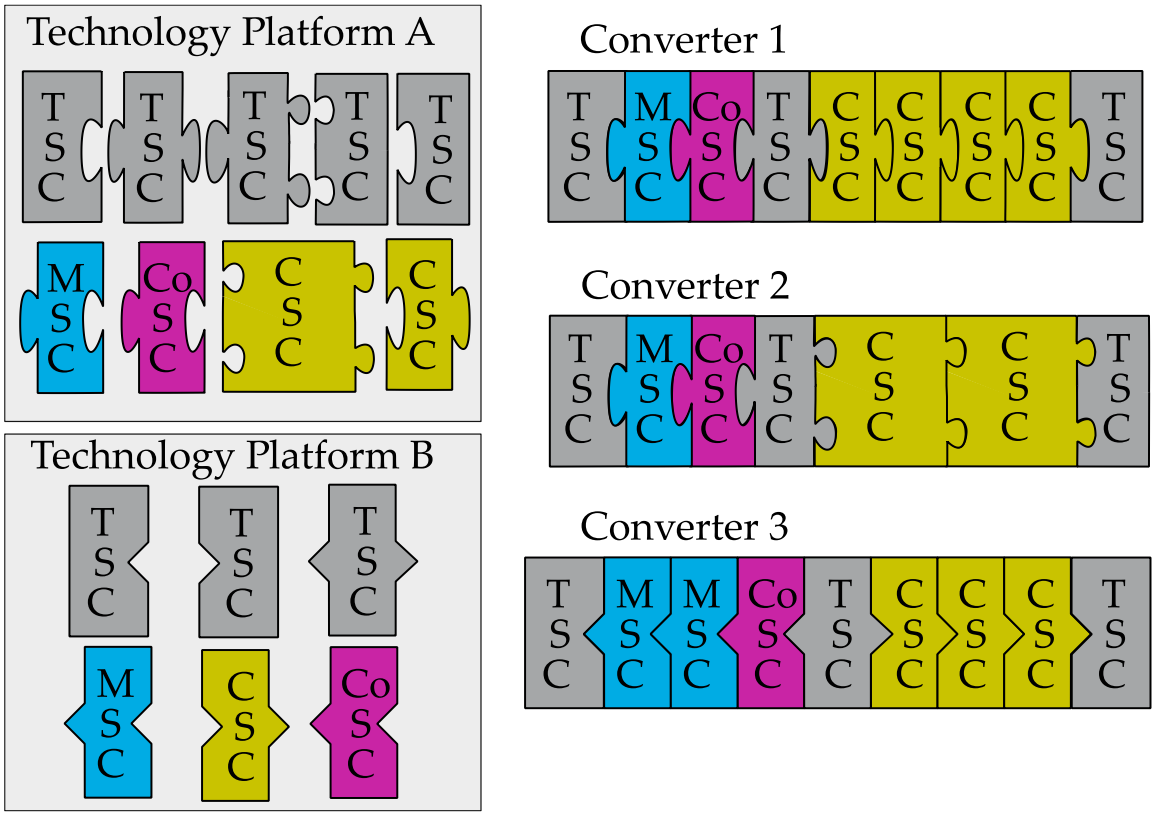

Figure 1.7 Artistic view of Power Converters Arrays as an aggregate of jigsaw puzzle pieces. The image presents pieces from different Technology Platforms that are incompatible with each other and that a Technology Platform may have several different CSCs and TSCs.

Table 1.2 List of Standard Cells in a Technology Platform.

Name	Composition	Function
Conversion Standard Cell (CSC)	Switches, passives components, gate drivers, passive cooling	Power conversion
Measurement Standard Cell (MSC)	Current sensors, voltage sensors, galvanic isolation, filters	Measurement
Control Standard Cell (CoSC)	Microprocessor, crystal, filtering capacitors, auxiliary supplies	Control, HMI, MMI
Terminal Standard Cell (TSC)	Bus bars, wiring connectors, Jumpers, B2B connectors, fluidic and/or cooling devices	Signal and power interconnection, electromechanical connection thermal management
Filtering Standard Cell (FSC)	Capacitors, inductors	Input/output filtering
Power connection Standard Cell (PSC)	Wire-to-board connectors, busbars	Connecting input and output terminals to wires

The power conversion stage of a PCA-based ASPEC is made by the association of conversion standard cells (CSC) associated with Terminal Standard Cells (TSC) that provides the CSCs electrical interconnections, physical, mechanical and thermal implementation. In order to achieve different voltage conversion ratios, CSCs can be associated in four different types of configurations: Input series output series (ISOS), input series output parallel (ISOP), input parallel output series (IPOS) and input parallel output parallel (IPOP), presented in Figure 1.8. In this work, the word "configuration" is used to describe the types of interconnections. Solutions that use ISOP and IPOS configurations are always preferred due to their natural balance mechanism [54].

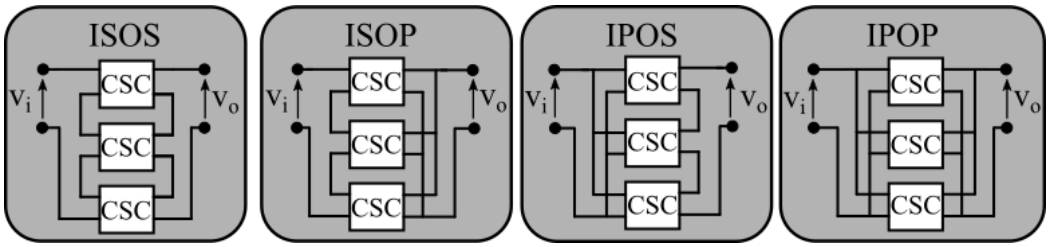

Figure 1.8 Possible connections among conversion standard cells.

In order to propose solutions in different fields of application, different Technology Platforms (TP) are proposed which share similar design, manufacture and implementation constraints. Each TP contains one or more families of SCs, which are able to provide all necessary sub-systems, many different converters power/voltage specifications as well as specific standards and regulations. Table 1.3 proposes a list of characteristics for any given TP and Figure 1.9 illustrates how these different characteristics may are used in different application fields.

Table 1.3 Characteristics of a Technology Platform

TP Criteria	**Description**
Interconnection techniques	Bus bars, cables…
Normative class	Automotive, avionics, medical…
Dielectric isolation	Voltage rating of isolation
Power class	High, medium or low voltage or current
Housing technology	Packaged solutions
Control and dynamic class	
Maturity class	Technology Readiness Level (TRL1-9)
Environmental class	RoHs compliant…

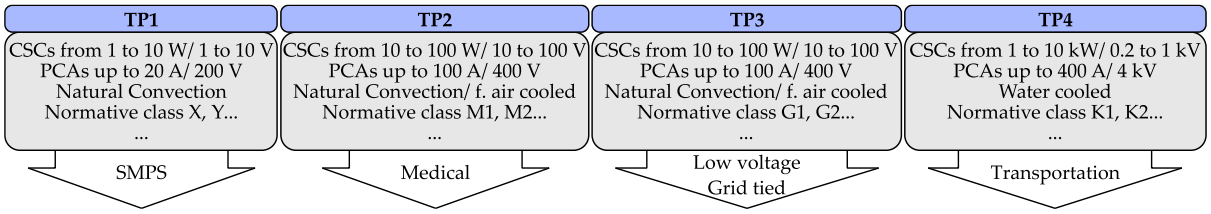

Figure 1.9 Examples of different Technology Platforms, the characteristics of their CSC and their application field.

The Technology Platform creation process consists in designing, optimizing and bringing to the highest manufacturing readiness level each family of standard cells [55]. These three steps are made in collaboration with an industrial partner since TP component selection must compromise between optimal performance, supply chain logistics, reliability, layout design, mechanical dimensions and cost, to cite a few industrial constraints. Only after all of these constraints have been taken into and the manufacturability of the standard cells have been validated that their characterisation process may begin.

Once created, a Technology Platform goes through a characterisation process whose objective is to determine precisely how the different families SCs behave in all possible implementation scenarios. In order to acquire this information, several experiments are performed with different ASPECs, carefully chosen to provide as much real-world data as possible on different association scenarios of the families of SCs under characterisation. Throughout this process, data that describes the behaviour of each individual SC can be acquired, and statistical models can be created to predict their collective behaviour for the association scenarios. With this previous knowledge of the behaviour of any possible ASPEC, this methodology allows for the possibility of estimating ASPEC performances for different operating conditions. This hindsight is almost impossible with traditional design methods since these rely on theoretical models whose accuracy not only may be limited by the operating conditions being simulated but also cannot account for inevitable modifications brought to the ASPEC by the industrialisation process.

The design rules and constraints associated with a Technology Platform are derived from the data obtained during its characterisation process. It allows the definition of technology boundaries within which a designer must stay to guarantee the feasibility and performances of the ASPEC under design. These boundaries translate into a set of design rules and constraints such as the maximum number of CSC that can be connected in a line for a given current, a given ambient temperature or a given cooling method. This set of rules are summarised in a Design Rules Manual (DRM) and implemented in the automated design environment through a Converter Synthesis, and a Design Rules Check tool.

An ADFM algorithm puts together the statistical models and design rules derived from the characterisation data of a Technology Platform to generate solutions automatically for specifications given to it by a designer. These solutions consist of a list of the various SC assemblies with details such as the required number of CSCs, their configuration, the placement of each SC, their corresponding TP if more than one is considered by the algorithm,

performance (efficiency, temperature), standards compliance, volume, weight and cost. With a final list displayed by the automated design environment, the most suitable solution can be chosen at the discretion of the designer. Once a suitable solution is chosen by the designer, a datasheet and application note can be automatically generated, providing a solid start to the documentation of the ASPEC before it has even been manufactured.

1.4 The Technology Platform G2ELab-Maatel

The TP G2ELab-Maatel (GM) was developed in parallel to this work, in the context of project Mamaatec, financed by the Rhone Alpes region. TPs have specific fields of applications and this specific TP is designed to produce converters with the specifications included in the list of characteristics presented in Table 1.4.

Table 1.4 The TP G2ELab-Maatel main characteristics

Input and Output Voltage Range	12 V to 600 V
Current Range	Up to 90 A
Dielectric isolation	1.5 kV
Assembly and interconnection technology	PCB
Cooling technology	Natural convection or forced air

This TP contains two different families of power standard cells built around two CSCs, the GM20V5A and the GM10V3A. Their names are related to their nominal voltage and current ratings. The GM20V5A has a nominal input voltage of 20 V and a nominal current of 5 A, being more suitable to applications from 20 V to 400 V. The GM10V5A has nominal values of 10 V and 3 A. It is more suitable to applications from 10 V to 200 V.

Several concept rules define how to build a PCA converter using the proposed GM SC family. The following rules are described in Table 1.5 and illustrated in Figure 1.10.

Table 1.5 Concept rules to build a PCA using the GM SC family

Rule	Description
Three dimensions PCAs	Any PCA may contain lines, columns and boards, making the TP three-dimensional
Line-oriented interconnections	At the beginning and the end of each line must be placed a Terminal Standard Cell
CSC configuration unicity	In each dimension (lines, columns and boards), one and only one type of configuration among CSCs (ISOP, IPOS, SISO, SIPO) can be implemented
Auxiliary board separation	Every PCA is equipped with an auxiliary board, placed above the power conversion part. It collects all currents flowing to and from CSCs and contains the Control Standard Cells (CoSC), Measurement Standard Cells (MSC), protection and filter standard cells and Power connection Standard Cells (PSC)

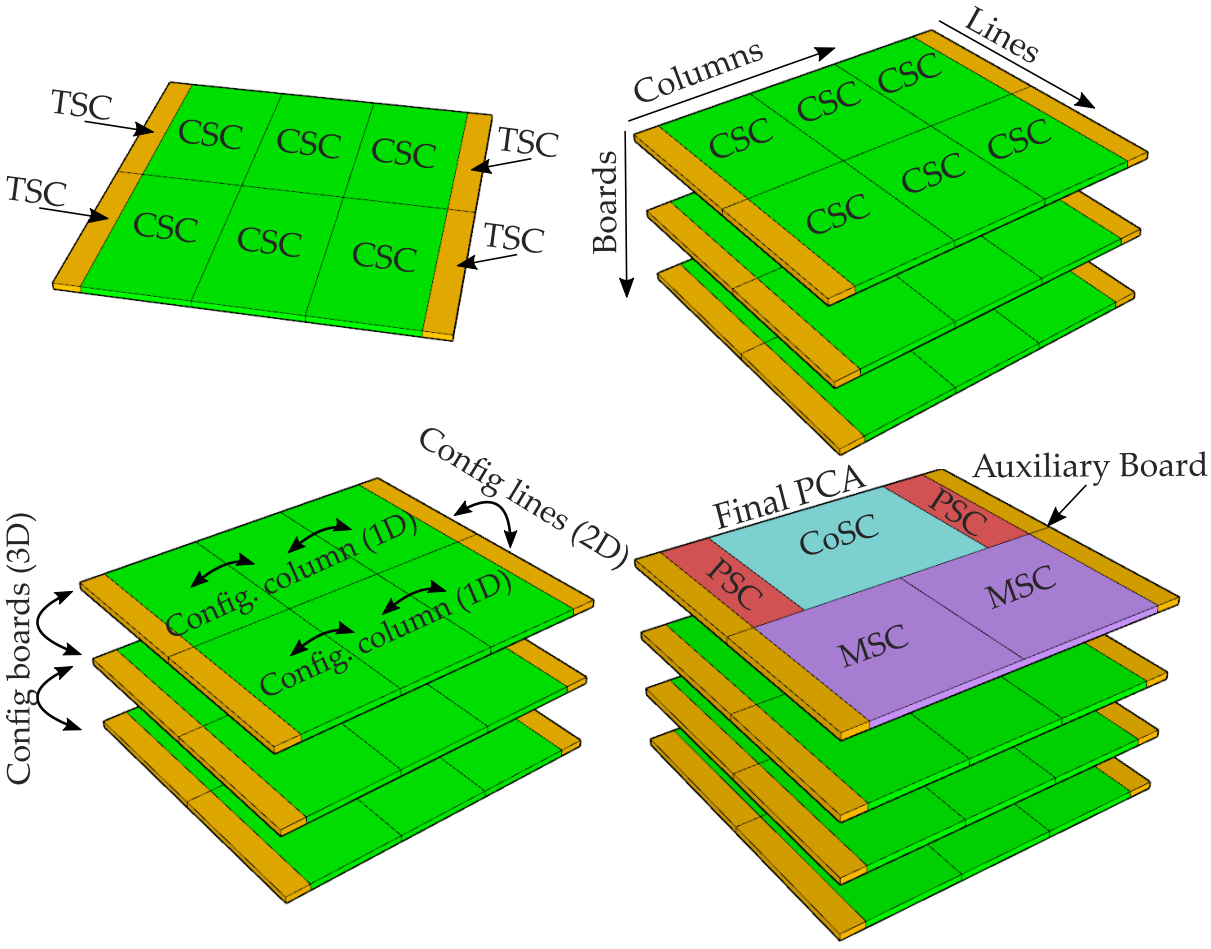

Figure 1.10 Illustrations of the rules to build a PCA with the TP G2ELab-Maatel

The design of a TP is a very detailed and complex task. This work will only present details about the TSC and the CSC because they are directly related to the contributions of this thesis.

Further details about the other SCs and about the collaborative design with an industrial partner are presented in [46].

The architecture of a PCA is the number of conversion cells that are arranged in lines (*nline*), columns (*ncol*) and a number of boards (*nboard*). As presented in Figure 1.11, different converters with the same number of cells can be built with several different architectures. Each architecture may implement different interconnection pieces and display different thermal behaviour, as the airflow is affected by the physical arrangement of the conversion cells. Figure 1.11 presents three conversion architectures namely *3x2x1*, *2x3x1* and *1x3x2*, being *nline x ncol x nboard* respectively, all containing 6 CSCs and theoretically being capable of performing the same power conversion ratings.

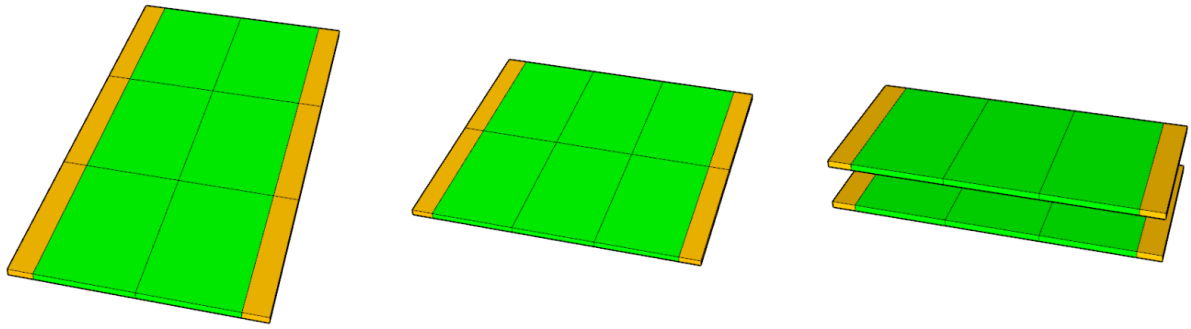

Figure 1.11 Three converters with the same amount of conversion cells with different architectures: 3x2x1, 2x3x1 and 1x3x2

In this work, the configuration of a PCA represents the type of connection, series and/or parallel, for the inputs and outputs of its CSCs. As explained in the previous section, four types of interconnections are possible and all of them can be mixed, into different configuration levels. As mentioned in [56], there are preferable arrangement schemes that ease global converter implementation.

Each converter dimension can only receive one configuration level. Thus, a converter can be connected in its first dimension (columns) in any of the four interconnection types (ISOP, IPOS, SISO, IPOP), and similarly for the second and third dimensions. It is possible to create converters with different configurations that have the same power and voltage conversion, as it is shown in Figure 1.12.

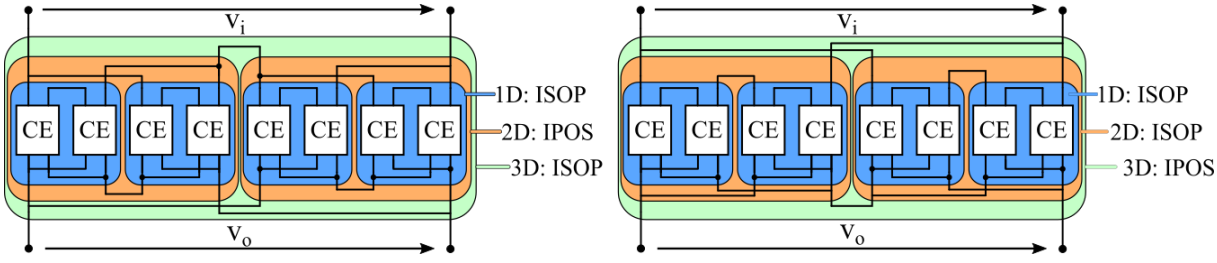

Figure 1.12 Two different configurations that result in the same input-to-output voltage conversion ratio.

This work focused on the characterisation and description process of the GM20V5A family, which is introduced in detail below.

1.4.1 CSC G2ELab-Maatel 20V5A

The power electronics converter topology chosen to perform the CSC is the dual active bridge (DAB), presented in Figure 1.13. This topology was chosen because it presents galvanic isolation and is capable of achieving high power density and high efficiency, especially when the input to output voltage ratio is kept close to the unity [57], [58].

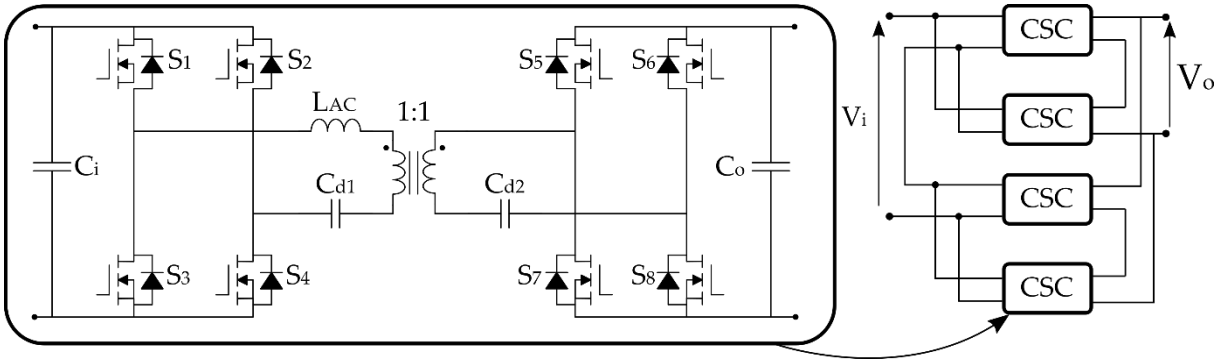

Figure 1.13 Dual Active Bridge (DAB) topology used to perform the role of CSC.

A phase shift modulation scheme is employed to drive the DAB, which results in a voltage conversion ratio given by equation 1.1. The power transfer is performed through the inductor L_{AC}, which is the sum of external discrete inductor, and the transformer leakage inductor. Figure 1.14 below provides illustration pictures of the presented CSC.

$$V_o = \frac{V_i R_0}{2 f_{sw} L_{AC}} \alpha(1-\alpha) \qquad 1.1$$

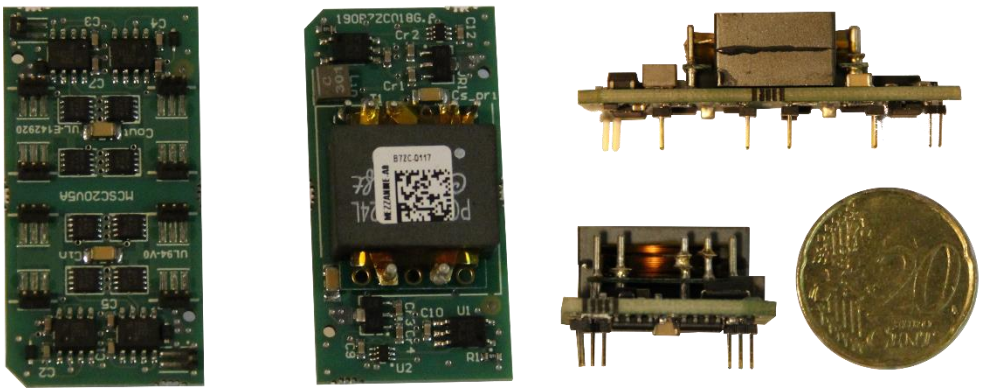

Figure 1.14 Pictures of the Conversion Standard Cell G2ELab-Maatel 20V5A.

A list of the main components present in the CSC is displayed in Table 1.6

Table 1.6 Components present in the CSC GM20V5A

Component name	**Function and description**
8 Si MOSFETs	These MOSFETS are arranged in two active bridges connected back to back
Input/output capacitors	These capacitors filter the DC voltage in the input and the output of the DAB
L_{AC}	This inductance is composed of a discrete inductor and the leakage inductance of the transformer
4 Gate drivers	Each one responsible for driving 2 MOSFETs in a leg forming a switching cell,
2 dual inverter buffers	Responsible for generating a complementary logic signal to drive the two legs of a full bridge with one single signal
2 Optocouplers	Used to isolate the control neutral point from each CSC neutral point.
2 Linear regulators	One on each side of the DAB converter to supply the adequate voltage to each electronic component.
Auxiliary passive components	Filtering capacitors, bootstrap capacitors and bootstrap diodes.

The main characteristics of the CSC is reported in Table 1.7.

Table 1.7 Details about the CSC GM20V5A

Factor	GM20V5A
Maximum Input Voltage	20 V
Minimum Input Voltage	8 V
Maximum Output Voltage	20 V
Minimum Output Voltage	8 V
Maximum output current	5 A (Highly dependent on cooling factor)
Nominal switching frequency (f_{sw})	250 kHz
Dimensions (length, width, height)	(24 mm, 47 mm, 13 mm)
Insulation	1.5 kV
Weight	30 g
PCB maximum temperature	90 °C

1.4.2 TSC G2ELab-Maatel 20V5A

The Terminal Standard Cells (TSC) is responsible for the electrical interconnection between lines and between boards. TSCs also distribute driving signals between the CoSC and each CSC. These signal connections are designed not to impose any limits on the maximum number of PCBs that can be stacked. Additionally, the TSCs provide mechanical support and, in some cases, air guidance for cooling. The details of the TSCs layout for the GM20V5A family are presented in Figure 1.15a). Figure 1.15b) presents the real implementation of the TSC in a converter; the area that corresponds to the TSC is highlighted with the red dashed lines.

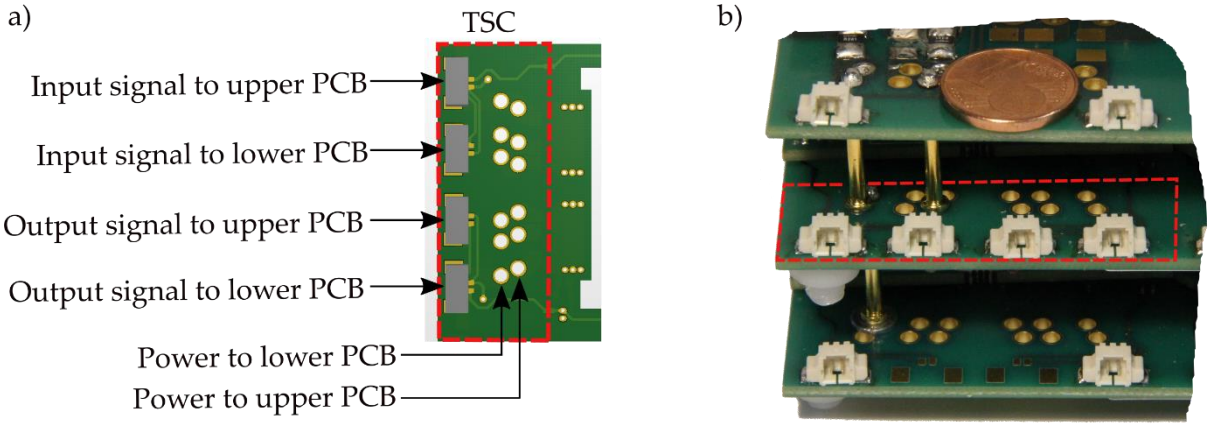

Figure 1.15 a) Details of the TSC 20V5A in a CAD 3D image. b) Photo of a PCA focusing on the TSC, the TSC is highlighted by the red dashed line

The TSCs theoretical current limit for board-to-board connection is 30 A. Above this theoretical limit, the connector will increase its losses and may hamper overall ASPEC performances. The characterisation process should provide clues about the real impact of this TSC.

In general, theoretical limits are important to set up a first range of safe operating area for the components used in the technology base. These limits also provide first estimations of the operating area with the best performance levels for a given PCA. However, these operating ranges and areas must be verified through the characterisation process.

An overview of all the theoretical limits of the TSC GM are given in Table 1.8.

Table 1.8 Details about the TSC GM

Factor	GM20V5A
Maximum Voltage Isolation (input to output)	1.5 kV
Maximum Voltage Isolation (Input V+ to V-)	400 V
Maximum current	30 A
Dimensions (length, width, height)	(18 mm, 47 mm, 13 mm)
Weight	15 g
PCB maximum temperature	90 °C

1.4.3 G2ELab-Maatel 20V5A family thermal aspects

A PCA created using the GM20V5A can operate with forced air-cooling or in natural convection. This work is focused on the air-cooled PCAs in order to study a larger spectrum of solutions. All experimental procedures used with PCAs in forced air cooling operation can be applied to study the PCA in natural convection.

The placement of the fan in a PCA based on the presented TP is presented in Figure 1.16. The air is blown in the direction of the PCA lines, so, theoretically, the air gets warmer as it passes through each line. The temperature of the air is illustrated by the red colour gradient in Figure 1.16.

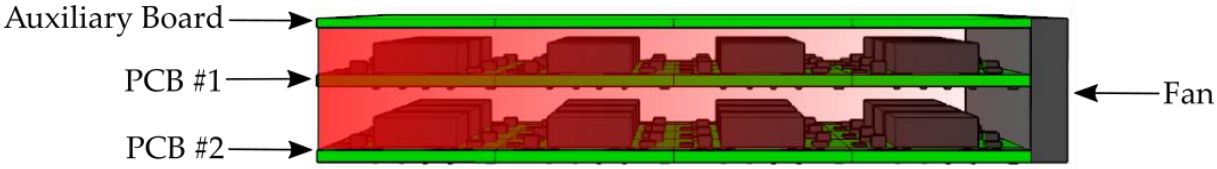

Figure 1.16 Lateral view of a PCA containing 4 lines, 3 columns and 2 boards. The red gradient symbolises the rise of temperature with the distance to the fan.

The TSCs connectors provide a natural barrier that crosses the converter in the direction of the airflow. They act as a wind tunnel, keeping the entire airflow within the PCA power conversion cross-section. This barrier ensures that the surface in which the fan blows its coolant is exactly the cross-section of a CSC multiplied by the number of CSC columns and by the number of power boards. This is illustrated in Figure 1.17, it is also highlighted the surface of the CSCs directly facing the fan.

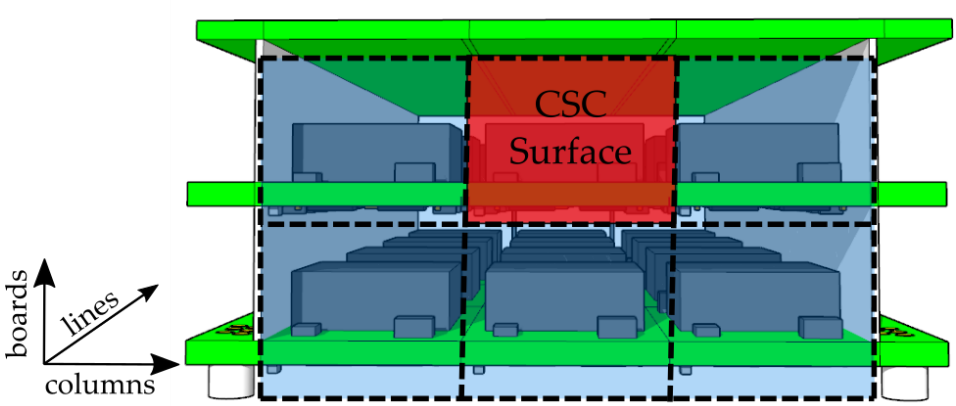

Figure 1.17 View of the PCA in the direction in which the airflow.

There is a clear relationship between the architecture of a PCA and its thermal performance. This relationship will inevitably pit architecture against maximum ASPEC temperature through its impact in the airflow. This work will use the characterisation process of the technology framework as a means to study this relationship.

1.5 Example of a PCA created following the method

In order to illustrate how the PCA concept works, the example below describes the design of an ASPEC. The specifications of the ASPEC are presented in Table 1.9. Its specifications correspond to those of a converter for charging and discharging a LiFePO4 36 V battery stack using a 120 V DC bus, including galvanic isolation.

Table 1.9 Specifications of a DC-DC converter for a battery charging application

Input Voltage (battery side)	32 V to 40 V
Output Voltage (source side)	120 V +/- 4 V
Output Current	8 A_{DC} max
Isolation	1.5 kV
Maximum dimensions	Width:10 cm Length :30cm Height: 10 cm
Cooling method	Forced air-cooled
Minimum efficiency at nominal power	91 %
Maximum weight	1 kg

The specifications are used as input into the ADFM algorithm. The algorithm then selects the Technology Platform, which is the most adequate to fulfil the required specifications. From the choice of the TP, the algorithm then provides all possible solutions using the families of SCs available in each TP. During this work, the only TP available was the G2ELab Maatel, which contains the GM20V5A CSC, presented in Table 1.7 and the GM10V3A which is a CSC limited at 10 V and 3 A. All possible solution found by the algorithm are presented in Table 1.10.

Table 1.10 List of PCAs that are able to perform the power conversion. Solutions that comply with all specifications are highlighted in grey.

	#	Arch-tecture	No. of CSCs	Config.	Max. Power (W)	Max. Input voltage (V)	Max. Output voltage (V)	Max. output Current (A)	CPR* (%)	Lengt (mm)	Width (mm)	Height (mm)	Weight (g)
GM5A-20V	1	2x6x1	12	PS-SP-0	1200	40	120	10	100	94	144	13	420
	2	6x2x1	12	SP-PS-0	1200	40	120	10	100	282	48	13	540
	3	1x6x2	12	PS-0-SP	1200	40	120	10	100	47	144	26	420
	4	2x3x2	12	PS-PS-SP	1200	40	120	10	100	94	72	26	480
	5	2x3x2	12	SP-PS-PS	1200	40	120	10	100	94	72	26	480
	6	3x2x2	12	SP-PS-PS	1200	40	120	10	100	141	48	26	540
	7	2x2x3	12	PS-SP-PS	1200	40	120	10	100	94	48	39	540
	8	7x2x1	14	SP-PS-0	1400	40	140	10	85.7	329	48	13	630
	9	2x7x1	14	PS-SP-0	1400	40	140	10	85.7	94	168	13	480
	10	7x1x2	14	0-PS-SP	1400	40	140	10	85.7	329	24	26	840
	11	1x7x2	14	PS-0-SP	1400	40	140	10	85.7	47	168	26	480
	12	2x4x2	16	PS-PS-SP	1600	40	160	10	75	94	96	26	600
	13	4x2x2	16	SP-PS-PS	1600	40	160	10	75	188	48	26	720
GM3A-10V	14	4x6x2	48	PS-SP-PS	1440	40	120	12	83.3	128	144	26	1152
	15	6x4x2	48	SP-PS-PS	1440	40	120	12	83.3	192	96	26	1296
	16	2x12x2	48	PS-SP-SP	1440	40	120	12	83.3	64	288	26	1008
	17	12x4x1	48	SP-PS-0	1440	40	120	12	83.3	384	96	13	1296
	18	12x2x2	48	SP-PS-SP	1440	40	120	12	83.3	384	48	26	1728
	19	4x4x3	48	SP-PS-PS	1440	40	120	12	83.3	128	96	39	1296
	20	4x4x3	48	PS-SP-PS	1440	40	120	12	83.3	128	96	39	1296

*CPR - CSC Power Ratio: Ratio of the operating power of the CSC in the converter application to the nominal CSC power.

Table 1.10 presents the architectures in which the CSCs are placed, where (nlxncxnb) correspond to (number of lines x number of columns x number of boards). The configuration presents the type of connections (SP for input series output parallel and PS for input parallel output series). The maximum values of input and output voltage are, in some solutions, higher than the specified voltage, but they can work at the desired voltage. The table also presents the CSC Power Ratio (CPR), which represents the percentage of the maximum power the CSCs will work.

The solutions highlighted in grey presents the PCAs that comply with all specification, in terms of voltage conversion, power rating, dimensions and weight. To give a practical example of the technology, the PCA number 13 was built. This PCA has 4 lines, 2 columns and 2 boards. The lines are connected in IPOS, the columns are connected in IPOS and the boards are connected in ISOP. A photo of the converter is presented in Figure 1.18 together with details of the placements of TSCs, CSCs and auxiliary board that compose the converter.

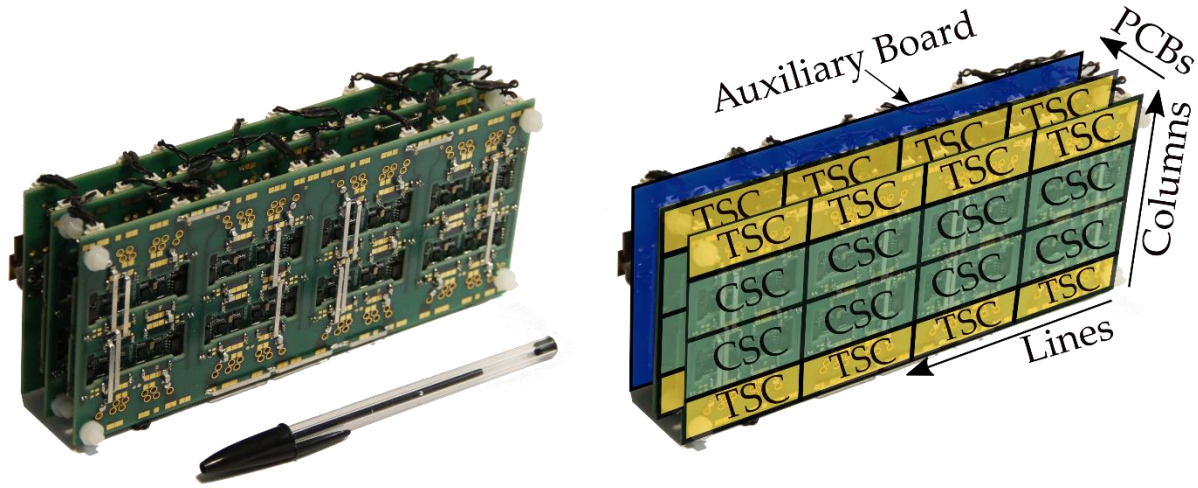

Figure 1.18 Left: PCA created to answer the desired converter specifications. It contains 16 CSCs, which are arranged in a 4x2x2 architecture and an IPOS-IPOS-ISOP configuration (columns/lines/boards). Right: Details of what the PCA consists of in terms of standard cells.

Experimental measurements have been made in two different testing conditions. The corresponding operating point of the converter are presented in Table 1.11. Figure 1.19a) presents an infra-red (IR) photo of the first setup and Figure 1.19b) presents the PCA under natural convection.

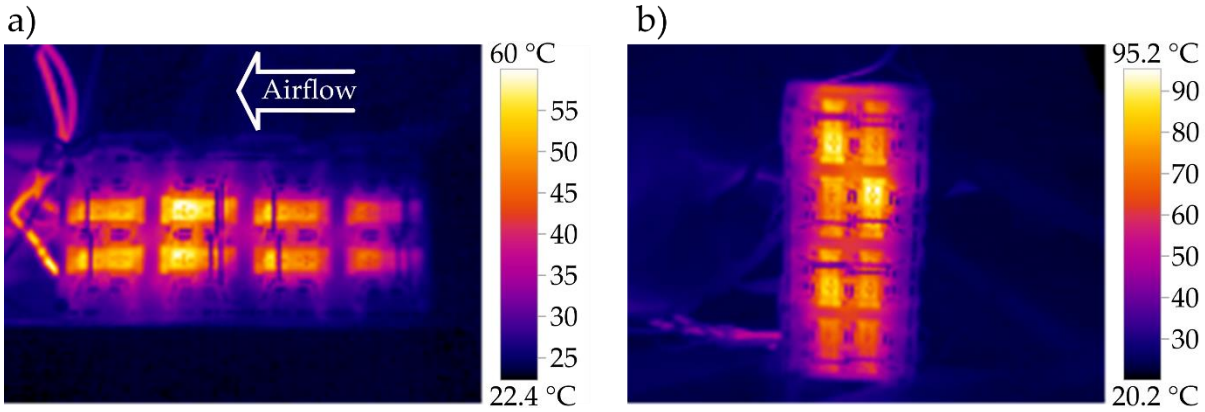

Figure 1.19 Infrared photos of the MCC. a) Forced airflow b) Natural convection.

Table 1.11 Details of the two operating points of the PCA when the IR photos were captured.

	Forced air cooling	Natural convection
PCA input voltage (average input voltage at each CSC)	34 V (17 V)	34 V (17 V)
Output voltage (average output voltage at each CSC)	120 V (15 V)	120 V (15 V)
Output current (average output voltage at each CSC)	8 A (4 A)	5.2 A (2.6 A)
Output Power	960 W	624 W
Ambient temperature	20 °C	20 °C
Air speed at the converter	1.5 m/s*	-
Max board temperature	60 °C	95.2 °C
Efficiency	91.7 %	91.6 %

*: Estimated value, it is not possible to have an accurate value as one side of the housing of the converter was opened in order to obtain the IR picture.

It can be seen in the IR pictures that in both setups the CSCs present different temperatures. In the forced air-cooling setup, it can be clearly noticed that the CSCs that are closer to the fans present lower temperatures. This confirms the original assertion that the air rises in temperature as it passes through the CSC lines. In the natural convection setup, the temperature among CSCs is more homogeneous, presenting temperature differences lower than 10 °C among the same components in different CSCs.

As only ISOP and IPOS configurations are employed, it is possible to send one driving signal to all CSCs and rely on its natural voltage/current balance mechanism [54]. In order to validate this natural balance phenomenon, the output voltage of each CSCs is analyzed individually. To do so, a third experiment is performed in which the output voltage was fixed at 124 V and the output voltage of each CSC was measured individually for 4 different values of output current. Figure 1.20 presents the schematic of the configuration in which the 16 CSCs are connected. Figure 1.21 presents the value of the output voltages of each CSC for the different values of output current. The test has been made using forced air cooling.

The expected equilibrium voltage for each cell is $V_e = 124\,V/8 = 15.5\,V$. However, it can be seen the CSC 10 presents a voltage of 15.9 V and the CSC 11 with 14.95 V, a total difference of 0.95 V. The maximum error of 0.55 V from the equilibrium point, which represents 3.5 % of the desired value. This voltage unbalance may have several different explanations, among which is the value of the inductor of the AC link, whose tolerance is +/-20%. A theoretical approach would struggle to model the complex interactions leading to this unbalance. This is where a thorough experimental characterisation can provide the data for creating statistical models to try to predict in much more detail this type of behaviour.

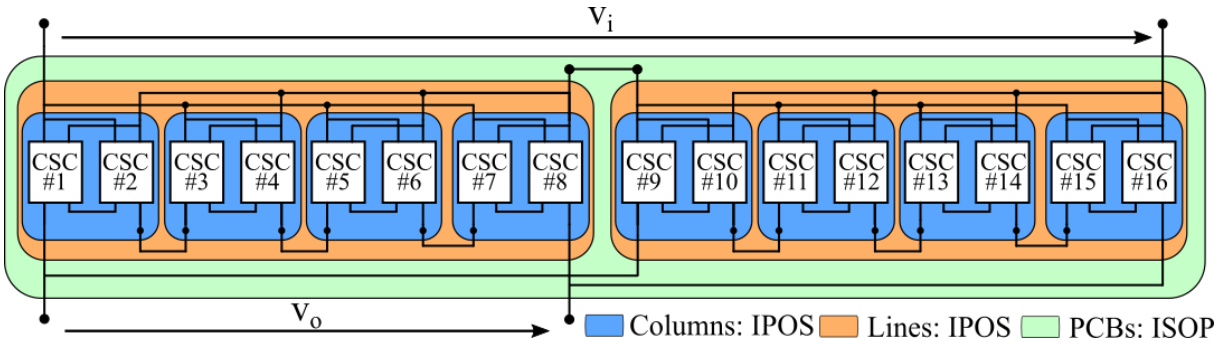

Figure 1.20 Details about the configuration of the PCA converter

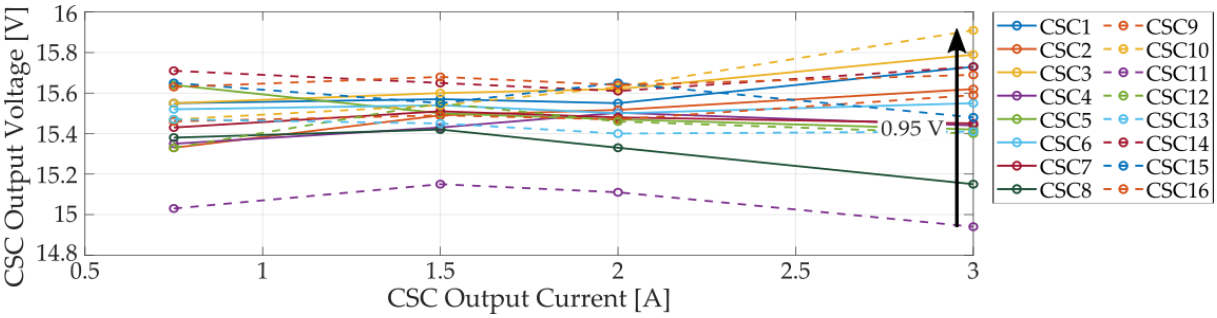

Figure 1.21 Measured data of the Output voltage in each CSC at various levels of output current

Among all solutions presented in Table 1.11, the PCA number 13 was chosen and built to illustrate the PCA ADFM methodology. A designer using this method could choose any other solution that presents higher efficiency and the best thermal behaviour. The prediction of this information is one of the unique features that the PCA ADFM method can bring. The methodology to create the models needed for these predictions is one of the major tasks of this thesis, the next section details precisely how the research is carried out.

1.6 The goals of this Thesis

After presenting the formalism of the Power Converter Array (PCA) methodology, its design process and an example of the design of an Application Specific Power Electronics Converter (ASPEC), it is possible to describe the objectives of this work and to understand where the research will contribute to the overall approach.

This work will aim to provide the link between the technology platform and the design environment. This link consists in supplying all the necessary **data** needed for achieving two main objectives:

- To describe the TP, create design rules and to design PCAs based on this data.
- Predict the behaviour and performance of all PCAs that can be built by the TP

Four possible strategies were considered to obtain the data:

1. Fully experimental dataset; build all possible PCAs that the PT can provide and perform a set of experiments in each one of them.
2. Create theoretical models; modelling the electric and thermal behaviour of the CSC and TSC by theoretical equations, then guess all possible effects that a PCA may present then predict the behaviour of all possible PCAs.
3. Make hybrid models; performing a full characterisation in one CSC and TSCs. Then create a model predicting the electro-thermal behaviour of PCAs based on the characterisation data and the possible effects of a multicell converter.
4. Statistical models based on experimental data; Build a representative sample of PCAs, acquire experimental data from them and fit statistical models to predict the information of the others.

The strategy used in this thesis was chosen by elimination.

Strategy 1 requires a huge amount of time and resources to build and test all PCAs. For instance, considering PCAs up to 5 lines, 5 columns and 3 boards, that are connected only in ISOP and IPOS configurations, there are over 150 different possible PCAs. Building all of these would cost over 100k€. Measurements would take over 180 days' worth of data acquisition. This does not take into account the time needed to process the data.

The strategy 2 and 3 propose two different methods of obtaining the knowledge about the Standard Cells, both are interesting and feasible. A theoretical electro-thermal model of the CSC and TSCs can be created since the behaviour of the converter is very well comprehended, as proposed by strategy 2. In addition, as strategy 3 proposes, to perform a characterisation of a single CSC and TSCs does not take much time or resources. However, to predict precisely the behaviour of the PCAs, both strategies would require an accurate knowledge of all the interactions between the physical variables that can possibly exist within any PCA architecture. Some of these effects are: Uncertainty of value of passive components due to the tolerance level, the variability of the value of passive components and switches by the temperature, temperature of a CSC by its position in a PCA, driving signal delay related to the position of the CSC, etc. These effects can be very complex and very hard to be understood without experimental data.

Since experimental data is needed anyways, and that experimenting on all possible architectures is not feasible, the only logical solution is to go for strategy 4.

The data used in this work were extracted from a characterisation process of several samples of PCAs designed by the G2ELab-MAATEL technology platform. More specifically, it is the GM20V5A CSC that will be considered, along with its colpanion Standard Cells, during the whole project.

The statistical models will relate to the two objectives of this thesis, namely, helping in the creation of design rules and provide predictions of PCA behaviour.

In terms of design rules, the models should provide precise information about the safe operating area of the technology, in terms of electrical and thermal variables. In practice, this means that the model should provide predictions of the efficiency and of the converter

temperature for any PCA architecture under any operating condition. This kind of information is then used to guide the TP design rules that must be followed in order to create reliable PCAs. In terms of predictions, the statistical models should provide reliable information about the behaviour and the characteristics of any PCA, in order to assist the PCA Automated Design For Manufacturing (ADFM) algorithm to find the solutions complying with the converter specification or to help a designer to choose among possible solutions. As it was illustrated on the example in section 1.6, a given converter specification can result in several solutions. If the models can describe precisely all the converters efficiency and temperature in all electrical and thermal situations, the designer will have a better chance of selecting the best option. In practice, the models should predict behaviours of PCA architectures that cannot be experimentally tested and provide the confidence interval of these predictions as well.

The whole work is divided into three main parts:

The characterisation process of the TP consists on obtaining information on PCAs with different configurations (ISOP, ISOS…), architectures and all possible operating range (power, temperature, voltages, cooling conditions…). To minimise the number of prototypes to be built, measurements to be made and ultimately data to be collected, it is important to adopt some design of experiments techniques. The first part of this work is then the definition of a **design of experiments** (DOE). The DOE will define which PCAs should be built and which operating points should be measured in order to take the most information about the CSC and the PCAs with minimum time/effort.

As the study is fully based on measured data, the second part is the design and the creation of a **characterisation platform** and the methodology used to acquire reliable data. This platform contains the required equipment (power supply, load, fans, heaters) in order to set all PCA on the desired operating points. Special attention is given to the regulation of each testing factor and to the precision of the measurements.

The third issue is about **statistical models**, which are responsible for using the acquired data to provide prediction about PCA architectures that have not yet been experimentally verified. Several techniques of statistical modelling are available in the literature, from more traditional such as linear regression, up to more modern such as non-parametric machine learning techniques. In this third part, these techniques will be evaluated to select the most adapted to the problem at end. The program of this thesis is presented in Figure 1.22.

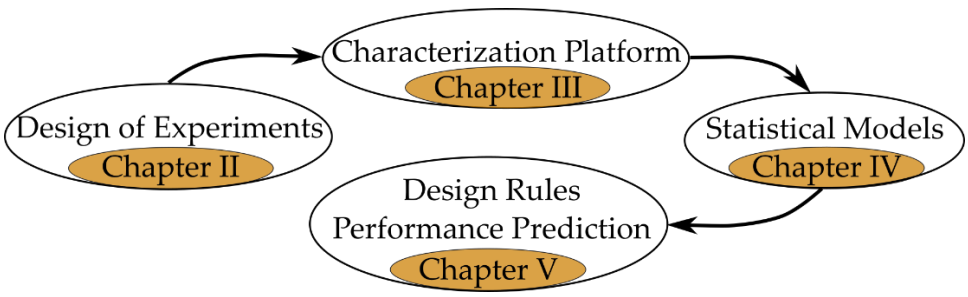

Figure 1.22 Division of the following chapters of this thesis.

In the last chapter, the two main objectives of the thesis are demonstrated with practical examples. Examples of the design rules are presented, and the models are used to show the limits of the safe operating area of the technology. In addition, some demonstration of the prediction of performance of converters is presented, illustrated by the performance of the converters listed in section 1.5.

2 Design of Experiments

This work aims to create mathematical models from a database of experimental data. This chapter will present: **which** are the variables that are going to be measured, why those variables were chosen, **how many and under which** operating points the converters will be tested and **how many** converters will be built.
At the end of this chapter, a design of experiments (DOE) will be formalized. It will serve as a guide to the experiences that will produce the data that will be used in the models.

2.1 Introduction

As stated in chapter 1, this work studies statistical models based purely on experimental data to predict the behaviour of a Power Converter Array (PCA). In order to create a precise model able to predict any PCA architecture behaviour with respect to several variables and over a wide range of operating conditions, a huge amount of experimental data is required. Chapter 1 estimated that it would be necessary up to an equivalent of 180 days of testing and up to 100k€ in investment to cover a part of all assembly possibilities for one technology of PCA. To avoid using an exhaustive approach to obtain this experimental data, this chapter will use experimental design references [59]–[61], [61] to select which experiences shall be done.
A design of experiments (DOE) is a procedure for planning experiments with the objective to maximize the amount of information obtained for a given amount of experimental effort [59]. Experimental design is used in a wide variety of fields from chemical experiments, medical research to engineering process optimisation. In this work, DOE is used to minimize the number of operating points that each PCA is tested (saving time) and to minimize the number of prototypes that are constructed (saving resources).
The experiment is defined with respect to three types of variables, namely input, output and uncontrolled variables. Input variables are divided into two groups: *Operating point variables*, that are imposed and regulated by the laboratory's equipment, and the *construction variables*, that are proper to each PCA prototype. Output variables represent the performance of the PCA and its thermal behaviour. Finally, the uncontrolled variables that may affect the output in an unforeseeable way. A panorama of the experiment variables is presented in Figure 2.1.

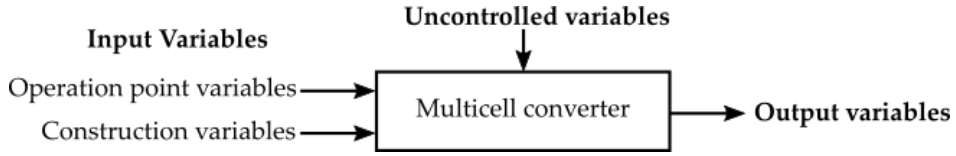

Figure 2.1 Variables studied in the experiments

The input variables are divided into two groups because there is a fundamental difference between them. Construction variables are linked to the hardware of the PCA prototypes to be tested. Any variation in these variables implies building a new PCA prototype, increasing the overall complexity and cost of the experiment. Operation point variables are more flexible: they can be modified by just setting different operating values to the bench equipment (power

sources, electronic charges, thermostats). Because of this difference, different DOE methods are used for studying each of those variables. The operation point variables are first analysed by a first run of experiments, giving a general idea of the behaviour of the output variables, facilitating the choice among the DOE methods. In contrast, the construction variables are analysed in a theoretical way and the DOE must consider the budget and the time available to perform the experiments.

2.2 Experimental variables definition

One objective of this work is to accurately predict the thermal behaviour and the performance of any PCAs architecture implemented from any standard cell family belonging to any technology platform. In this work, thermal behaviour is best expressed by the overall operating temperature of a PCA and performance are translated as efficiency.
PCA efficiency is a fundamental output variable to select the best architecture. PCA operating temperature is directly related to the feasibility itself, especially with respect to heat removal capabilities that need to be set. Both output variables are dependent on the amount of losses produced by the PCA. Both operating temperature and efficiency are linked through losses, making them both critical output variables that any designer must manipulate to create a converter that satisfy specifications.
Other output variables are also very important and meaningful, such as radiated and conducted EMI signatures, dynamic responses to disturbance and setpoint variations, reliability over time and mission profiles. However, this work focuses only on PCA efficiency and in the PCA operating temperature.

2.2.1 Input variables

As mentioned before there are two groups of input variables: operation and construction variables. Operation point variables, are directly related to the PCA operating point settings, electrical, and thermal. Construction variables are directly related to the PCA architecture and configuration. Architecture being defined in this work as the number of lines, columns and boards associated to build the PCA and configuration as the type of electrical interconnections made between cells in their inputs and outputs. Construction variables also describe the way the PCA is implemented with respect to thermal issues. The input variables that affect PCA efficiency and operating temperature are listed below

- **Output Current (Io):** As the current flowing through the PCA increases, more power is processed leading to higher switching and conduction losses, in the general case. It can be expected that the output current will therefore affect significantly the PCA efficiency and internal temperature. The conversion cell is theoretically designed for a maximum current rating, although in practice this value is dependent on the cooling capabilities that are implemented, which are mainly the ambient temperature of the heat removal fluid and the cooling variables.
- **Input Voltage (Vi):** The maximum input voltage is limited by the blocking voltage of the switches. While operating at the higher possible voltage, at a given current level,

the PCA can process more power, with a minimum impact on conduction losses, leading to higher efficiency. As a result, the input voltage is a critical input variable for a PCA performance representation.

- **Output voltage (Vo):** Like the two previous input variables, the output voltage is important to map the various operating conditions that will affect PCA efficiency. This variable can also be represented by the voltage gain (G) which is the ratio of output to input voltage (Vo/Vi) or by the voltage difference (DV) which is the difference between the input voltage and the output voltage (Vi-Vo). Depending on the topology of the conversion standard cell it is more conventional to analyse G or DV to interpret the output voltage.
- **Ambient Temperature (Ta):** Ambient temperature is the first cooling variable that impacts both PCA efficiency and operating temperature. Several components in a PCA change their characteristics with temperature, such as the magnetic elements, power switches and capacitors. In addition, the performance of the PCA must be validated on a wide range of temperature values in order to comply with existing norms.
- **Heat coefficient (h):** Thermal resistance from converter-to-ambient is the second cooling variable that impacts greatly the PCA performance and internal temperature. Like the ambient temperature, the global thermal resistance from the PCA to the ambient affects the temperature of the converter, allowing it to work at different power ratings. It provides also an important information for the PCA implementation itself. Depending on the heat removal technology, the thermal resistance input variable can be qualified by a more useful parameter. The technology used in this work, uses forced air cooled for heat removal, so the air speed is the parameter to qualify the heat removal coefficient, which represents the thermal resistance between the PCA and its ambient.

These first 5 variables are related to the operating point of a conversion cell. Although, as discussed in chapter 1, PCAs proposed in this work have other variables that influence the performance of the converter. The construction variables:

- **Architecture:** As it was described in chapter 1, the architecture represents the number of conversion cells that are arranged in lines (nline), columns (ncol) and a number of boards (nboard). The architecture adds a variable for each dimension according to the configuration. This variable represents the number of cells in width and length and the number of boards in height.
- **Configuration:** The configuration is the type of connection (series or parallel) at the input and output of the CSC. As it was described in chapter 1, each dimension (lines, columns and boards) have 1 and only 1 type of connection. The configuration definition adds 3 more variables to the experiments: 1st dimension (1D), 2nd dimension (2D) and 3rd dimension (3D).

It is hard to predict how the construction variables affect the efficiency and temperature of a PCA from a theoretical point of view. Some hypotheses can be made such as the number of lines that affects how the air flows throughout the converter, leading to higher temperature; the number of lines, columns and boards lead to more interconnections leading to higher

losses; some configurations might lead to unbalance between conversion cells. However, these remain a hypothesis that must be proven via experiments. In the case of this work, the result of the experiments will be used to train statistical models whose results will show how these input, output and uncontrolled variables affect efficiency and the PCA operating temperature.

2.2.2 Output variables

As introduced above, two output variables have been selected for their impact in terms of PCA characteristics and PCA implementation constraints: Efficiency and Operating Temperature.

- **Efficiency**: The efficiency of the PCA is the ratio of output to input power. It represents the amount of losses of a PCA for a given operation point. It can be derived from input and output power measurements or from a direct measurement of the produced thermal energy in a climatic chamber. The efficiency is very important for the PCA Automated Design For Manufacturing (ADFM) methodology proposed in this work because it defines the operating limits of a given architecture and its associated configuration. If too many cells are connected in parallel, the efficiency will be affected and the possible configuration/architecture combination will not be selected as a suitable solution by the ADFM PCA algorithm. Logically, efficiency will become one of the most significant criteria in any PCA selection.
- **Converter Temperature**: It is very important to know precisely the temperature of the PCA as it limits the converter's safe operating area. The variables that mainly affect the temperature are power, ambient temperature and airflow values. As a CSC is built from the association of several individual components, each one with its own temperature limits. A first analysis must be done in order to define which is the most sensitive component and how the temperature can be measured without impacting the cooling capabilities.

A summary of all the input and output variables which will be studied in this work is proposed in Table 2.1. It comprises 11 input variables, out of which 5 are related to the operation of the PCA and 6 are related to its construction.

Table 2.1 Input and output variables

Input variables				Output variables			
Variable name	Variable abbreviation	Unity	Type of variable	Variable name	Variable abbreviation	Unity	Type of variable
Input voltage	Vi	[V]	real	Efficiency	**η**		real
Voltage difference	DV	[V]	real	Converter temperature	Tc	[°C]	real
Output current	Io	[A]	real				
Heat coefficient	h	[m/s]	real				
Ambient temperature	Ta	[°C]	real				
Number of lines	nline		integer				
Number of columns	ncol		integer				
Number of boards	nboard		integer				
1rst dimension	1D		integer				
2rst dimension	2D		integer				
3rst dimension	3D		integer				

Since operation variables can be manipulated at no extra cost and construction variables have a severe impact on the total cost of the experiment, two different strategies will be applied to define their experiments. The two next subsections will present different approaches.

2.3 DOE for the "operation point" variables

The choice of a DOE depends on the objectives of the experiment and the number of variables to be investigated [59]. The objective of this work is to create statistical models that predict with acceptable confidence the output variables as a function of the input variables. A first step when designing the experiment is to decide in how many levels each variable is going to be tested. A level represents a set of conditions under which a certain variable is tested. The smaller the number of levels, the smaller the number of experiments to be performed for a given number of variables.

To decide how many levels a certain variable requires, a small set of experiments should be performed to identify the general response of each output variables with respect to each input

variable. Three types of responses are illustrated in Figure 1.2. A linear response is shown in Figure 2.2(a): in this case, 2 levels of input variables is enough to estimate the output variable. Figure 2.2 (b) shows an output variable that has a quadratic response: in this case 3 levels can capture the essential information of the variable. Finally, Figure 2.2(c) shows a cubic function, where a minimum of 4 levels are needed to obtain the essential information. The levels must be selected around maximum, minimum or inflexion points which will provide the statistical models with important data to identify the relationship between the input and output variables [59].

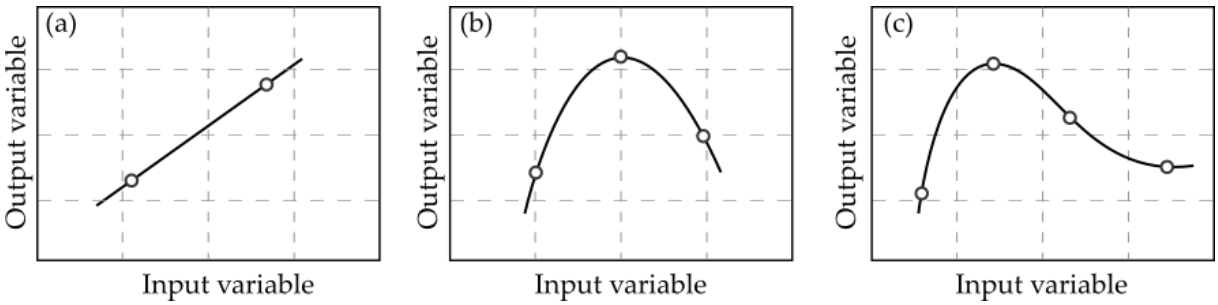

Figure 2.2 Possible responses as functions of an input variable: (a) linear response, (b) Quadratic response, (c) Cubic response. Adapted from [59].

This work adopted the one variable at a time (OVAT) method to analyse the relationship between input and output variables. The OVAT test is a common strategy for an experiment: it consists of variating one input variable while keeping all others fixed. This test, when the input variables are varied with small increment step, can provide precise information about the behaviour of the outputs, facilitating the selection of the levels in the final DOE.

Interactions among input variables cannot be estimated using OVAT since the input variables are never simultaneously changed [62]. The interactions among input variables can interfere in the shape of the output variables, changing maximum, minimum and inflexion points. For this reason, the selection of levels of the input variables will be as follows: Linear: 2 levels, Quadratic: 3 to 4, Cubic or more complex: 4 to 5.

Three identical prototypes were constructed, each one containing one conversion cell. An OVAT test was made with a very small increment step in the input variables in order to obtain a very fine response of the output variables. In addition, as the prototypes are identical, this test gives a good idea about the variance between prototypes. The three conversion cells used in this test are presented in Figure 2.3.

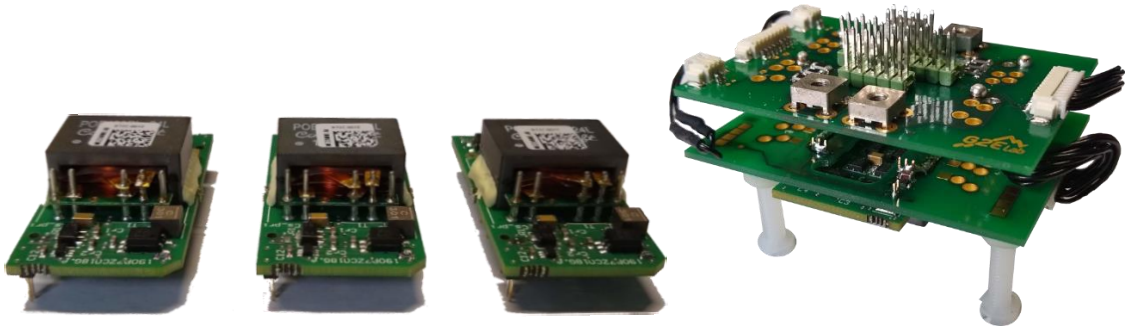

Figure 2.3 Left: The three conversion cells used in the OVAT experiment. Right: Conversion cell assembled with the auxiliary board forming the 1x1x1 converter.

Table 2.2 presents the setups of the OVAT test. Five different setups were made, each of them varying one specific variable. As a reminder, Io stands for Output Current (A), Vi means Input Voltage (V), DV means delta voltage (Vi-Vo) (V), Ta means ambient temperature (°C) and h means airflow (m/s). The variables denoted as fixed were kept constant within a tolerance level. Table 2.2 shows the variance range of each fixed variable for each test.

Table 2.2 One variable at a time test setup.

	Input Variables				
Setup	Io	Vi	DV	Ta	h
I	0.5 to 4.5 A	Fixed	Fixed	Fixed	Fixed
II	Fixed	10 to 19 V	Fixed	Fixed	Fixed
III	Fixed	Fixed	-2 to 2 V	Fixed	Fixed
IV	Fixed	Fixed	Fixed	20 to 70 °C	Fixed
V	Fixed	Fixed	Fixed	Fixed	2 to 12 m/s

Figure 2.4 presents the Setup I, where the output current was set to vary between 0.5 A and 4.5 A. The figure on the left shows the efficiency variation and the figure on the right the converter's temperature variation. The tolerance range of fixed input variables varied during the tests are shown in a box inside the charts. As the efficiency response to variations in the output current is non-linear, the current levels selected in the DOE were 0.75 A, 1.5 A, 2 A and 3.5 A. The temperature has a quadratic response and these 4 levels are enough to capture the behaviour.

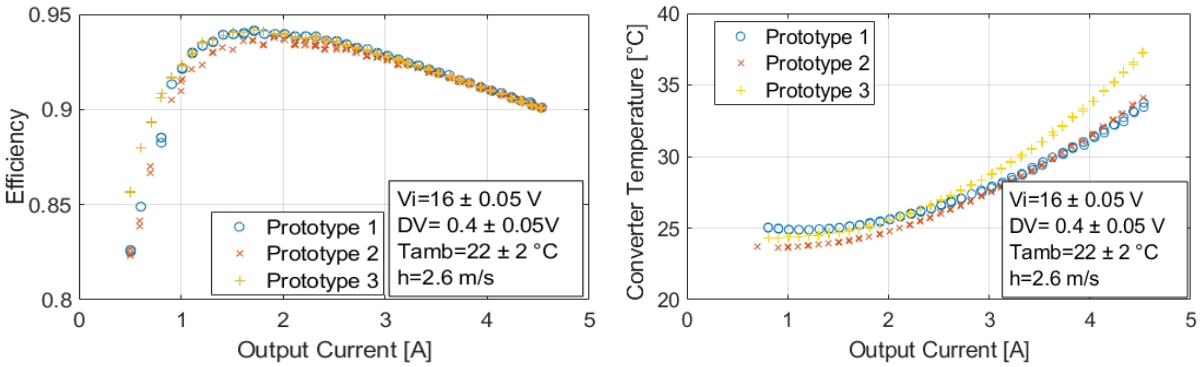

Figure 2.4 Setup I, output current (Io) versus efficiency (left figure) and versus converter temperature (right figure) for the three prototypes.

Figure 2.5 shows the Input voltage versus efficiency on the left and versus the converter's temperature on the right. The efficiency response is exponential for varying voltage inputs. The temperature presents a slight variation, however its increase is proportion to that of the voltage. It may seem strange at first, because the PCA presents higher efficiency at higher voltages, however as the PCA process more power, the losses absolute values are higher, producing more heat. To analyse this variable three levels are selected: 10 V, 14 V and 18 V.

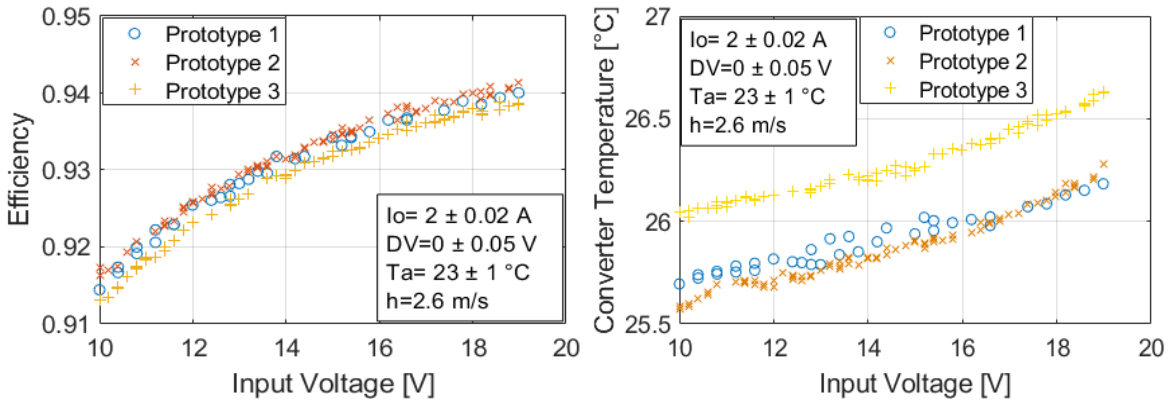

Figure 2.5 Setup II, input voltage (Vi) versus efficiency (left figure) and versus converter temperature (right figure) for the three prototypes.

The setup III is shown in Figure 2.6, where the output voltage (Vo) varied while all other variables remained fixed. In this way the behaviour of the voltage difference (Vi-Vo) could be analysed. Between 0 V and 1 V of difference, the efficiency and the temperature present a quadratic behaviour, and above 1 V and bellow 0 V it presents different linear behaviours. It was decided that 5 levels are required to test this variable: -1 V, 0 V, 0.5 V, 1V and 2 V.

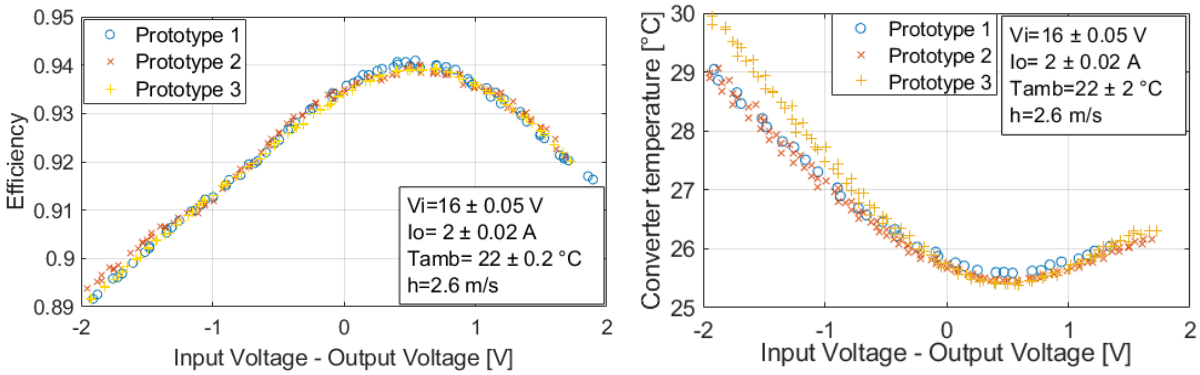

Figure 2.6 Setup III, input to output voltage difference versus efficiency (left figure) and versus converter temperature (right figure) for the three prototypes.

Figure 2.7 shows the PCA behaviour as a function of the ambient temperature. During this test the Prototype 1 failed when operating over 70 °C. For this reason, the results are presented only for prototypes 2 and 3 with a maximum temperature of 70 °C. The efficiency presented no significant variation, inside a range of 0.007 points, and no clear tendency. Due to the linear behaviour of the PCA temperature, only two ambient temperature values were selected: 30 °C and 55 °C.

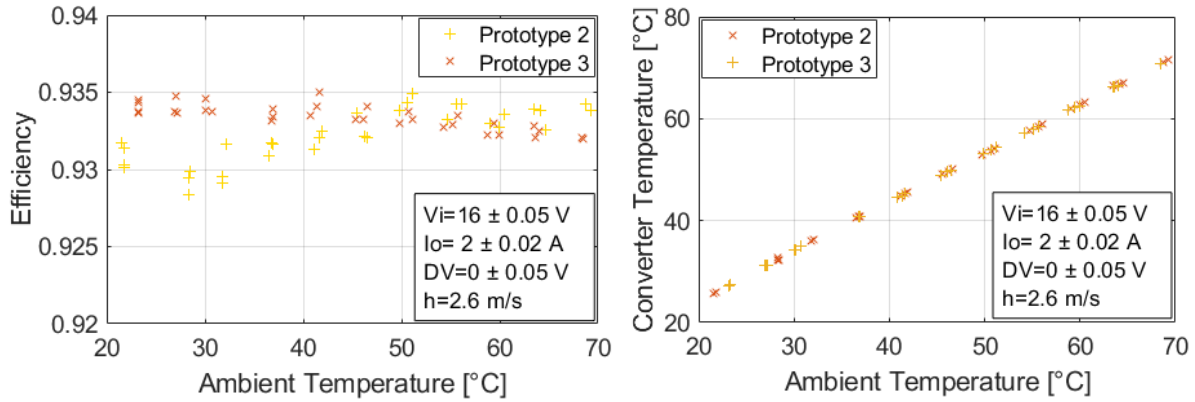

Figure 2.7 Setup IV, ambient temperature (Ta) versus efficiency (left figure) and versus converter temperature (right figure) for two prototypes.

Finally, the results of the experience with the setup V where the air speed was allowed to vary are presented in Figure 2.8. The variation of efficiency, similarly to the ambient temperature, is insignificant. However the PCA temperature has non-linear behaviour. The selected points to study this variable are: 2 m/s, 4 m/s and 8 m/s.

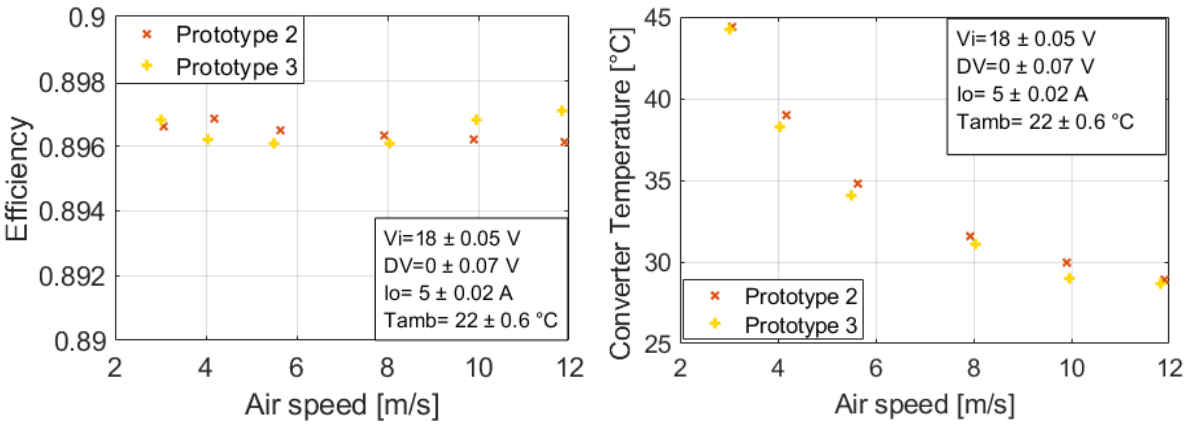

Figure 2.8 Setup V, air speed flowing in the converter (h) versus efficiency (left figure) and versus converter temperature (right figure) for the prototype no. 3.

Opposed to the OVAT, a **full factorial design** consist of testing all possible combination between the selected levels. It extracts the information about the effects of each input variable over the output variables individually and also the joint effects that two or more variables over the output variables. An overview of the levels selected with the OVAT experience are summarized in Table 2.3. Creating a full factorial design experiment with these selected points results in 360 experiments.

Table 2.3 Defined measurement points.

Operation Point				
Vi [V]	**DV [V]**	**Io [A]**	**Air [m/s]**	**Tamb [°C]**
[10; 14; 18]	[-1; 0; 0.5; 1;1.5]	[0.75; 1.5;2;3.5]	[2; 4; 8]	[30; 55]

There are several techniques to reduce the number of experiments such as Box-Behnken designs or Central Composite Designs. However, as the experiments are done in an automatic setup, the 360 experiments are considered as a feasible quantity. In addition, this big amount of data will be useful to test several statistical modelling techniques in chapter 4.

2.4 DOE for configuration and architecture

The construction variables (configuration and architecture) require building and testing several prototypes. As it is expensive to build a prototype, the DOE must wisely choose a reduced but yet meaningful number of prototypes for the experiment.

Different configurations can be performed with the same prototype just by changing the interconnection clips. In this way, the DOE in this work can be divided into: Deciding which prototypes to be constructed (architecture) and deciding which interconnections to be made (configuration).

2.4.1 Defining the architecture of the prototypes

Before choosing a set of architectures, it is necessary to know which dimension of the architecture has the greatest impact on the efficiency of a PCA. This allows for a more realistic

choice of architectures which are actually representative of real-life scenarios. In order to have a general idea of how the efficiency is impacted by the architecture, a simple theoretical model is studied first. This model is based on the idea that the resistance of the interconnection pieces, that connects lines, columns and boards, are known. So, it is possible to estimate the losses the interconnection pieces produce for a given current.

Most of the losses of the interconnection pieces come from the parallel connection of CSCs. When the CSCs are arranged in columns and in boards, the current of the parallel connected cells sums up in the interconnection pieces. However, when CSCs are connected in lines this effect does not happen. Figure 2.9 shows an example that illustrates this effect. In it each CSC was considered to operate at 5 A in their inputs and outputs.

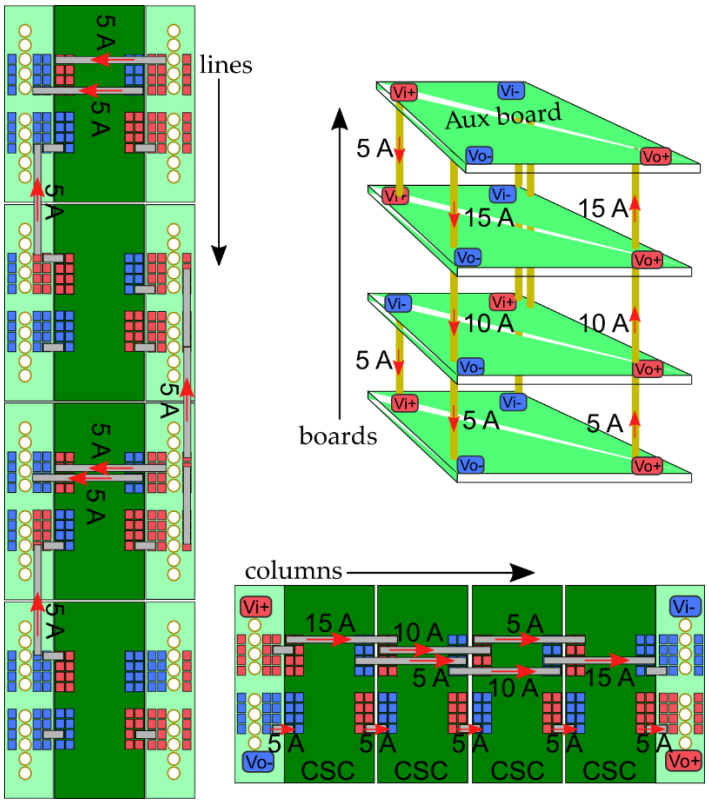

Figure 2.9 Illustrations detailing the current flow in the interconnection pieces.

Figure 2.10 shows the theoretical results for the efficiency considering the losses in line, columns and board interconnections. It was considered a current of 5 A per CSC, similarly as presented in Figure 2.9. The predictions show that the number of columns affects the most the efficiency, losing more than 0.15 point of efficiency in an arrangement of 9 CSC. The number of lines, theoretically does not imply extra losses, because more terminal cells are added and the current of different CSCs does not share the same pieces. The number of boards also affects the efficiency, but not as much as the number of columns.

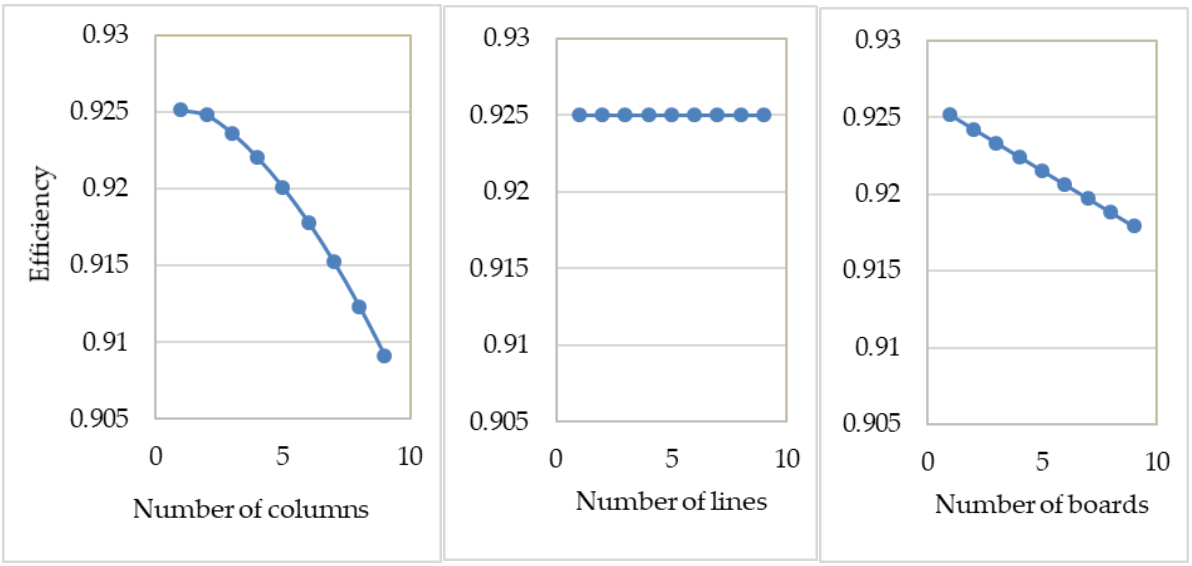

Figure 2.10 A theoretical result of how the efficiency drops with the number of columns, lines and boards.

As presented before, the architecture consists in three variables: the number of lines (nline), number of columns (ncol) and number of boards (nboard). These variables are independent and can be chosen independently. So, imagining a CSC technology that is limited to a maximum of nline=5, ncol=5 and nboard=3, there are 5*5*3=75 possible architectures. Ideally, the three variables of the architecture could be analysed independently, but the manufacturing process of boards are cheaper when done in quantity. So, the total cost of the experiment is reduced when identical boards with a given ncol and nline are constructed, and then be stacked up to form a *ncolxnlinex2* and *ncolxnlinex3*.

The number of columns is limited to 5 in this work because the maximum current supported by the interconnection clip that carries the current to the output connector is 30 A. So, 5 conversion cells in a line, connected in parallel working at 5 A each would result in 25 A, more than 80% of the component limit. However, it is certainly possible to design a PCA with 10 columns, limited at 3 A per cell, or 30 columns limited at 1 A per cell. In this work the boundaries are set at 5 lines, 5 columns and 3 boards.

To define which PCA is constructed for performing the tests, the only variables that are analysed are the number of columns and the number of lines. As both can vary from 1 to 5, there are 25 possible choices. Between the possibilities, 6 of them have more than 14 conversion cells: these possibilities are considered too expensive for the scope of the project because they would require equipping the test bench with specialized power supplies and electronic charges. Among the 19 remaining solutions, it was decided to do a sampling that contains at least 1 board containing 1, 2, 3, 4 and 5 lines and 1, 2, 3, 4 and 5 columns. The selected boards to be fabricated are presented by the orange dots in Figure 2.11.

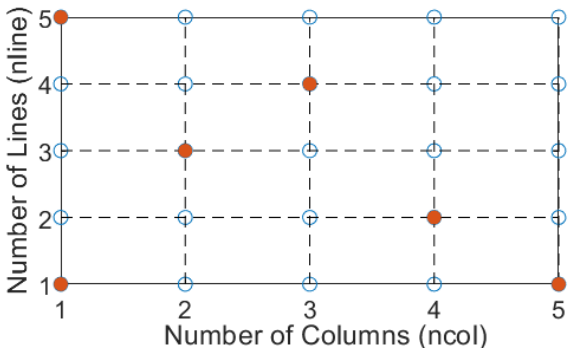

Figure 2.11 Possible architectures in a board. In orange: boards that are fabricated for the experiments in this work.

2.4.2 Defining the configuration of the prototypes

The configuration consists of 3 variables, first dimension (1D), second dimension (2D) and third dimension (3D). In this work, only ISOP and IPOS configurations are studied due to the natural voltage balance. However, IPOP and ISOS configurations are also feasible. The configuration variables are tied to the architecture, as the dimensions only exist for nline, ncol and nboard ≠ 1. This concept is clarified in Table 2.4, which presents which architectures have one, two or three dimensions.

Table 2.4 Possible combinations of architectures and configurations for the multicell converters. (j∈N/2≤j≤5) (k∈N/2≤k≤3)

Architecture			Possible configurations		
(ncol,nline,nboard)			1D	2D	3D
(1x1x1)			-	-	-
(jx1x1)	(1xjx1)	(1x1xk)	ISOP or IPOS	-	-
(jxjx1)	(j, 1, k)	(1xjxk)	ISOP or IPOS	ISOP or IPOS	-
(j, j, k)	(j, j, k)	(j, j, k)	ISOP or IPOS	ISOP or IPOS	ISOP or IPOS

As the converters are bidirectional, one hardware can perform two different conversions, e.g. the PCA (2x5x1) ISOP-IPOS have the exact same hardware as the (2x5x1) IPOS-ISOP. To give a notion of the number of different converters that can be constructed, Figure 2.12 presents each PCA as a dot in a three-dimensional plot for solutions up to 5 lines, 5 columns and 3 boards.

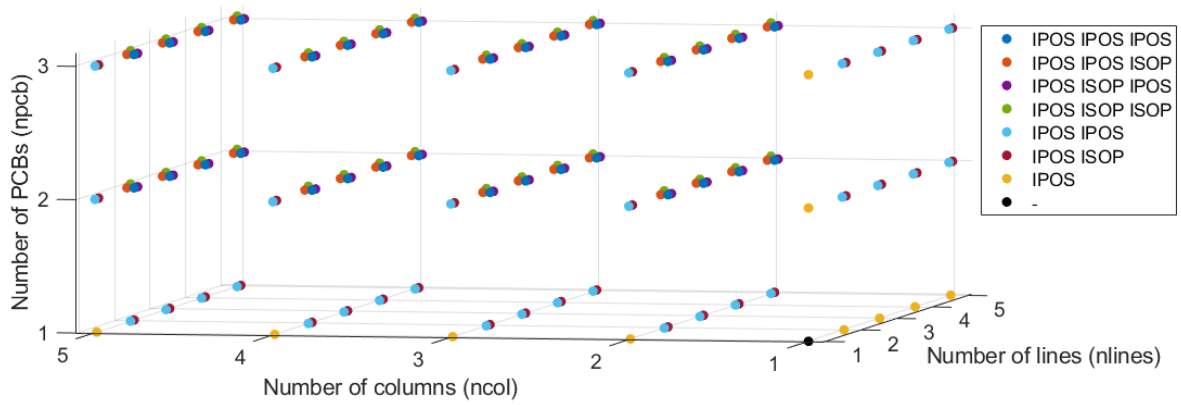

Figure 2.12 All possible hardware that can be created following the PCA methodology.

The total solutions can be calculated as

1-dimension converters:

$$\max(nlin) + \max(\text{ncol}) + \max(\text{nboard}) - 3 = 10$$

2-dimension converters:

$$2(\max(nlin) - 1)(\max(\text{ncol}) - 1) + (\max(nlin) - 1)(\max(\text{nboard}) - 1) + (\max(ncol) - 1)(\max(\text{nboard}) - 1) = 64$$

3-dimension converters:

$$4\,[(\max(nlin) - 1)(\max(\text{ncol}) - 1)\,(\max(\text{nboard}) - 1)] = 128$$

The total number of different PCAs that can be created with 5 lines, 5 columns and 3 boards are 203. Using the 6 boards that are detailed in Figure 2.11, there are 43 converters that can be built. They are listed in Table 2.5.

Table 2.5 Configurations of possible PCAs that can be constructed. Abbreviations SP for ISOP and PS for IPOS.

	Quantity of PCBs			
PCB	**1**	**2**	**3**	**Solutions**
1x1	-	PS	PS	3
1x5	**PS**	PS-PS, PS SP	PS-PS, PS SP	5
2x3	**PS-PS, PS-SP**	**PS-PS-PS**, **PS-PS-SP**, PS-SP-PS, PS-SP-SP	PS-PS-PS, PS-PS-SP, PS-SP-PS, PS-SP-SP	10
3x4	**PS-PS,** PS-SP	**PS-PS-PS**, **PS-PS-SP**, PS-SP-PS, PS-SP-SP	**PS-PS-PS**, PS-PS-SP, PS-SP-PS, PS-SP-SP	10
4x2	**PS-PS, PS-SP**	PS-PS-PS, **PS-PS-SP**, PS-SP-PS, PS-SP-SP	**PS-PS-PS**, PS-PS-SP, PS-SP-PS, PS-SP-SP	10
5x1	**PS**	PS-PS, PS SP	PS-PS, PS SP	5
				Total: 43

From the PCAs shown in Table 2.5, only 15 converters will be tested, the configuration and architecture of the selected converters are the ones presented in bold in Table 2.5.

2.5 Computing the Sample Size

To verify that the variation of an input variable does statistically represent a variation in an output variable, some replication measures might be required. A replication means repeating the same measurement on a different sample of the same population. In other words, this section aims to find the number of repeated prototypes that must be constructed to have statistical support that the conclusions are accurate.

This work follows the method presented in [63]. The reference demonstrates that from a population sample with a known standard variation (σ), it is possible to calculate the sample size (N), in order to validate (or not) a hypothesis with a given percentage of certainty (Uα, Uβ) for a variation of the output variable of (δ).

The formula to calculate the sample size is:

$$N = (U_\alpha + U_\beta)^2 \frac{\sigma^2}{\delta^2} \quad 2.1$$

The steps for understanding the variation of one variable in an output are as follows. First the standard deviation is calculated. Second an expected variation must be defined. Third a hypothesis is made. Fourth a risk level in the hypothesis be correct is chosen. The example below applies this 4-step method.

Hypothesis: The efficiency of a PCA will decrease at least of 0.003 from a 1x1x1 architecture to a 1x5x1 architecture.

From this affirmation two hypotheses are formalized. The null hypothesis (H0) states that the average value of both populations efficiency is equal (the architecture does not present a significant variation). The alternative hypothesis (Ha) declare that the efficiency in the PCA with architecture 1x5x1 will be at least 0.003 less than the PCA 1x1x1. The number 0.003 in efficiency was chosen because the accuracy of the measurement equipment cannot be more precise than it.

H_0: $\overline{\eta_{1x5x1}} = \overline{\eta_{1x1x1}}$

H_a: $\overline{\eta_{1x5x1}} + 0.003 < \overline{\eta_{1x1x1}}$

The second step is to define at which confidence risk the hypothesis will be verified. Assuming that the variation of the efficiency of replicate converters functioning of the same operating point has a normal distribution, and if it is desired a 98% chance of denying H0 and a 95% chance of accepting Ha, the values of Uα, Uβ are 2.054 and 1.64 respectively.

For estimating the standard deviation, the results from the experiment done with the three prototypes presented in section 2.3 were used. Figure 2.13 presents 36 operating points with three converters 1x1x1, at each operating point the standard deviation was calculated. The highest value of standard deviation was 0.065, while the output current was 1.3 A. In order to emulate the worst-case scenario, this will be the value used to calculate the number of prototypes required.

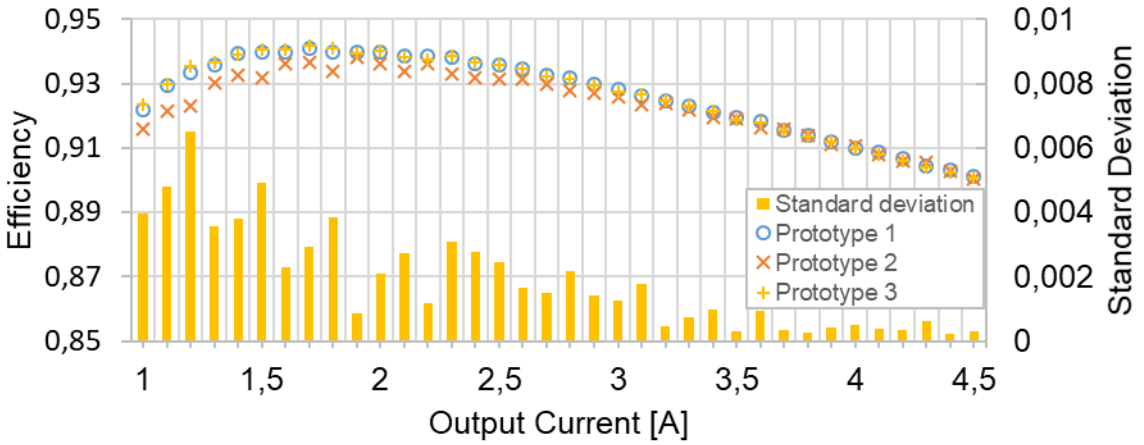

Figure 2.13 Standard deviation between the three prototypes for each operating point while variating the output current.

After substituting the values in the formula presented in equation 2.1, the resulting value of number of samples required was 1.77, which means that by realizing measurements on two prototypes it is possible to identify a variation in the efficiency of 0.003 with a 98% confidence level.

Based on this theory, all experiments in this work are done with 2 identical converters. The standard deviation is recalculated for each set of experiment, and if values above 0.0065 are obtained, a third identical PCA is built and measured. The variation can be caused by a malfunctioning cell, a PCA assembly error or other technical problems.

2.6 Conclusion - Checklist for the experiments

The conclusion of this chapter is made in the form of a checklist [60]. This checklist summarizes the complete experimental procedure and is a simple way to find information about the experiments.

(a) The main objectives of the experiment.

The main objective of the experiments is to gather enough data to feed a statistical model that is capable of predicting the efficiency and the temperature of any PCA (up to 5 lines, 5 columns and 3 boards) presented in Figure 2.12 and inside the operating point ranges presented in Table 2.3.

A secondary objective is that the model can make prediction for converters up to 7 lines, 7 columns and 4 boards, and in a wider range of operating. This extrapolated range will be tested at the end of this work.

(b) Sources of variation

(I) Treatment variables and their levels

A total of eleven variables were presented in section 2.2. Their levels are presented in Table 2.3 and in Figure 2.11.

(II) Experimental CSCs

The experimental PCAs were built using the CSCs designed following the g2elab-Maatel Technology Platform 2018. They were designed during the year of 2018, fabricated from December 2018 to January 2019. To complete the implementation of the converters used in the experiments, specific motherboards and auxiliary boards were fabricated for each architecture and configuration tested.

(III) Noise variables

The main noise variables identified were:

Component tolerances: Although the conversion cells are identical and fabricated following the same procedure, every cell is prone to the variance of components values. E.g. the leakage inductor of the transformer, the ac link capacitor, the input and output capacitor, all have a tolerance of 10% in their value.

(c) The rule by which the experimental units to the treatments

A detailed experimental procedure is presented in chapter 3, precisely describing the time delay between each measurement and the total time for each set of experiment.

(d) The measurements to be made, the procedure of the experiment, and the anticipated difficulties.

The electrical measurements to be made are the input and output voltages and currents. The current values are obtained by voltage measurements across shunt resistors. The input and output voltage and the voltage measured across the shunt resistors are made with a power analyser. The precision of the efficiency measurements is expected to be less than 0,5 %. More details about the errors of the equipment are presented in chapter 3.

The thermal measurements of the PCA are done by one (or more, depending on the PCA architecture) pt100 sensor. The ambient temperature measurement is made by 6 pt100 sensors placed inside the wind tunnel. The expected error is less than 3 °C. More details on errors are presented in chapter 3.

(e) Pilot experiment

The results presented from Figure 2.4 to Figure 2.8 came from the first pilot experiment. To achieve these results several small experiments were made before, with few prototype failures, allowing the boundaries and the maximum electrical steps to be defined.

(f) The modelling techniques

Different modelling techniques will be tested and compared. They are presented in chapter 4.

(g) Outline of the analysis

Due to the big amount of data that will be collected and the different techniques of modelling, it is expected that at least one modelling technique can be able to predict the whole space of solutions within an error of 0.5 % on efficiency and 5 °C accuracy on temperature.

(h) Number of observations

Following the levels presented in Table 2.3, there are 360 selected operating points. As there are 15 converters to be tested, it results in 5400 measurements, replicated 2 times, totalizing 10800 measures.

(i) Design Review

The experiments are done in an automated test bench and it is estimated that it is possible to perform 360 measures per day. The whole experiment design can be made in 30 working days' time. This is considerable feasible for the scope of the project.

3 Characterisation Platform

This work aims to create mathematical models from a database of experimental data. This chapter will present: **the construction of a testbench** capable of regulating the five operating point variables and compatible with the construction variables defined in the DOE , **details on the equipment** used to realize the tests, their precision and limitations and **present the testing conditions** setup in order to produce the data**.**

3.1 Introduction

The operating point of a multicell converter is set by five input variables: input voltage, output voltage, output current, ambient temperature and a heat removal parameter. To perform the experiences and to acquire good quality data, each input variables must be controlled and measured over a wide range of operation. In addition, due to the huge amount of measurements stipulated by the DOE, the tests must be done in an automatic and reproducible way for all sensitive parameters.

The DOE stipulated the input variable values that must be applied to the converter. The experimental equipment must then have a satisfactory precision to control the input variable values accordingly to the DOE. The measurement of each variable is performed by specific measurement equipment. This chapter describes both the selection of the equipment to apply the good testing conditions to the converter and the equipment to carry on the measurements.

The operating point variables are divided into two types: the electrical variables and the thermal variables. Electrical variables require a power source, a load (active or passive) and control over the driving signals of the converter.

The thermal variables require a specific test device to perform the tests for a specific technology converter. Chapter 1 presented the concept of Technology Platform (TP), which contain a family of standard cells sharing the same technological basis. Different TPs may have different cooling system, different range of dimensions, different housing. So, every TP has different requirements for testing the thermal variables. This chapter first defines which are the requirements of a test bench for a generic TP, and later it presents the construction of a specific test bench adapted the TP used in this work.

As the experiments are made on PCAs without addressing the housing itself neither fans, the cooling factors are free to be tested and related directly to the electric variables. In this way, it is possible to characterise the converter in the same way heatsink manufacturers characterise their products: relating the rise in the temperature of the converter to the processed power (°C/W) with the cooling factor (air/water speed flow).

In the last part of the chapter, a measurement protocol is formalized, detailing the order in which the measurements are made, taking into account the dynamics of the converter and the dynamics of the test bench. In addition, it is presented some analysis of measurement precision, to identify the error in every measurements. Finally, it is stipulated the format that the output data and the creation of a database to be exploited by the modelling techniques in the next chapter.

3.2 Experimental Setup Design

The DOE introduced and specified in chapter 2 defined the values at which the input variable must be tested. It is presented in Figure 3.1 the operating point variables and the output variables, together with the equipment responsible for driving and collecting the measurements of each variable. The data acquired by the measurement equipment is the data that is used to fit the prediction models. The equipment can be divided into two groups: the control equipment (responsible for setting the desired value to each variable) and the measurement equipment (responsible for measuring each input and output variable).

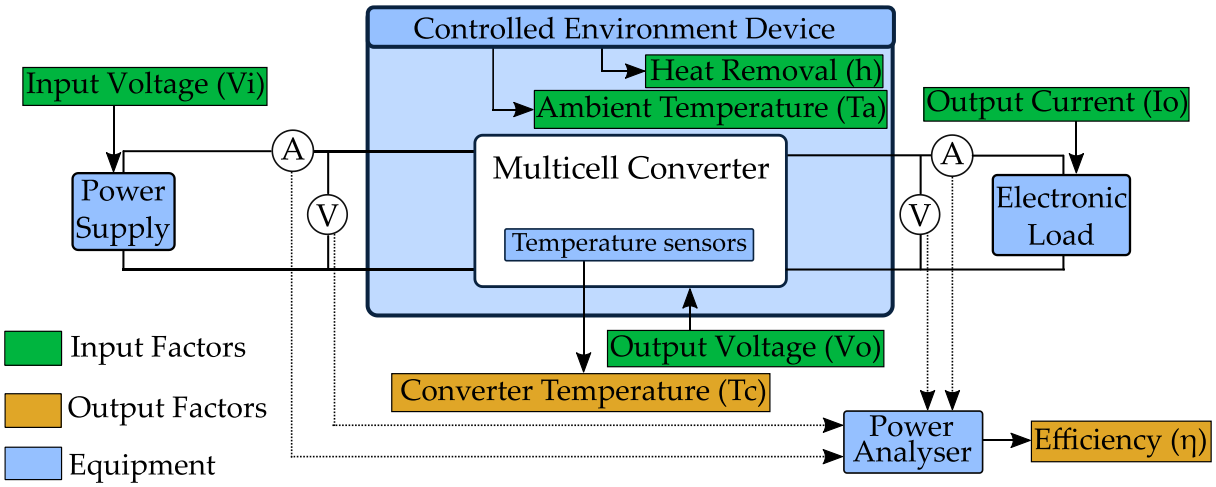

Figure 3.1 Panorama of the input and output variables and the equipment used to control and measure each variable of a generic Technology Platform.

The specifications of the control equipment are guided by the operating point variables of the DOE. For example, the power supply is chosen according to the maximum input voltage and input current defined by DOE. Similarly, the measurement equipment must be adapted to the values of the variables that are being measured.

As the experiments with PCA deals with many different converter characteristics, it might be required to change some equipment from one test to another. PCAs with several CSCs with its inputs connected in series present high input voltages. In contrast, PCAs with several CSCs inputs connected in parallel lead to low input voltage and high input current. Hardly a power supply is able to fit the requirements of extreme both tests. Similarly, it is very unlikely that the same measurement device covers a wide range of values for each variable to be measured. This chapter presents the choice of each equipment used in the experiments, always trying to find a simple solution without losing precision.

The thermal variables are dependent on the converter cooling technique. Three solutions are mainly used in power electronics: natural air-cooling, forced air-cooling and water-cooling. Regardless of the implemented cooling technology, the experiments require that the ambient conditions, the air or water temperature, must be controlled. Depending on the thermal

technology, additional variables such as fluid speed or air-cooling channelling must be considered. In this work, since the power converter technology considered is PCB based, only natural and forced air-cooling solution are studied.

In forced air-cooling, a fan is used to push the coolant air into the heatsink. When a physical heatsink is available, a datasheet can be used to set up the fan characteristics according to the amount of heat to remove due to the power losses. When the power converter is not designed with heatsinks, the components are cooled down with the air flowing over and around them. The PCB is an important contributor to the cooling process, but it is very difficult to estimate how efficient the heat removal is. An important aspect of this work is the use of experiments, rather than simulations, to estimate this and other thermal behaviours which would be otherwise very difficult to model.

As presented in figure 3.1, the experiments require a controlled environment bench. The test bench has the following characteristics:

- It must be capable of physically fitting all converters that are defined in the DOE
- It must be able to control the ambient temperature
- It must control the heat removal variable (for air cooled converters, it should control the air speed, for water cooled converters, the speed/pressure of the liquid)
- It must emulate a generic housing for the converters, able to produce abacus for effective housing and cooling designs.

To guide the design and the construction of this test bench, first, it is made an analysis of the dimensions of the PCA converters that are going to be tested. Second, the range and the technique to control the ambient temperature is defined. Third, the cooling technology, if it is air-cooled, water cooled or natural convection impact significantly on the bench development. Lastly, the housing of the converter must be analysed so that the tests are made in conditions as close as possible to the real implementation.

In order to use the controlled environment bench correctly, it is required to run a first set of experiments to identify the dynamics of the equipment. To do so, it is performed a test applying a temperature reference step, and it is observed the time response for the measure reach the reference, the temperature stability and the steady state ripple. This first run is also useful to optimise the total time needed to carry on the full DOE, as the time for the thermal variables to reach steady state represents a huge amount of time over the whole experiment.

As it was stated before, the experiments must be made automated as much as possible to save operator time and to maximise reproducible test conditions. To do so, all equipment need to be connected and driven by a central management unit (CMU). The CMU is responsible for the communication with each equipment, for giving the information of the operation point the converter must be at, the time to wait for the converter to reach steady state, and then, perform all measurements at the same time.

3.3 Wind Tunnel Construction Details

As the TP tested in this work is a PCB based, air cooled technology, the controlled environment device must be able to control the speed of the airflow applied to the device under test (DUT). The heat removal variable is changed by acting on the air speed at the converter level. The controlled environment device in the particular case of this technology is a wind tunnel.
In order to control the ambient temperature, it is proposed to place heating resistors at the entrance of the wind tunnel, just after the fans. In this way, it is possible to control the temperature of the air that flows through the converter, to estimate converter behaviour with respect to ambient temperature. Figure 3.2 presents the schematic of the wind tunnel, detailing the equipment used to implement the control of the thermal conditions.

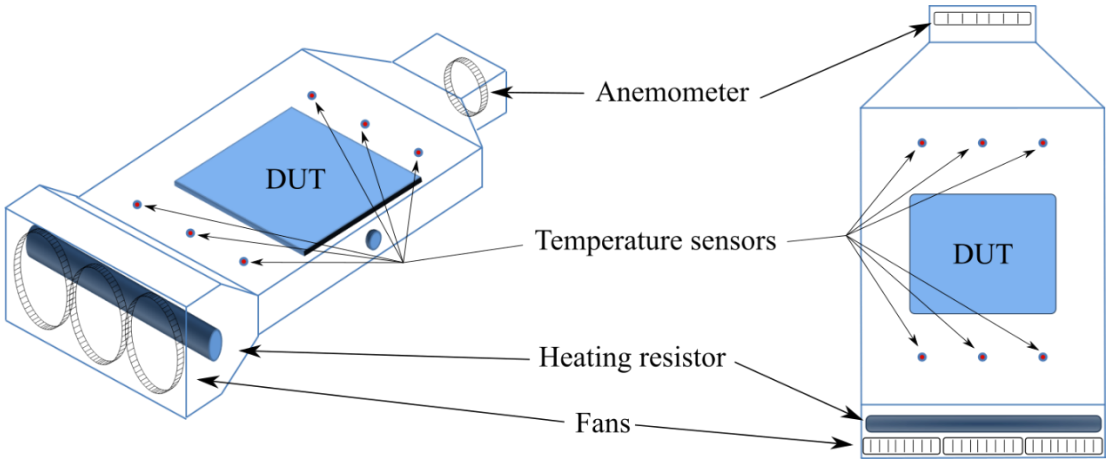

Figure 3.2 Construction plan of the wind tunnel.

To define the dimensions of the wind tunnel, first are analysed the size of the converters that are going to be tested. The experiments performed in this work are made with converters designed with the TP G2ELab Maatel presented in chapter 1. The geometrical details of the conversion standard cells (CSC) and terminal standard-cells (TSC) and the resulting dimensions of the PCAs are presented in Table 3.1. To clarify how the formulas are defined, Figure 3.3 presents the construction details of how the CSCs and TSCs are arranged in the PCA converter.

Table 3.1 Geometrical details of the CSC and TSC used in the experiments
G2ELab-Maatel 2019 Technology Platform

Conversion Standard Cell	25 x 47 x 15 mm
Terminal Standard Cell – left	18 x 47 x 15 mm
Terminal Standard Cell - right	17 x 47 x 15 mm
Converter Width	$CSC_{(width)}$ x ncol + $TSCleft_{(width)}$ + $TSCright_{(width)}$
Converter Length	$CSC_{(length)}$ x nline
Converter height	$CSC_{(height)}$ x nboard + $Auxiliary\ board_{(height)}$

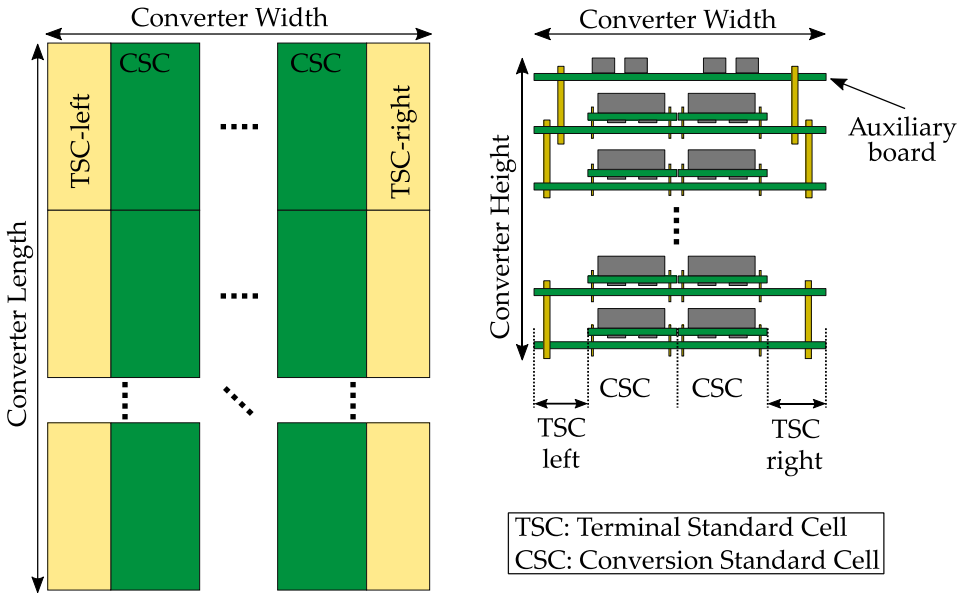

Figure 3.3 Geometrical details of the multicell converters.

The standard cell height is defined, including mounting and cooling constraints. As a result, a nominal standard cell height is defined but it can be modified with respect to critical design and optimisation issues. By applying the dimension formulas given in Table 3.1 on Table 3.2 it is possible to find the dimensions of the largest converters that are defined in the DOE. The largest length is the converter with 5 lines, the largest width is the converter with 5 columns and the highest converter is the one with 3 boards. Table 3.2 summarise the largest dimensions, which serve as a guideline for the construction of the wind tunnel.

Table 3.2 Maximum dimensions of the multicell converters tested in this work

Dimensions	Converter with maximum dimensions in the DOE (nline x ncol x nboard)	Values
Maximum converter width	5x1x1	160 mm
Maximum converter length	1x5x1	235 mm
Maximum converter height	4x2x3	80 mm

Given the maximum dimension of the converters, the inner dimensions of the cavity of the wind tunnel were defined as width: 230 mm, length: 300 mm height: 100 mm. The complete device was divided into six pieces and built with a 3D printer. Figure 3.4a) presents the top and side views of the constructed wind tunnel.

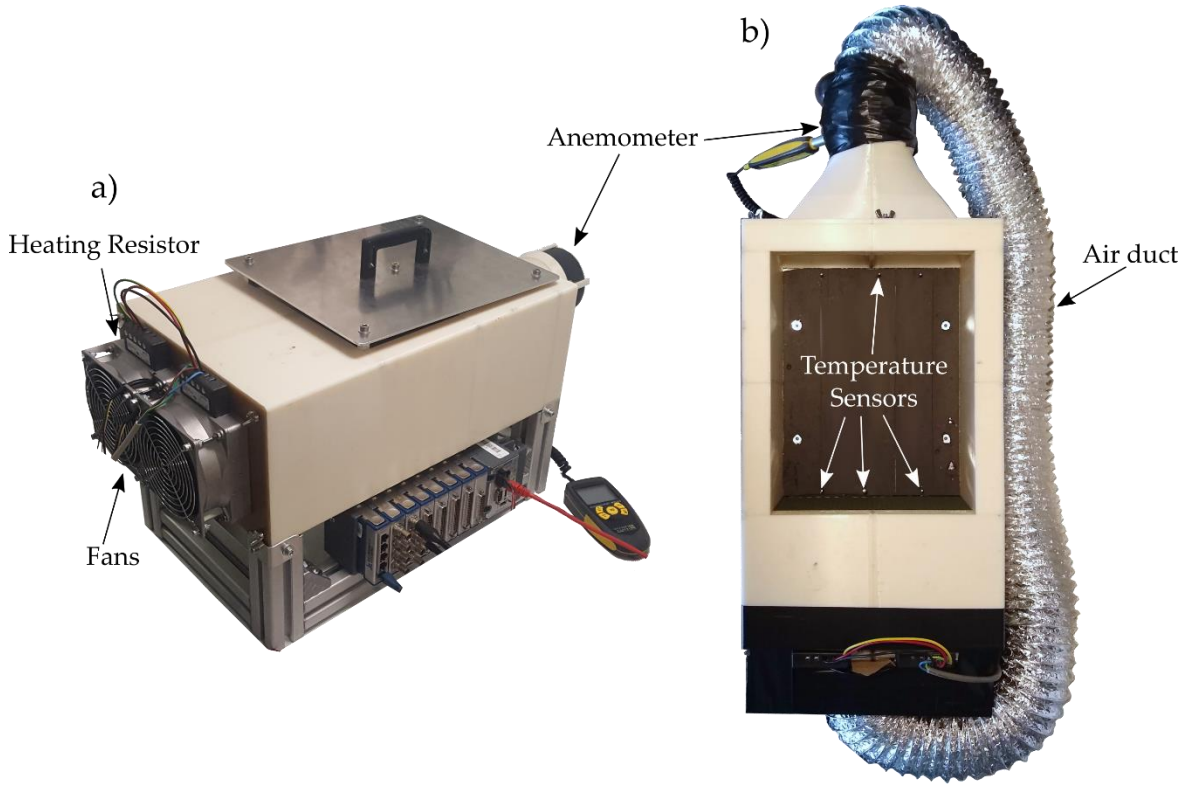

Figure 3.4 a) Wind tunnel. b) Top view of the wind tunnel with the air duct in place to recycle the warm air.

The temperature controller is an Eurotherm 2408. It can drive the heating resistor in on or off state. A PID controller is internally available in its system; it is possible to set the values of proportional, integral and derivative gains. The PID controller gains were regulated following a Ziegler-Nichols method. Figure 3.5 presents the elements used in the ambient temperature regulation.

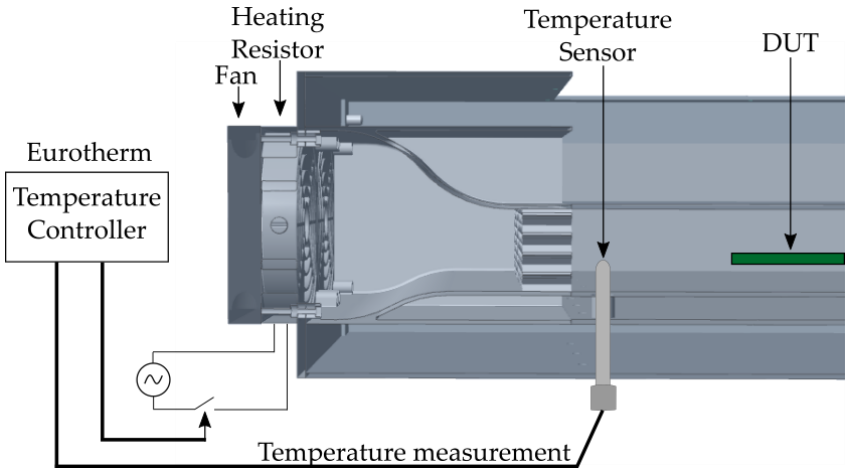

Figure 3.5 Key components responsible for the ambient temperature control.

The heating resistors and fans used are two units of Stego HVL 031. The two heaters together can develop up to 800 W of power. In order to achieve high temperatures, it was proposed to recycle the warm air by an air duct. The air duct is highlighted in Figure 3.4b). With this setup, the inner temperature of the wind tunnel can reach up to 70 °C at a wind speed of 5 m/s, a satisfactory value to perform all desired tests.

In order to perform accurate measurements of temperature, a calibration procedure is realized. A converter under test with 8 temperature sensors is placed inside the wind tunnel. Measurements are made with the converter temperature sensors and with 4 temperature sensors inside the wind tunnel. The converter is not supplied. A step in reference of the ambient temperature is made from ambient temperature to 55 °C. Figure 3.6a) presents the temperature measurements from all sensors as function of the time during the reference step without any calibration. At time t=0 s and at t=5000 s, all sensors are in steady state it is considered that they measure the same temperature. Based on the measurement at these two temperatures, it is derived a linear function for each temperature sensor as presented in Figure 3.6b).

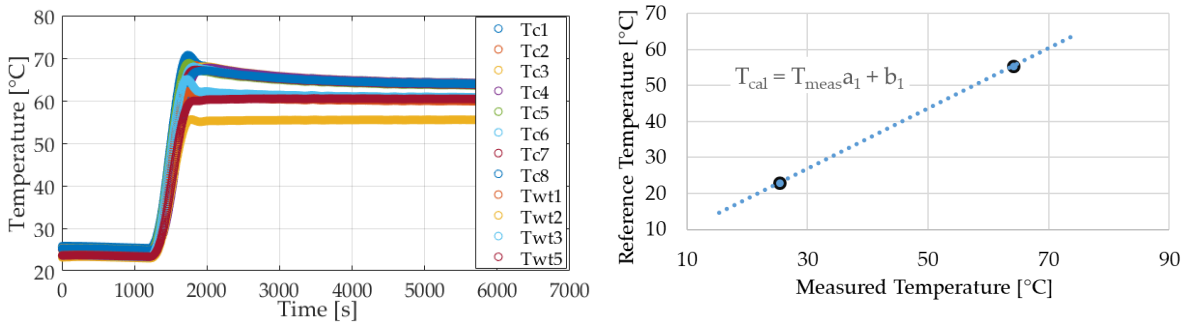

Figure 3.6 Left: Moving average value of each temperature sensor in a reference step from ambient temperature to 55 °C without calibration. Tc1 to Tc8: Converter temperature sensors. Twt1 to Twt5: Wind tunnel temperature sensors. Right: Calibration method applied to each sensor.

A linear function was derived for each sensor. The results of the same experiment presented in figure 1.6 is presented in figure 1.7, but now each sensor is calibrated with their respective linear function. To validate that the linear function is capable of performing accurate results in the calibration process, a second test was made with a temperature reference of 40 °C. The results of this test are presented on the graphic on the left of figure 3.7. The maximum temperature difference from the reference sensor was of 0.4 °C. This result is satisfactory for the range of temperature that the wind tunnel will be working with.

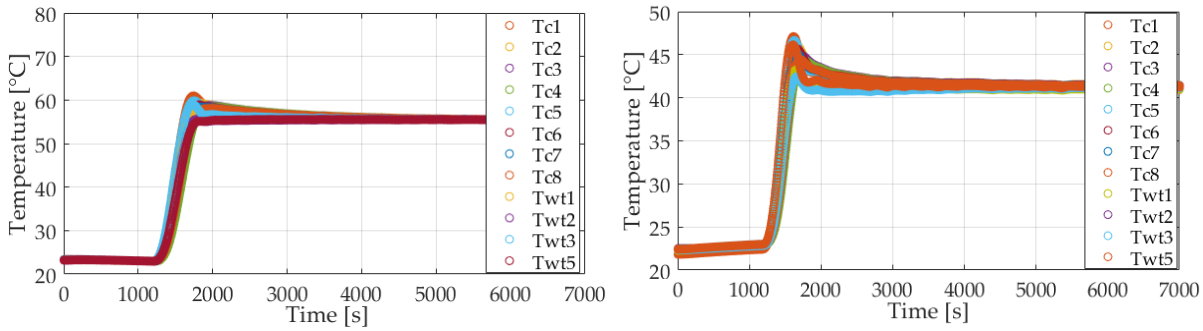

Figure 3.7 Moving average value of each temperature sensor after the calibration for two temperature reference: 55 and 40 °C

For every different converter that is tested this procedure to calibrate the temperature sensors are performed.

3.4 Experimental Setup Implementation

This section presents all the equipment used to control each input variable and all the equipment used to perform the measurements. The subsections are divided into electrical variables and thermal variables.

3.4.1 Electrical Variables

3.4.1.1 Input Voltage

The input voltage applied to the PCA under test is set and regulated by a TDK Lambda power supply: it can supply up to 100 V under 33 A. It is connected through a serial port to the CMU. For the tests that required input currents above 33 A, a second identical power supply was added in parallel and driven in slave mode.

The measurement of the input voltage is made by a Fluke NORMA 5000 Power analyser. Its precision is ±0.03 % of the measured value.

$$\sigma_{Vi\%} = 0.03\% \qquad 3.1$$

3.4.1.2 Output Voltage

As the PCA converters are composed of several DABs Conversion Standard Cells, operating with a phase-shift modulation scheme, the output voltage is defined by equation 3.2 [64].

$$V_o = \frac{V_i R_0}{2 f_{sw} L_{AC}} \alpha(1-\alpha) \qquad 3.2$$

For fixed values of input voltage (V_i), output load (R_o), switching frequency (f_{sw}) and ac-link inductor (L_{AC}), it is possible to set the output voltage (V_o) by varying the phase-shift angle (α). To do so, the CMU communicates directly with the converter's digital controller via a serial connection. To set the output voltage, the system follows the logic block diagram presented in figure 3.7. The output voltage is measured by the Norma 5000, the data is transferred to the CMU, which derives and transfers a new phase shift value to the power converter digital controller.

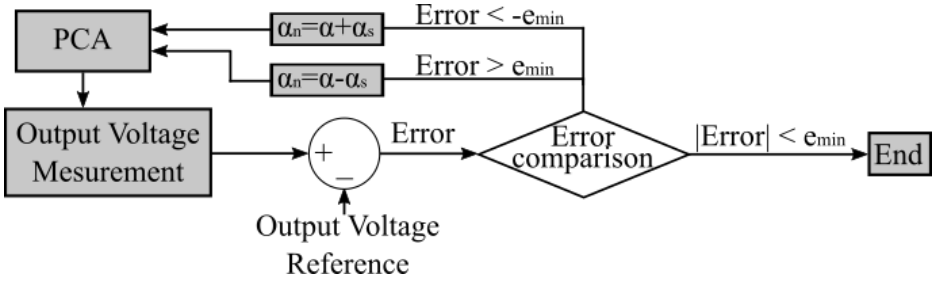

Figure 3.8 Output voltage control loop.

Where:

e_{min}: is the minimal acceptable error, it varies for each converter, following the rule:

$e_{min} = n°\ of\ converters\ with\ the\ outputs\ connected\ in\ series\ x\ 0.05\ V$

α: degrees of phase shift in °

α_s: one step of degree variation. Set to 0.03° due to the precision of the DSP.

Using this system, it is possible to set the output voltage of the converter without risking regulation interactions with supply and active load that are both regulated. As the voltage measurement is made via the power analyser, each loop iteration happens with a 500 ms delay, resulting in a very slow dynamic response. This ease to decouple regulations but it introduces extra time to set up each new electrical operating condition.

The accuracy of the output voltage measurement is

$$\sigma_{Vo\%} = 0.03\% \qquad 3.3$$

3.4.1.3 Output Current

The output current is defined by the output load. The load used in this work is an electronic load H&H model ZS5680. Working in resistance mode, it has a precision of ±1 % ±0.3 % of current range.

The measurement of the output current is made via a shunt resistor up to 33 A. The choice of a shunt resistor to measure the current was made because it is hard to find ammeter capable of measuring high current. The value of the voltage across the shunt resistor is all the time measured by the Norma 5000 power analyser. Using the same measurement device over the entire DOE range is good if a precise characterisation of the various shunt is made.

The precision of the output current measure is

$$\sigma_{I\%} = \frac{\sigma_{Vsh}}{V_{sh}} + \frac{\sigma_{Rsh}}{R_{sh}} = 0.03 + 0.1 = 0.13\% \quad 3.4$$

3.4.1.4 Efficiency

The efficiency of the converter is calculated with the electrical measurements presented in equation 3.2

$$\eta = \frac{V_o I_o}{V_i I_i} \quad 3.5$$

In addition, of the three electrical variables described before, to calculate the efficiency it is required to measure the input current.
The input current is measured also with a shunt resistor together with a Norma 3024677. Its voltage is measured with the same Norma 5000 with the same accuracy as the output current. The accuracy of the input and output power and the efficiency measurement can be calculated as:

$$\sigma_{P\%} = \frac{\sigma_V}{V} + \frac{\sigma_I}{I} = 0.03 + 0.13 = 0.16\% \quad 3.6$$

$$\sigma_{\eta\%} = \frac{\sigma_{Pi}}{P_i} + \frac{\sigma_{Po}}{P_o} = 0.16 + 0.16 = 0.32\% \quad 3.7$$

3.4.2 Thermal Variables

3.4.2.1 Ambient Temperature

As mentioned before, in order to set and regulate the ambient temperature the fan blows air in a heating resistor. A temperature sensor placed inside the wind tunnel sends the temperature data to a temperature controller device. The temperature sensor is a PT100, which presents a precision of +/-1 °C. Although, due to the inertia of the heating resistor, the ambient temperature oscillates around 3 °C of the temperature set point. This issue is presented in the next section with the dynamics of the wind tunnel.

3.4.2.2 Forced air cooling

The converters tested in the experiments are industrialised and ready to be used. The last parts missing are the housing and the fan. To reproduce the operation of the converter as close as possible to a real application case, the wind tunnel has to emulate as close as possible the housing effect. In order to do this, the converters have to be confined in a precise shape, so the air can flow similarly to a real case application. As presented in Figure 3.9, a set of pieces of polystyrene were created to emulate the housing effect for each converter shape.

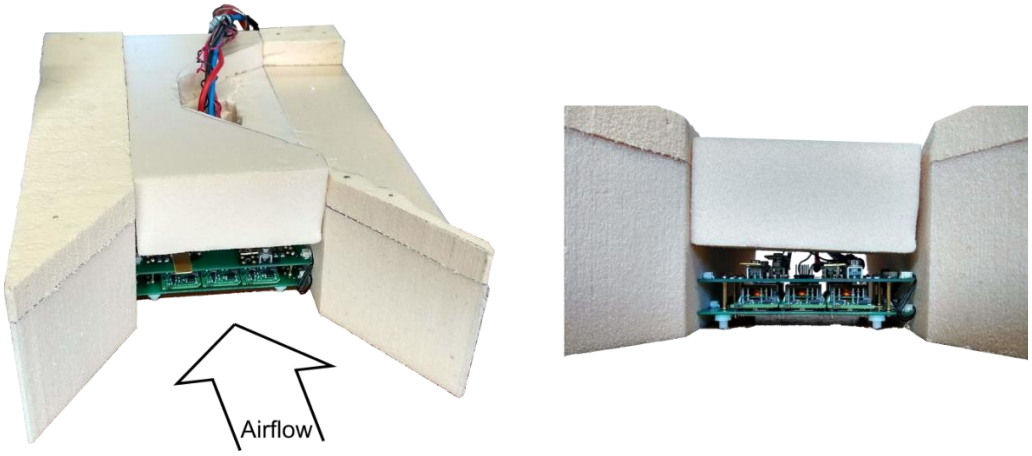

Figure 3.9 Pieces of polystyrene created to channel the airflow inside the wind tunnel. Different set of pieces are used for converters with different architectures.

It is required one set of polystyrene pieces for each different architecture in terms of numbers of columns and numbers of boards.

The wind speed is measured by an anemometer that is fixed at the end of the wind tunnel. As can be seen in Figure 3.10, the wind speed measured by the anemometer is performed in a surface area that is different from the surface area where the Converter under test (CUT) is placed. The wind speed flowing through the converter is estimated by relating the area of the anemometer with the area where the converter is placed as presented in equation 3.8.

$$V_{CUT} = \frac{V_{an} S_{an}}{S_{CUT}} \qquad 3.8$$

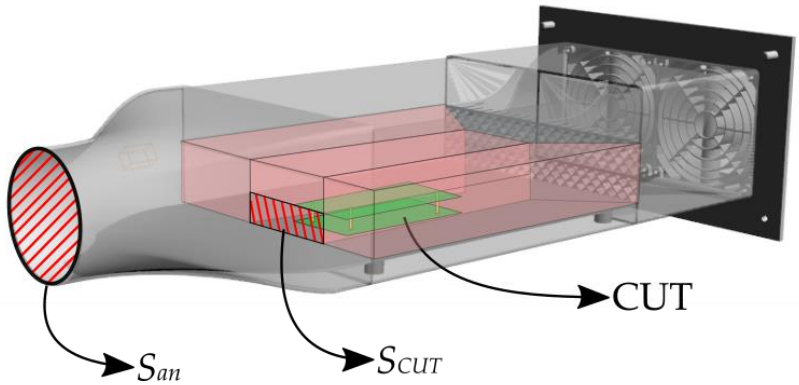

Figure 3.10 View of the wind tunnel with transparency. The surface of the anemometer (S_{an}) and the surface of the converter under test (S_{CUT}) are highlighted.

The anemometer selected is a Chauvin Arnoux C.A.1224 with a precision of 3% ± 0.1 m/s.

3.4.2.3 Converter Temperature

It is desired to measure at least one value of the temperature of the converter for each operating point. Although each multicell converter has several conversion cells, each conversion cell has several components and each one might have a different temperature. To decide which component or converter device temperature should be observed, a first study was carried out.

The first study consisted of capturing thermal images of the converter and comparing the warmest components to the position where a thermal sensor could be placed without affecting the airflow. A 6 CSC converter was placed inside the wind tunnel as presented in Figure 3.11a). Pieces of polystyrene were made especially for this test with a hole in the top piece in a way that the IR camera could focus the converter. The complete setup is presented in Figure 3.11b).

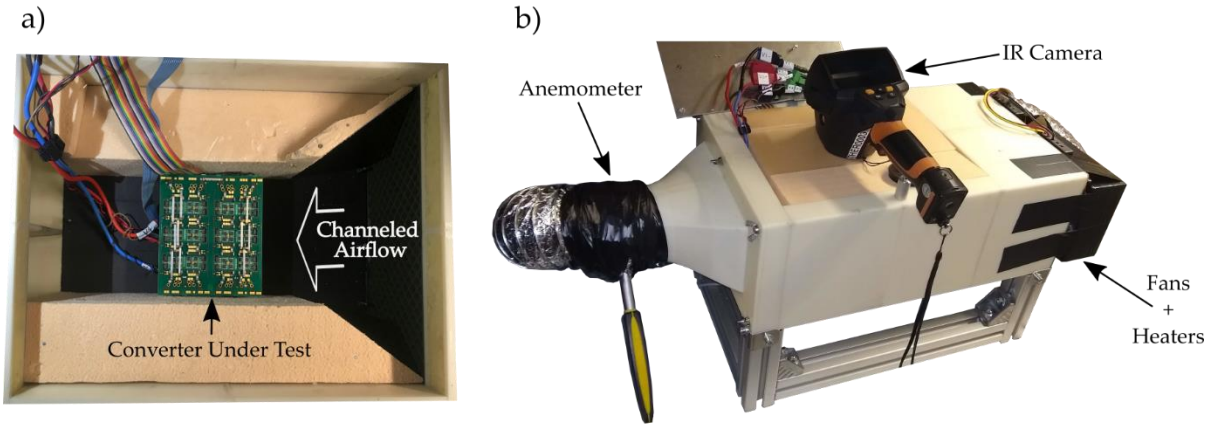

Figure 3.11 a) Wind tunnel interior with a 2x3x1 PCA. b) Wind tunnel setup during the IR camera test.

The converter had two thermal sensors installed, one on each line, attached to the lateral side of the transformer to ease its implementation. Details of the installation of the sensors are presented in Figure 3.12. The photo on the left presents a 1x5x1 converter and the placement of the sensor at the edge of the CSC vector/line. The photo on the right shows the position of the sensor that is made with thermal paste and a thermal tape, this time on a single CSC converter prototype.

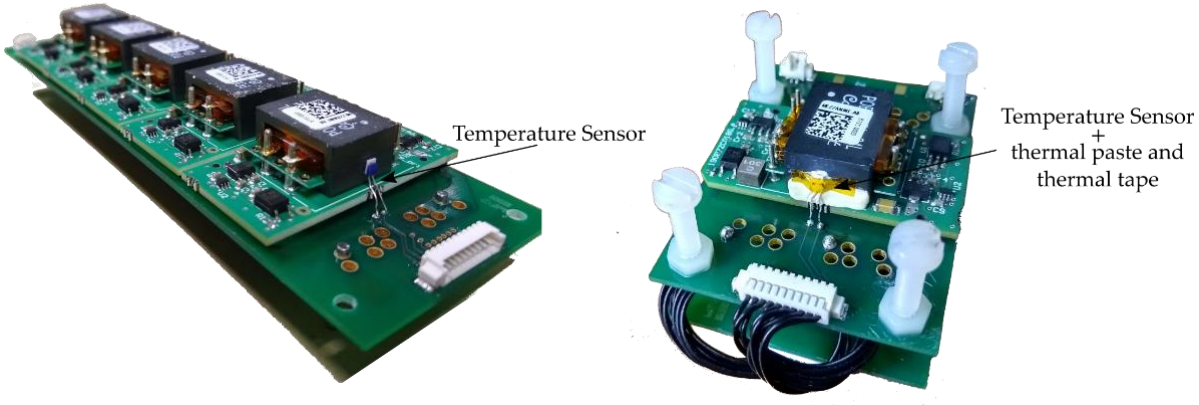

Figure 3.12 Left: temperature sensor placed in a 1x5x1 PCA. Right: temperature sensor fixed in a 1x1x1 PCA.

Figure 3.13 shows two thermal photos of a multicell converter 2x3x1 operating with output currents of 1.5 A and 5 A, (Vi=16 V, DV=0 V, Ta=25 °C and h=1.4 m/s), their efficiencies were 93.6% and 90.1% respectively. The test was made with airflow direction from right to left (as presented in figure 1.12). The IR pictures were made with a Testo 875i IR-camera, which has

an accuracy of ±2 °C with the settings when the photos were taken. The photos give the information of the warmest temperature in the top side of the converter.

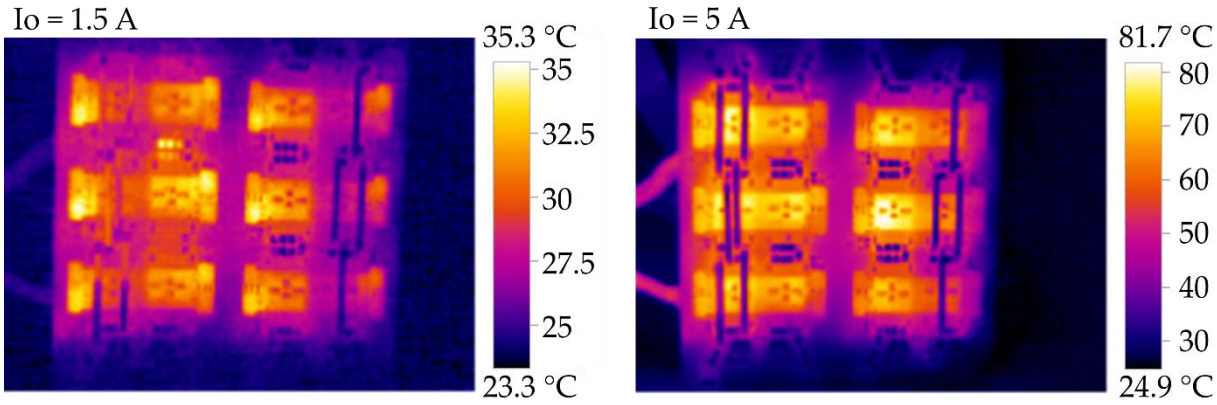

Figure 3.13 Thermal images of a 2x3x1 converter with different output current. Left: Io=1.5 A and efficiency of 93.6%, 0.1W/cm², Right: Io=5 A; η=90.1%; 0.5W/cm². The other input variables were kept constant during the test: Vi=16 V, DV=0 V, Ta=25 °C and h=1.4 m/s.

A set of experiments were made in order to find a mathematical relation of the measured temperature with the PT100 sensor at the transformer, with the MOSFET temperature obtained by the IR photo. Figure 3.14 (left) presents the temperature of the transformer (measured with the PT100 sensor) and the temperature of the MOSFET (measured with the IR-camera) versus the output current. The test was made two times, once with air speed of 2 m/s (dashed lines) and a second time with an air speed of 1.4 m/s (continuous lines). It can be seen that for both air speeds the temperature difference between the MOSFET and the one of the sensor at the transformer increases as the current increases. In order to estimate the MOSFET temperature by the measurements made by the sensors at the transformer, Figure 3.14 (right) presents the transformer temperature versus the MOSFET temperature. This primary result presents a linear relation and the air speed does not present a significant impact on this relationship.

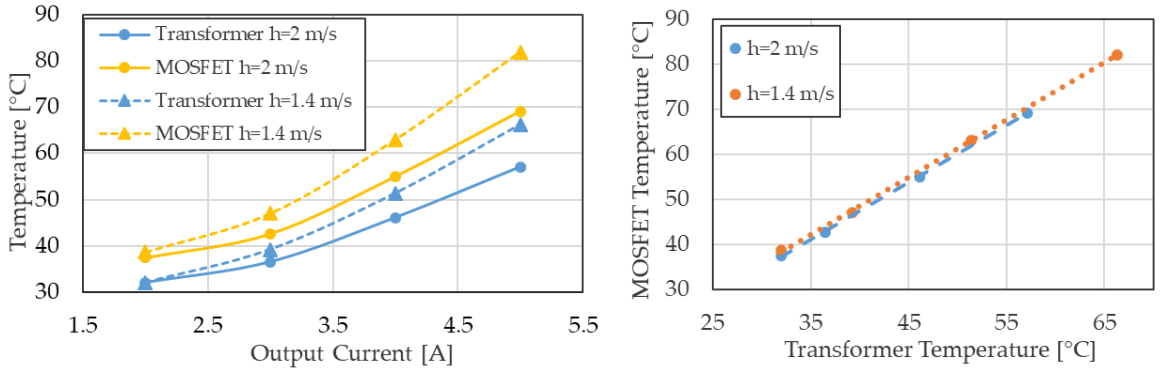

Figure 3.14 Comparison between the temperature measured at the transformer and the temperature at the MOSFETs. Left: Output current versus Temperature. Right: Transformer temperature versus MOSFET temperature

The direction of the airflow certainly impacts the consideration made with respect to this method to measure the converter temperature. This method is employed only to the measurements when the airflow flows perpendicular to the placement of the sensor.

3.5 Measurement Procedure

The measurement procedure follows the actions presented in the diagram displayed in fig 3.15. An operating point is transferred from the CMU to all control equipment. A pre-defined time duration is waited for the PCA to reach steady state, and finally all variables are measured simultaneously. This sequence is presented in Figure 3.15.

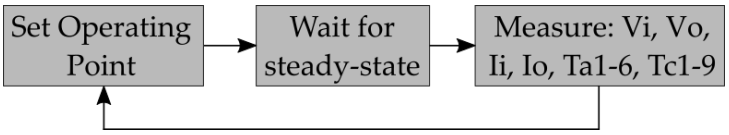

Figure 3.15 Measurement procedure diagram.

In order to perform the automatic set of measurements, it is important to define the time between each measurement based on the time the converter and the wind tunnel take to reach steady state conditions. To analyse the dynamics of each input and output variables, two stages of the experiment were analysed: first, the time each input variable takes to reach its steady state once the input reference is changed; second, the time it takes for all the output variables to reach steady state.

Input variables are divided into two groups, as presented in the last section: electrical variables and thermal variables. The former ones have very fast dynamic compared to the later. Input voltage and output current can change in a matter of milliseconds. The output voltage can take up to a few seconds due to the control algorithm implemented voluntarily to slow down that variable dynamic as mentioned in the previous section. The electrical variables will not be studied in details because their dynamics are irrelevant in comparison with the ambient temperature variable and the converter temperature variable. The ambient temperature dynamic response to a step reference is depicted in Figure 3.16. It presents a reference step from 30 °C to 50 °C. From this image, three important observations are made:

- The 20 °C step took approximately 515 s to reach steady state.
- The ambient temperature can oscillate up to 3.0 °C.
- The oscillation period is 220 s.

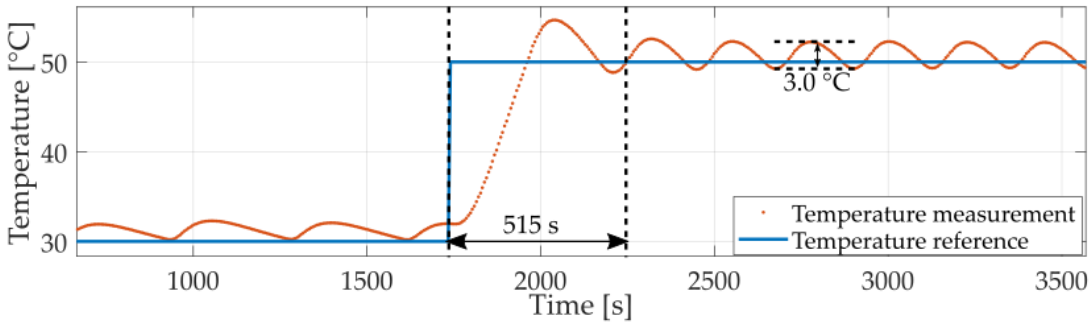

Figure 3.16 Dynamic behaviour of the ambient temperature in the wind tunnel.

The time duration for the temperature to reach steady state determines the minimum time required before performing a measurement after a temperature reference step. The temperature oscillation is caused by the temperature controller control strategy (on-off). This behaviour is not considered as a major concern as the analysed data is going to be the rise of temperature in the converter (Converter's temperature – Ambient temperature).

Another important parameter to be analysed is the thermal resistance of the converter. It is possible to analyse this parameter by varying the amount of losses in the converter by varying an electrical variable and measuring its temperature. In this way, it is possible to know the dynamics witch the converter temperature behaves. It was performed a test with a 1 CSC converter where it was applied a current step (from 2 A to 3.5 A).Figure 3.17 presents the data obtained in this test. It is plotted the output current, the converter temperature and a moving average of the temperature in order to define the moment the temperature reaches its steady state.

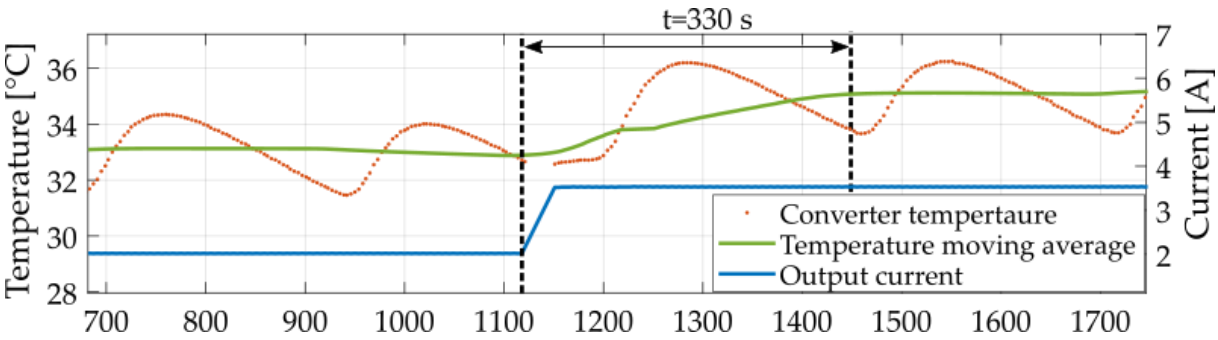

Figure 3.17 Test results in a 1x1x1 converter in order to analyse the converter thermal resistance. A current step (from 2 A to 3.5 A) is applied. The moving average considered one period of measurements.

As the ambient temperature inside the wind tunnel takes more time to reach the steady state, it is decided that the ambient temperature is the last variable to be changed. In this way, the plan of the DOE is made to minimize the number of times this variable is changed. The airspeed has the second slowest dynamics, so it is the 4th parameter to be changed, followed by the 3 electrical variables that presents the same dynamics. The final mission profile that defines in which order the input variables are changed is presented in Figure 3.18.

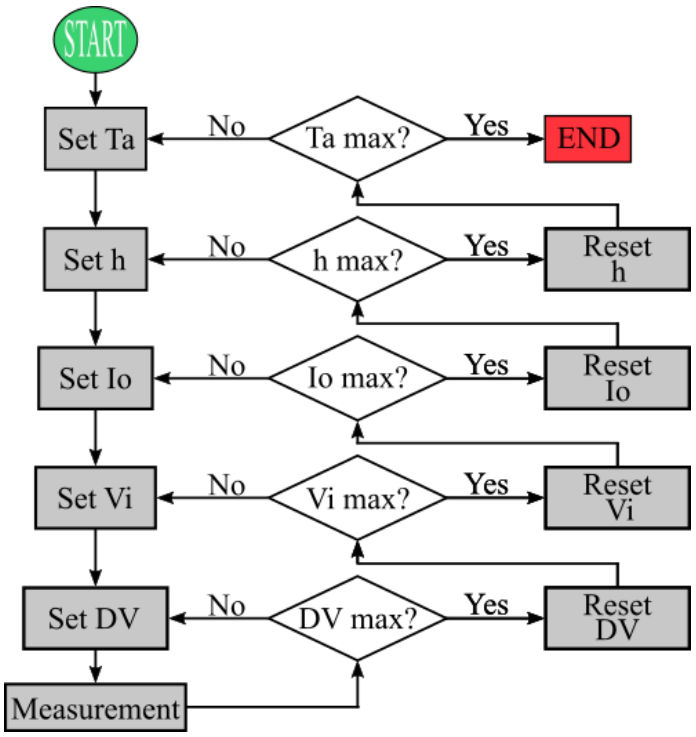

Figure 3.18 Algorithm of the experience.

The mission profile of the whole experience is presented in Figure 3.19. It can be seen that the variables of low dynamics are changed less often than the variables with faster dynamics. Following this order to set the input variables values the experience duration is as short as possible. In order to insure the safe operation of the converters, the mission profile avoids doing steps from maximum values to minimum values.

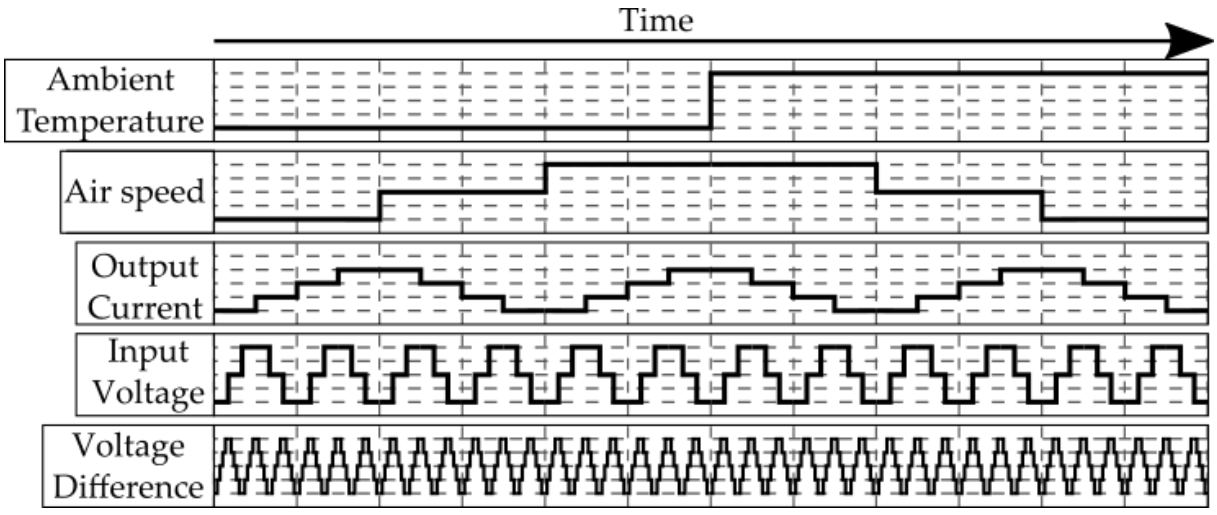

Figure 3.19 Mission profile of a complete experience.

3.6 Measurement Protocol

In order to establish a reproducible experiment procedure, all actions presented before are formalized in a protocol. The protocol defines the human actions that take part in the experiment, and the automatic actions, programmed in the system.

The whole experiment campaign consists in measuring several converters in several operation points. As the central computer drives all input variable equipment, it is possible to automate a round of experiments with one converter. However, several actions must be done by the test operator to complete the whole experiment campaign, such as:

- Place the converter inside the wind tunnel
- Adapt the inside of the controlled environment device to fit the housing of the PCA
- Relate the anemometer section area with the converter section area
- Perform the calibration of the converter temperature sensors
- Generate a mission profile sheet with the adequate input variable values to the PCA under test
- Verify if it is required to change a control equipment (power supply, load)
- Verify if is required to change a measurement equipment,
- Load the experiment file in the central computer
- Start the experiment

The experiment file defines the order of the measurements. It contains all the values that are transferred to each control equipment and the time delay between each measurement. It is unique to each PCA.

Once the test is finished, a .csv file is generated containing all measurements for each operating point. Finally, there is one file for each PCA. It is added in each line of each measurement the value of the construction variables of the converter, the architecture: (nline, ncol, nboard) and the configuration (1D, 2D and 3D) with the dummy variables: 0 for no connection, 1 for IPOS, 2 for ISOP. In this way, the files are ready for the statistical modelling process.

All the prototypes tested in this work are presented in Figure 3.20.

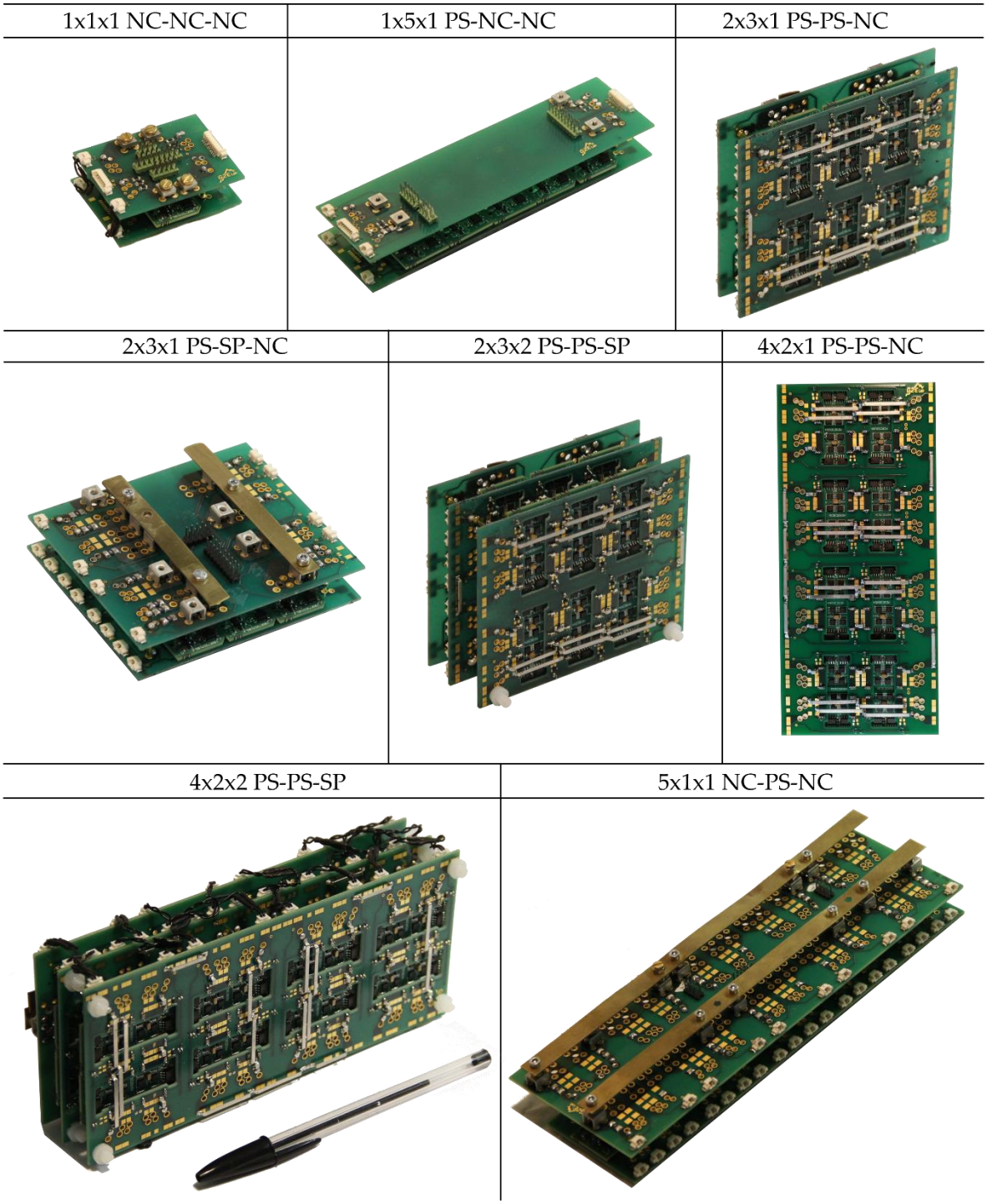

Figure 3.20 PCAs tested in this thesis.

4 Statistical Modelling

Chapter objectives:

- Present different statistical modelling techniques
- Apply different modelling techniques to the dataset obtained from the experiments
- Compare the quality of the results of the predictions for each modelling technique

4.1 Introduction

With the objective of creating statistical models to predict the behaviour of Power Converters Arrays, this thesis was divided into three parts. The first was the selection of the experiments, presented in chapter 2 (DOE). The second was the construction of the test bench and its related experiments presented in chapter 3. The third and final pillar of this work focuses on the interpretation of the data or, in other words, how to obtain the most of information about the behaviour of the converters out of the data available.

This chapter starts presenting details about the vocabulary and some basic concepts of statistical modelling. Supported by the basic concepts, the chapter introduces different modelling methods and discusses which methods are best suited to make predictions about the output variables in the context of power converter arrays.

All experimental data is displayed in a dedicated section for the dataset, which is later used to derive two models to perform predictions. One model is responsible for predicting the efficiency of PCAs and the other to predict the temperature of PCAs. The model accuracies are tested with extra experimental data, and finally, predictions are made to test interpolation and extrapolation capabilities.

4.2 Some statistical modelling basic definitions

Statistical modelling is the process through which mathematical *models* use *measurements* from real-world *variables*, bundled in *datasets*, to *learn* from the data and make *predictions* with a certain degree of error. To better understand these models, this section will introduce a series of fundamental concepts related to statistical modelling: variables, datasets, measurements, models, predictions, supervised and unsupervised learning, variance and bias error, and quality of prediction [65].

Variables in statistical modelling can be characterised as quantitative or qualitative. Quantitative variables can be measured and expressed by numbers and could be compared to an "analogue" or "continuous" variable. Qualitative variables express classes or categories and could be compared to "digital" or "discrete" variables.

Datasets regroup all variables, which were obtained in the *measurement* process through some sensor in real-world experiments. Datasets may contain important information about a system or a process, but they may also contain varying degrees of error inherent to the nature of their measurement methodology.

Models in statistical modelling are a mathematical equation that can convert input data into an output prediction. The process of choosing which "weight" to give to which variable is called "fitting". Thus, a model is "fit" to a certain Dataset. Fitting makes a model capable of finding information hidden within the dataset, but it also makes it vulnerable to its hidden errors.
Predictions are the outputs of a model for new input data that were not present in the dataset. As the name implies, a prediction is not an exact answer, and it will always be prone to error. Thus, a prediction estimates the response within a certain interval of confidence.
Learning is done either in Supervised and Unsupervised conditions. Supervised learning consists of problems that have an output data (response) for each input data. Its objective is to find the model that best predict the response given the input data. Unsupervised learning, in contrast, does not have a defined output. Its objective is to find the natural structure of the sample data. This work focuses on Supervised Learning.
Supervised Learning is done either by *Classification* or by *Regression.* Classification focuses on predicting discrete output variables, such as "yes/no" or "good/bad", based on the input data. A regression problem focuses on predicting continuous output variables, such as efficiency or temperature, based on input data. This work will focus on regressions.
The error has two elements: bias error and variance error. Bias error comes from the choice of the mathematical function that describes the output. For example, using a linear function to predict a response that has a cubic behaviour leads to high bias error. The variance error comes from the fact that a model has been fit too close to the data, taking its error for real information. To illustrate the principle of bias and variance error, Figure 4.1a) presents a dataset (red dots) that was created based on the green curve. The green curve represents the ideal function that the model should find. Figure 4.1b) presents a linear regression, which, in this case, has a high bias error, but zero variance error. Figure 4.1c) presents a very flexible model, that has zero bias error, although, it has a high variance error.

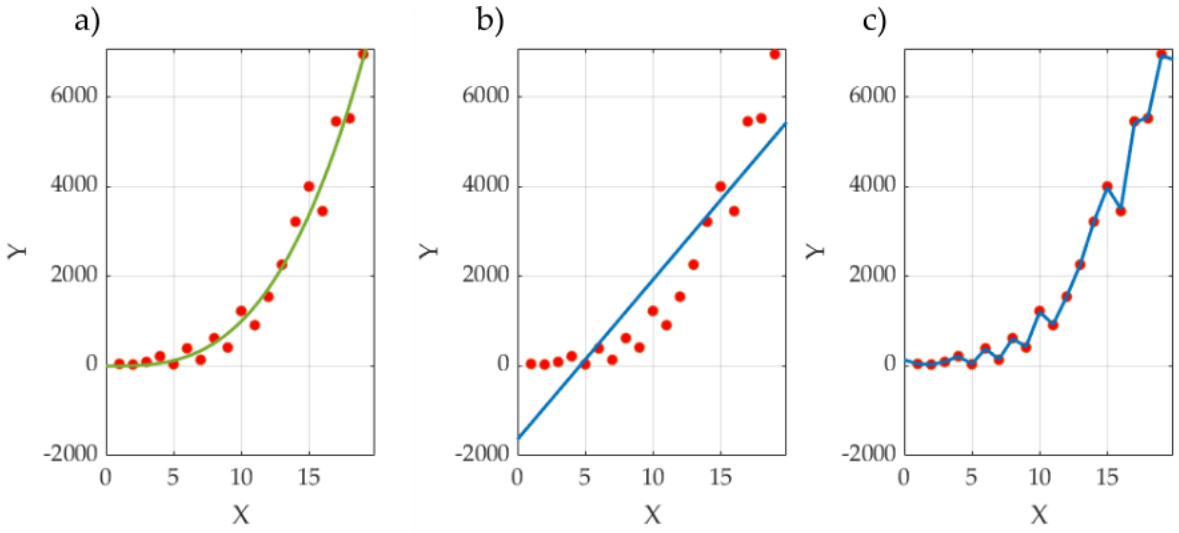

Figure 4.1 Examples of bias error and variance error. a) Red dots: sample data, green curve: function used to generate the sample data. b) Blue curve: linear regression fit, an example of fit with high bias error. c) Blue curve: Linear interpolation, example of fit with high variance error.

Statistical modelling can be perceived as a trade-off between variance error and bias error [65]. Different modelling techniques result in different compromises between these two types of errors. It is up to the analyst to understand the dataset and to choose the most adequate solution.

The quality of the model can be estimated by splitting the dataset into training data and testing data. The training data is used to fit the model, while the testing data is used to test its accuracy. This work uses the k-fold cross validation (KFCV) approach, which randomly divides the dataset into k groups of equal size. One of the groups is used as a validating set while the other k-1 groups are used to fit the model. This process is repeated k times, each time the validation is made with a different group. The parameters which yield the smallest error are used as the final model.

This chapter aims to build/fit a regression model through supervised learning, expressing the connexion between all 11 input variables to predict the efficiency and the operating temperature of a given PCA. As several modelling techniques can be used in regression problems, the next section proposes their cross-comparison, selects the most suitable one and applies it to the data obtained from the previous chapters.

4.3 Regression technique selection

Regression models can be broadly classified as parametric and non-parametric models. Parametric based models follow a two-step model-based approach [65]. First, an assumption about the shape of the function is made (e.g., the converter efficiency has a relation with the output current squared and a linear relation with the input voltage), as shown in equation 4.1.

$$\eta(I_o, V_i) = a_1 I_o^2 + a_2 V_i \qquad 4.1$$

The second step consists in estimating the parameters $a_1$and a_2 with a training data in the fit (or training) process. Different methods can be used to find the best values of the parameters; the most common is the least-squares approach [65].

Non-parametric methods, in contrast, do not make assumptions about the shape of the model function. These methods use the entire Dataset as input to an abstract equation/algorithm that will try to predict as precisely as possible the output data without being too rough or wiggly [65]. Since no pre-assumption is made about the shape of the function, non-parametric models can fit a wide variety of shapes, making the modelling process much simpler, especially in problems with many dimensions. However, non-parametric models require more data than parametric models to achieve good predictions, and they cannot be used to interpret the result. Parametric and non-parametric methods are at the core of the trade-off between bias and variance error. While parametric methods tend to have low variance error, they may present high bias errors, if the shape of the function was chosen poorly. On the other hand, non-parametric methods can be very flexible and achieve a low bias error to overfit the training data, resulting in a high variance error. Moreover, beyond error issues, there is also the issue of interpretability.

Interpretability is the capacity of the model to give a human user some sort of knowledge regarding the system or process from which the data is taken through the weights given to the variables of the dataset after its fit. Thus, variables that are given a large weight can be perceived as being more critical to the system or as having a more significant impact on its performance.

Parametric models are inherently more interpretable than their non-parametric counterparts. Since interpretability requires a model to have some sort of explicit equation, parametric models can show not only the type of equation that yields a better prediction but also the contribution of each variable through its weights. Non-parametric models do not have one explicit equation that expresses the output as a function of the inputs. For this reason, they are much less interpretable than parametric models.

In the case of this work, if a linear model is fitted using the 11 variables as input and the efficiency as output as presented in eq. 4.2, its parameters a_6 and a_7 could provide information about how the number of lines or the number of columns affect the efficiency of PCAs in general. However, this linear model would probably yield predictions with a high bias error, because, as it was presented in chapter 2, most of the variables have a non-linear effect on the efficiency.

$$\begin{aligned}\eta\left(V_i, I_o, DV, T_{amb}, A_{speed}, n_{line}, n_{col}, n_{board}, 1D, 2D, 3D\right) \\ = a_1 V_i + a_2 I_o + a_3 DV + a_4 T_{amb} + a_5 A_{speed} + a_6 n_{line} \\ + a_7 n_{col} + a_8 n_{board} + a_9 1D + a_{10} 2D + a_{11} 3D\end{aligned} \quad 4.2$$

In order to illustrate the advantages and drawbacks of different modelling methods, three examples are presented; a parametric model, a non-parametric model, named k-nearest neighbours regression and the Gaussian process model. These three methods use a dataset of 22 points where I_0 is the input variable, and the efficiency is the predicted output. In order to evaluate the variance error of the model, a second fit is made with each technique with a dataset containing 36% of the original dataset (8 points).

The parametric model is shown in Figure 4.2. This model was fitted by the equation 4.3, which gives the shape of the model. For a one-dimension problem, as this example, it can be easy to choose the equation that represents the shape of the response accurately. Then the parameters a_1,a_2,a_3 and a_4 were fitted by the least square method.

$$\eta(I_o) = a_1 + a_2 e^{a_3 I_o} + a_4 I_o \quad 4.3$$

The second fit presented in Figure 4.2 was made with the same equation and reduced amount of data, however new values for the parameters a_1,a_2,a_3 and a_4 were calculated. As can be seen, the parametric model in this example is not much penalised by the reduced amount of data of the second dataset and is thus very robust against the variance error.

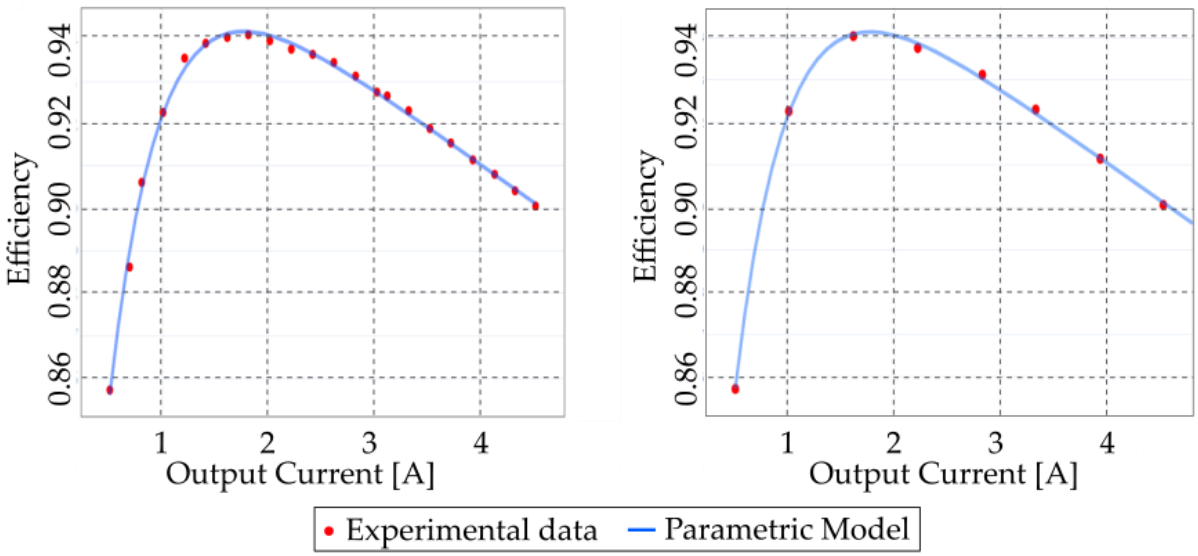

Figure 4.2 Example of a parametrical model. Left: Fit of a parametric equation using the 22 data points. Right: Fit of a parametric equation using only 8 data points.

The parametric method can be very accurate; however, the choice of the equation is decisive for obtaining predictions with low error. The choice of the equation gives the shape of the answer, so, if an equation that is not compatible with the shape of the answer is chosen, the model will present a high bias error, despite the values of the parameters $a_1,a_2 \ldots a_n$.
The non-parametric method called k-nearest neighbours was fitted with the same dataset as the parametric model. This method predicts the value of a response y_o for any given x_o as the mean value of the responses of the 'k' closest neighbours of the x_o value. Figure 4.3 presents the fit of this method for $k = 1$.

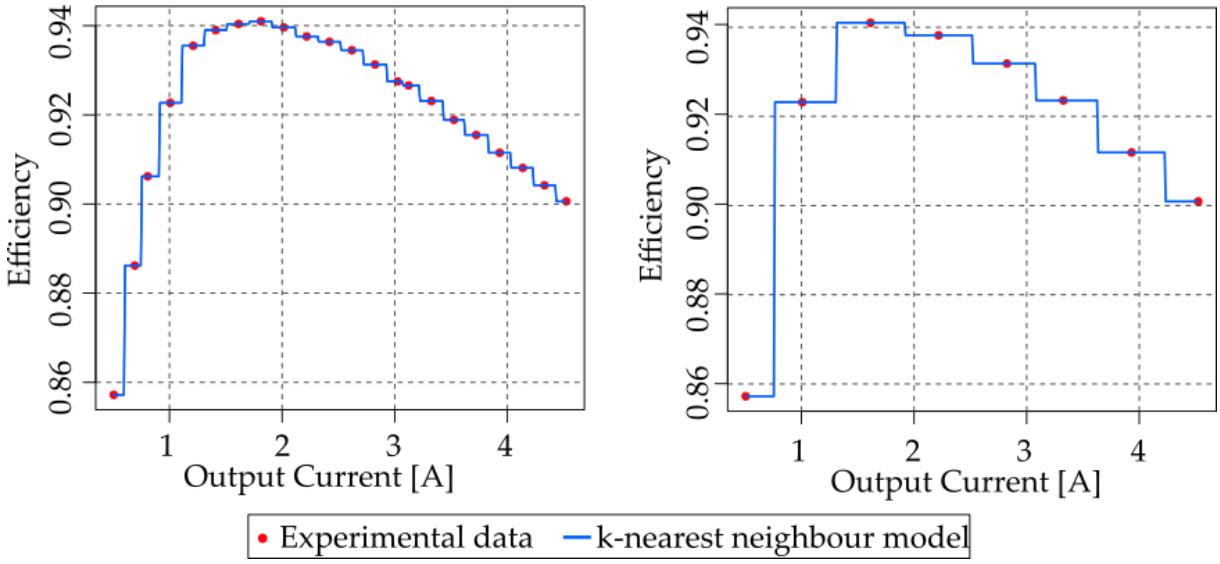

Figure 4.3 Example of a non-parametric method: the k-nearest neighbours regression. Left: Fit using the 22 data points. Right: Fit using 8 data points.

This example illustrates a model that is not defined by an explicit parametric function. It can be seen as an algorithm that is first trained with a sample data, that later is capable of predicting output value for different input values. Thus, no prior knowledge of the model is required to find the shape of the output (no bias error). However, the lack of data penalises the model as can be seen in the second fit of Figure 4.3, making it sensitive to the variability error.

The most relevant characteristic of non-parametric methods that this thesis wants to explore is that they do not require any prior knowledge about how the inputs affect the output. Despite the number of dimensions that are studied and even if there are coupling effects with two or more dimensions in the response, the non-parametric methods can 'figure out' the shape of the response with minor effort. However, this method requires a large amount of data which has been shown to be prohibitive in chapter 2.

A special case of non-parametric models is the Gaussian Process Regression (GPR). This method is defined as a meta-parametric technique (or semi-parametric) because, even if it does not have physical parameters, it has so-called *hyper-parameters* that can provide the user with a certain degree of tuning. Further details about its working principles are presented in section 4.4. An example of a fit using the GPR is presented in Figure 4.4. A squared exponential kernel was used to fit the data (kernels will also be explained in the next section).

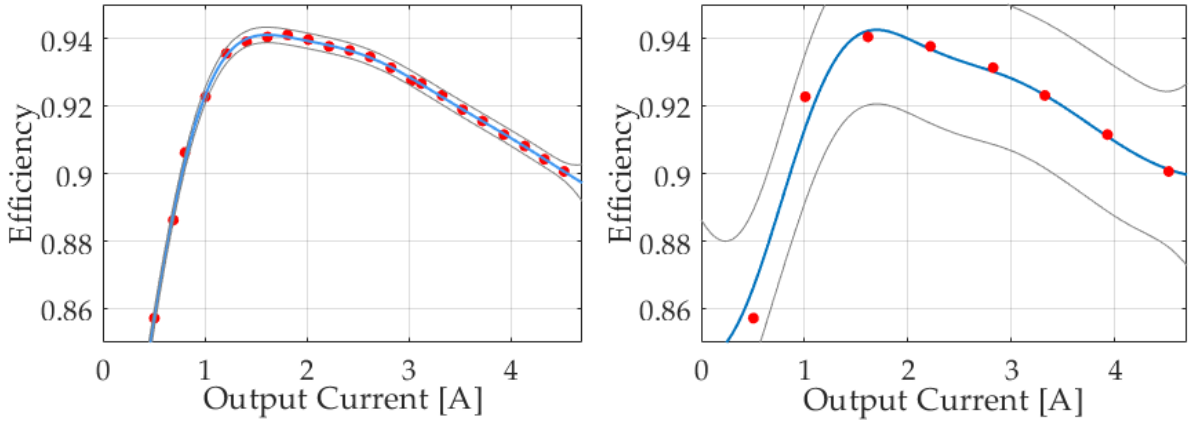

Figure 4.4 Example of a Gaussian process regression. Blue curves: Predicted value; Grey curves: The 95% confidence interval boundaries. Left fit using the 22 data points. Right: Fit using 8 data points.

The GPR, as a meta-parametric method, has the advantages and the drawbacks of both parametric and non-parametric methods.

The advantages of the GPR method is that it does not require prior knowledge about the shape of the response, making it robust against the bias error similarly to non-parametric methods. It is not very penalised for fewer amount of data, as shown in the second plot in Figure 4.4, making it robust against the variance error. The GPR gives fully probabilistic predictions. This means the model can give a reliable estimate of its own error along with its prediction.

In terms of disadvantages, the GPR does require the definition of some aspects of the shape of the equation used in the model through the choice of kernels and hyper-parameters. Kernels allow the user to add prior knowledge and specifications about the expected behaviour of the system model, introducing some degree of bias. Hyper-parameters allows the user to fine-tune these models according to some insight, thus influencing its variance error [66].
All the work done on the two previous chapters provided a certain degree of prior knowledge about the behaviour of PCAs, while still not being enough to infer an explicit equation to model this behaviour. This middle-ground between parametric and non-parametric approaches is perfectly suited, given the mathematical evidence, to the GPR method. This is the reason why the GPR was chosen as a method to fit the data from this work.

4.2 Dataset

The experiments performed in this work followed the input variables defined in the DOE as close as the test equipment accuracy. Figure 4.5 presents a complete experimental characterisation cycle for the PCA 511010. This converter has been submitted to 360 different operating points, and 9 measurements were repeated for each operating point. The total number of measurements points per characterisation cycle is 3240, representing nearly 30 h of tests per converter.

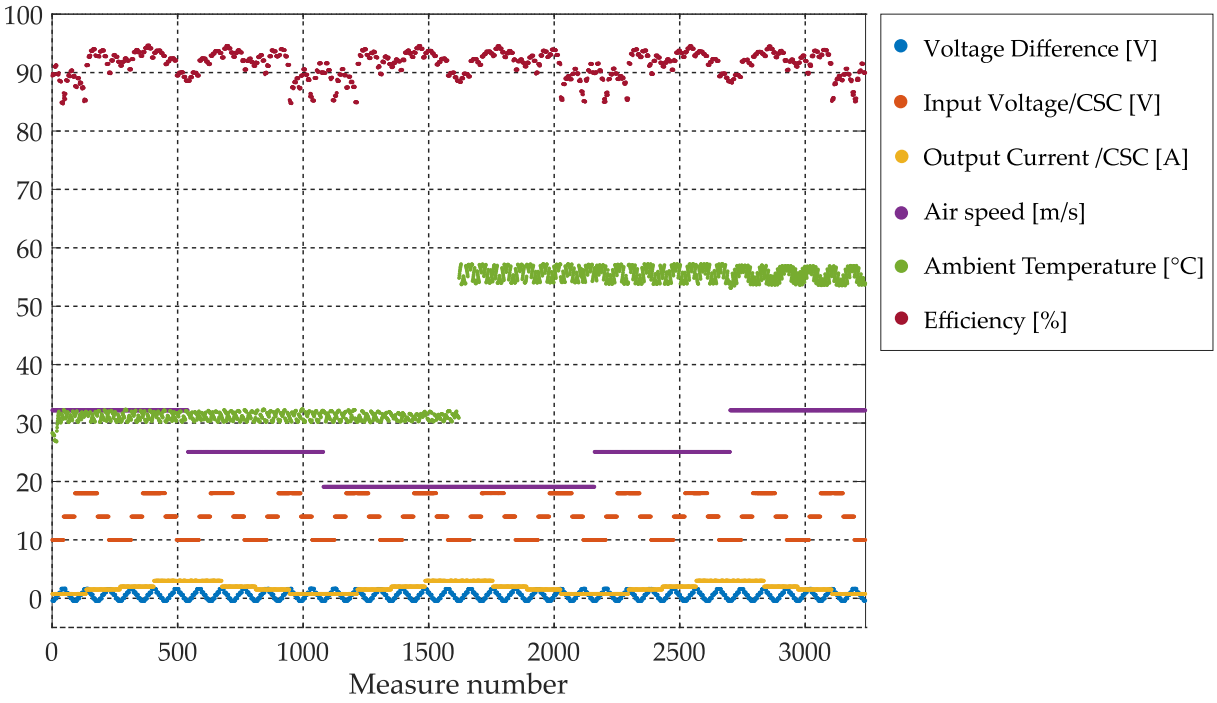

Figure 4.5 A complete experimental characterisation cycle for one converter.

The models will be evaluated for performing two different tasks: interpolation (predictions inside the boundaries in which the dataset contains data) and extrapolation (predictions beyond the boundaries). Initially, in chapter 2, it was selected 15 converters to cover the space

up to 5 lines, 5 columns and 3 boards. However, seven different converters were tested, less than initially proposed in the DOE mainly due converter failure and time constraints. For this reason, the boundaries that define the interpolation region are more restrictive than initially planned.

The total amount of experiment points tested were 2548. At each operating point, 9 repeated measurements were acquired, resulting in a total of 22932 measurement points. This work used the average value of the 9 repetitions in order to lower the equipment measurement errors, especially with respect to the ambient temperature oscillation that were presented in chapter 3.

All the 2548 experiment points are presented in Figure 4.6. Each input variable is presented individually as a function of the two outputs: Efficiency in the left y-axis and converter temperature in the right y-axis. The data presented in chapter 2, in the one variable at a time (OVAT) test, is also added to the dataset.

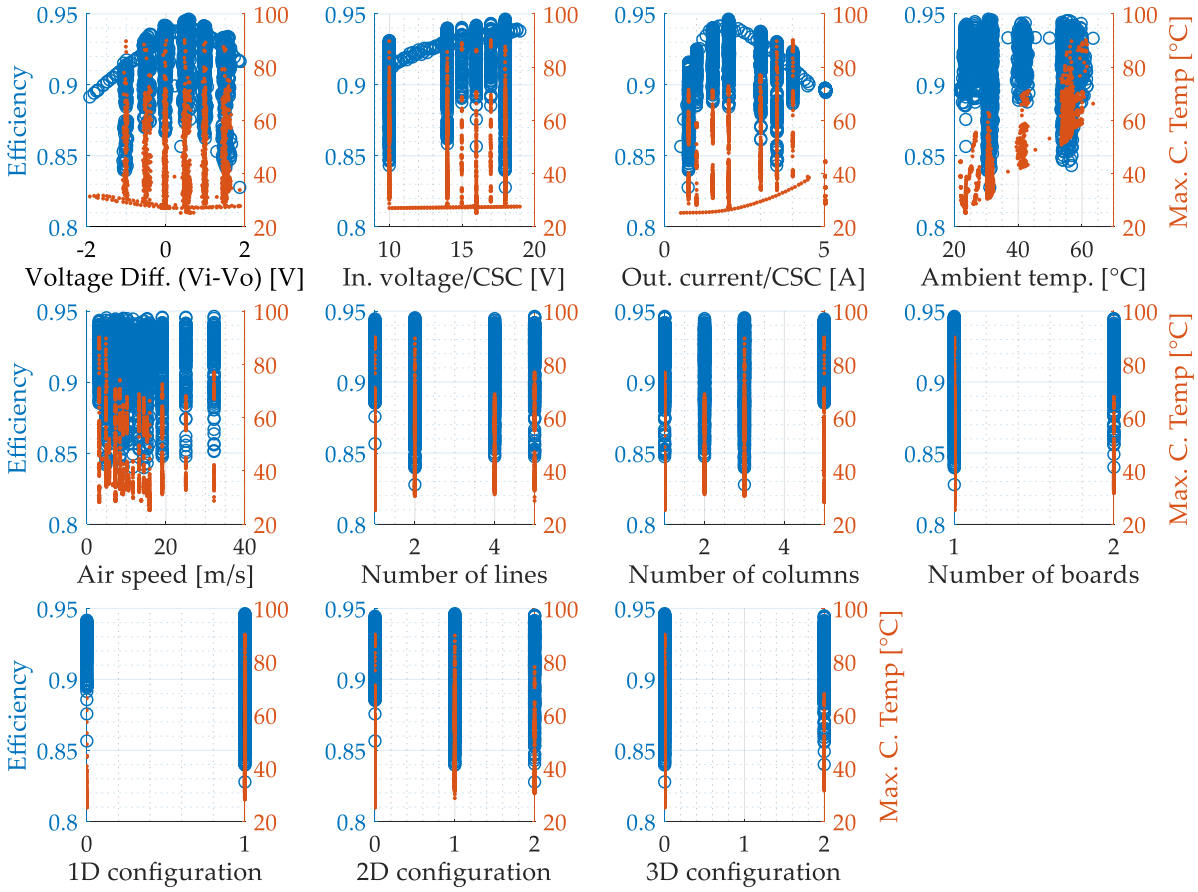

Figure 4.6 The complete dataset. Each plot contains one input variable on the x-axis and the two output variables on the y-axis (Efficiency in the left y-axis and the maximum converter temperature in the right y-axis). All 2548 experiment points are presented in each plot.

Table 4.1 presents the eleven input variables, their nature (QT for quantitative or QL for qualitative), and their maximum and minimum values. The qualitative variables are the 1D, 2D and 3D connection settings. These variables can assume 3 states, no-connection, with a value of zero (0), IPOS with a value of one (1) and ISOP with a value of two (2).
For fitting purposes, qualitative variables must be transformed into dummy variables, which must be treated as binary data (0 or 1) in a way that no mathematical relation is created among connections. The "dummy variables" are the following:

- 1DSP: 0 or 1
- 1DPS: 0 or 1
- 2DSP: 0 or 1
- 2DPS: 0 or 1
- 3DSP: 0 or 1
- 3DPS: 0 or 1

Table 4.1 Boundaries of the input values

Input Variables										
Input voltage (Vi)	Voltage Difference (DV)	Output current (Io)	Airflow speed (Aspeed)	Ambient Temp. (Ta)	nline	ncol	nboard	1D	2D	3D
QT	QT	QT	QT	QT	QT	QT	QT	QL	QL	QL
{9.98… 18.98}	{-1.92… 1.87}	{0.5… 5.0}	{3.1… 32.1}	{21.9… 63.5}	{1… 5}	{1… 5}	{1… 2}	{0… 2}	{0… 2}	{0… 2}

The models created in this work will also be used to extrapolate beyond the boundaries of its training data. As seen in chapter 1, many solutions of PCAs can exceed the 5 lines and 5 columns, which are the highest values tested. Although there is no data to analyse if the extrapolations are reliable or not, the results will be judged by physical insight e.g. efficiency must decrease at higher currents, converter temperature should increase with higher ambient temperature, etc. The ranges of extrapolations are presented in Table 4.2.

Table 4.2 Ranges in which extrapolations the models will try to predict

Input Variables										
Input voltage (Vi)	Voltage Difference (DV)	Output current (Io)	Airflow speed (Aspeed)	Ambient Temp. (Ta)	nline	ncol	nboard	1D	2D	3D
QT	QT	QT	QT	QT	QT	QT	QT	QL	QL	QL
{10… **20**}	{**-3… 3**}	{0.5… **7**}	{**1**… 32}	{**0**… 63.5}	{1… **7**}	{1… **7**}	{1… 2}	{0… 2}	{0… 2}	{0… 2}

4.4 GPR Modelling Process

The Gaussian Process Regression (GPR) is the method used in this work to fit the models for converter efficiency and temperature predictions. This complex modelling technique has been recently applied in subjects related to electrical engineering such as in [67] to predict the health of batteries, in [68] to estimate the lifetime of IGBT devices and in [69] to model the switching behaviour of MOSFETs.

All of the references above treat problems where there is no obvious model equation (bias problem), and the number of measurements is limited for some reason (variance problem). However, some prior knowledge is available for the system under study.

To better understand why the GPR is a good solution for these types of problem, this section provides some broad definitions before proceeding to fitting the data and evaluating the model performance.

4.4.1 Gaussian Process Regression Definition

To understand how a GPR works, picture a parametrical function, such as a linear regression, defined by *f*, which is supposed to fit the response data $Y = [y_1, y_2 \dots y_n]$ by using the input data $X = [X_1, X_2 \dots X_n]$, where $X_1 = [x_1, x_2 \dots x_p]$, being n the number of measurements and p the number of variables. The linear regression can be defined as

$$f(x) = X^T w \tag{4.4}$$

Where w is a vector of weights.

As can be seen, the function *f* is completely defined by the vector of weights w.

The prediction of the model is then the result of the function plus an intrinsic error ε, which is assumed to follow a Gaussian distribution with zero mean and standard deviation of σ ($N(0, \sigma^2)$)

$$Y = f(X) + \varepsilon \tag{4.5}$$

Looking at this problem from a probabilistic point of view, it is possible to demonstrate that the probability density of the observation, given the input data X and the parameters w, is equal to a normal distribution with mean $X^T w$ and standard deviation $\sigma^2 I$

$$p(Y|X, w) = N(X^T w, \sigma^2 I) \tag{4.6}$$

The latter quantity corresponds to the likelihood of the output Y (the probability of having the output Y), knowing the model/function/weights. In order to find the best function that fits the data, this likelihood function must be maximised (in w), in other words, finding the w that maximises this probability. This can be done through a series of tries and errors, leading to fitting methods such as least squares. The problem of bias and variability errors remain an issue throughout the process. An alternative solution is to use Bayesian Inference.

Bayesian Inference is a probability theory concerned on how new evidence changes the perception of the initial problem. For instance, if more measurements are performed with more PCAs, how does this new evidence provide information that can help find the best equation to predict the behaviour of converters which have not been measured? In these circumstances, there is a *prior* knowledge, which is what was known *before* new measurements were

performed and a *posterior* knowledge, which is what is known *after* this new information is taken into account. If the posterior knowledge is maximal, then the probability of finding the right function that best describes the problem is 1 (or 100%).

From a Bayesian point of view, maximising our knowledge with new data corresponds to maximising a *posterior probability function*. This is the equivalent of maximising the probability of finding the correct function/vector of weights, from our knowledge of the output data.

In mathematical terms, this can be expressed by the equation X where A and B are events.

$$p(A|B) = \frac{p(B|A)}{p(B)} \cdot p(A) \qquad 4.7$$

Where $p(A|B)$ defines the posteriori probability of observing event A given the available evidence of event B

$\frac{p(B|A)}{p(B)}$ defines how the evidence of event B supports observing event A

$p(A)$ is the prior knowledge of event A.

Using the Bayes theorem for the problem in equation 4.6, it is possible to have an analytical expression of the posterior probability function of the weight of the problem considering the observations of the output and input (which is the equivalent of a fit) shown in equation 4.7

$$p(w|Y,X) = \frac{p(Y|X,w)p(w)}{p(Y|X)} \qquad 4.8$$

Where

$p(w)$, the prior probability function (or how likely it was to find the right weights without using the input and output data from the experiments)

$\frac{p(Y|X,w)}{p(Y|X)}$, represents how the observations of the output given the input provide new information about the weights

By maximizing the *posterior probability function*, the Bayesian Inference mathematically guarantees that the result will be the best possible set of weights that represent the target function.

This same technique can be considered from a much broader perspective. Instead of looking for the weights of a given function, it is considered looking for a generic function among all possible mathematical functions. The theory above states that the solution can be found by maximizing the posterior likelihood given by equation 4.8.

$$argmax_f\big(p(f|Y,X)\big) = argmax_f\left(\frac{p(Y|X,f)}{p(Y)} \cdot p(f)\right) \qquad 4.9$$

When using a Gaussian Process Regression (GPR), it is assumed that the *prior probability density* corresponds to a *Gaussian distribution* with zero mean and covariance matrix Σ_p.

It can be proved that, under the latter assumption, the posterior density follows, as well, a normal distribution centred in $\acute{w}$ with a standard deviation of A^{-1}

$$p(f|X,Y)\ N(\acute{w}, A^{-1}) \qquad 4.10$$

Where

$$\acute{w} = \sigma^{-2}A^{-1}XY \qquad 4.10$$

$$A = \sigma^{-2}XX^T + \Sigma_p^{-1} \qquad 4.11$$

The variable $\acute{w}$ in equation 4.10 corresponds to the value that maximises the posterior density function, which means it provides the best solution for the problem stated by equation 4.8 given all the evidence taken into account.

Equations 4.10 and 4.11 show that the model that maximises the probability of good predictions from a GPR model depends uniquely on input variables X, output variables Y, the measurement standard deviation and the covariance matrix Σ_p. The problem thus becomes finding the covariance matrix that best suits the data at hand.

A kernel in GPR is the function used to calculate the covariance matrix Σ_p. This kernel is chosen by the user according to any prior knowledge of the data, which introduces some bias error. Since a kernel has its own parameters (called meta-parameters since they are applied indirectly to the data), it allows for a certain degree of control over the GPR fit, which in turn introduces some variance error.

The GPR method yields a fit that mathematically guarantees a minimal error of the prediction if it is provided the appropriate kernel and its associated meta-parameters. The problem of creating a model using GPR thus becomes a search for the kernel that best suits the problem under study [66]. This study is detailed in the section below.

4.4.2 Converter Efficiency GPR model

The first GPR model presented in this work focuses on predicting the efficiency of the PCA as a function of all of its 11 input variables. Given the insight gained from the one-variable-at-a-time study in chapter 2, it seems fair to assume the target function should have some strong non-linearity.

This work opted for exploring four classic GPR kernels suited for non-linear systems: exponential (EX), Matern 5/2 (M52), rational quadratic (RQ) and squared exponential (SE). They all were fitted following a 5-fold cross-validation. Their root mean square error (RMSE) and their training time are presented in Table 4.3.

Table 4.3 The root mean squared error and training time of each model and its correspondent kernel.

Kernel (Σ_p)	RMSE [points of efficiency 10^{-3}]	Training time [min]
Exponential (EX)	2.85	28.9
Matern 5/2 (M52)	1.27	23.9
Rational quadratic (RQ)	1.34	22.1
Squared exponential (SQ)	1.43	12.9

The RMSE presented in Table 4.3 measures the training error of the models, or how close the predictions are to the expected results used during training. It is important to note that this metric does not necessarily show how good are the predictions, but rather how close these are to the available training data. The data used to fit the model can be used to perform some

initial analysis of the quality of its results. However, an independent set of test data must also be used to finalise the validation of the model.

An initial analysis of the quality of the prediction of the kernels can be made by comparison between the predictions and the physical knowledge of the system. This is presented in Figure 4.7 where the models are used to predict the efficiency of the converter as a function of its output current. The other 10 variables are kept constant, and their values are presented in the legend of their respective plots. The grey dots in Figure 4.7 are the 95% confidence region of the prediction given by the model, while the blue dots are the actual predicted values.

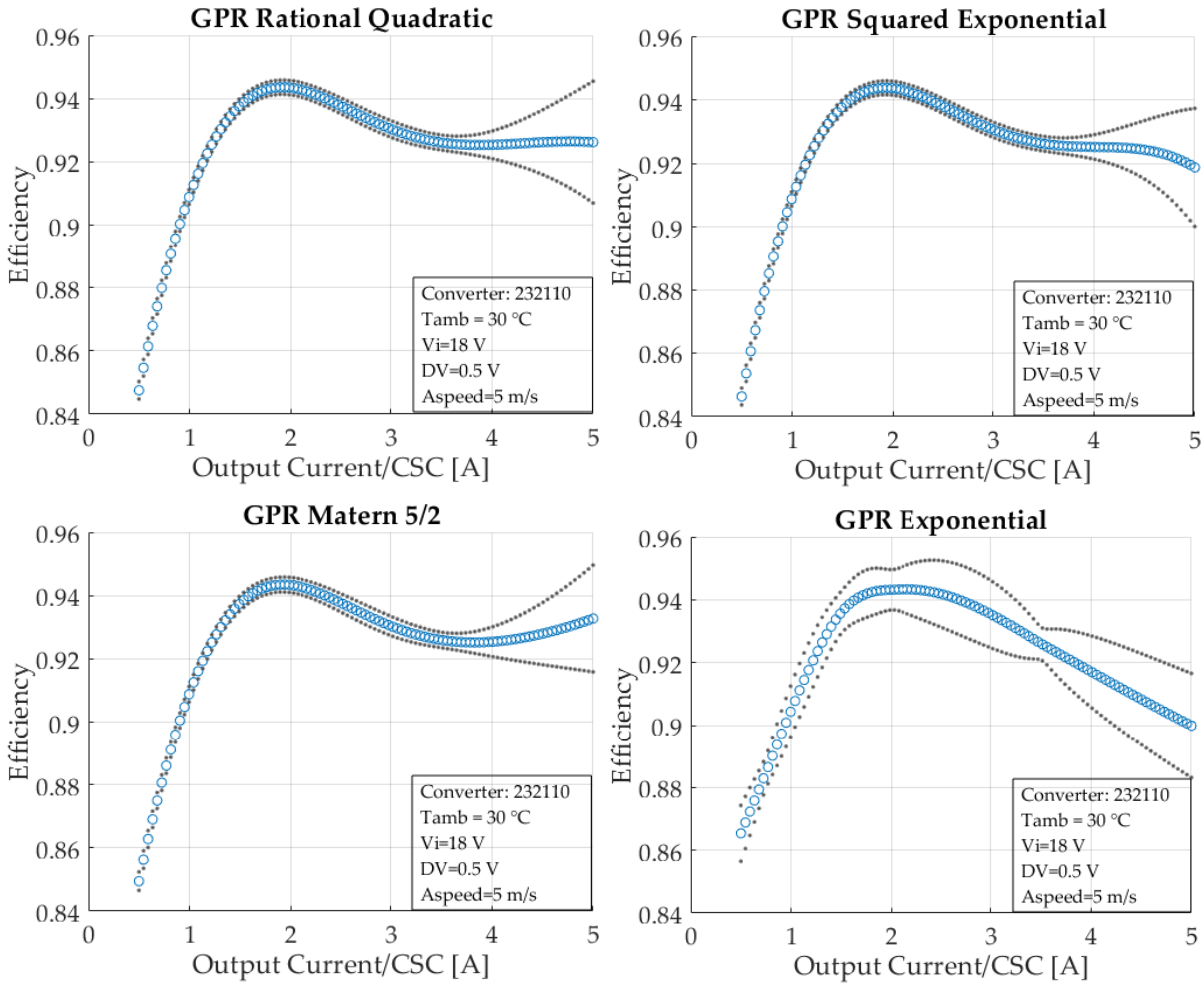

Figure 4.7 Predictions of the efficiency versus the output current with the 11 input variables assuming values close to points presented in the dataset. Blue circles: predicted values. Grey dots: 95% confidence interval. The converter code 232110 stands for: 2 lines, 3 columns, 1 board, 1D: IPOS, 2D: IPOS, 3D: NC.

From Figure 4.7, it is possible to see that the M52, the RQ and the SE perform a very precise prediction until 3.5 A, which is the region that concentrates most of the training data. Beyond this current, these kernels have incoherent results, incompatible with the physical reality. The EX kernel presents a lower overall precision, but its results beyond 3.5 A represent a physically acceptable prediction.

To validate the model interpolation capability, a new and independent dataset is used. A new PCA must then be fabricated and tested for this purpose. This work used an architecture of 3 lines, 4 columns and 1 board, and a configuration of 1D: IPOS, 2D: IPOS, 3D: NC, as presented in Figure 4.8.

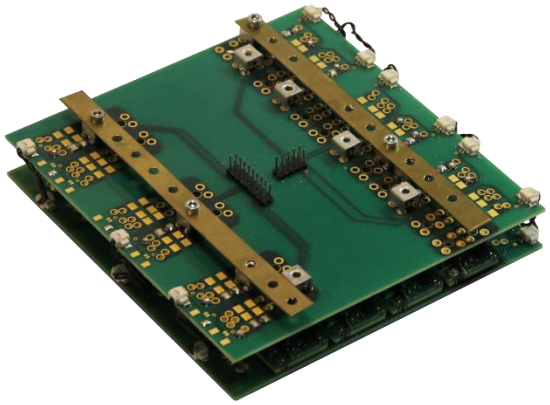

Figure 4.8 PCA 431110: 4 lines, 3 columns, 1 board, 1D: IPOS, 2D: IPOS, 3D: NC. The measurements made with this converter were not used as training data.

The PCA 431110 was submitted to a total of 1240 experimental measurements in 139 different operating points with 9 repetitions for each point. To validate the performance of the kernels, the exact same operating points applied to the converter during its experimental measurements are used as input data and the predictions are compared with the real efficiency measured during the experiment. The 139 operating points tested with the PCA 431110 are presented in Figure 4.9.

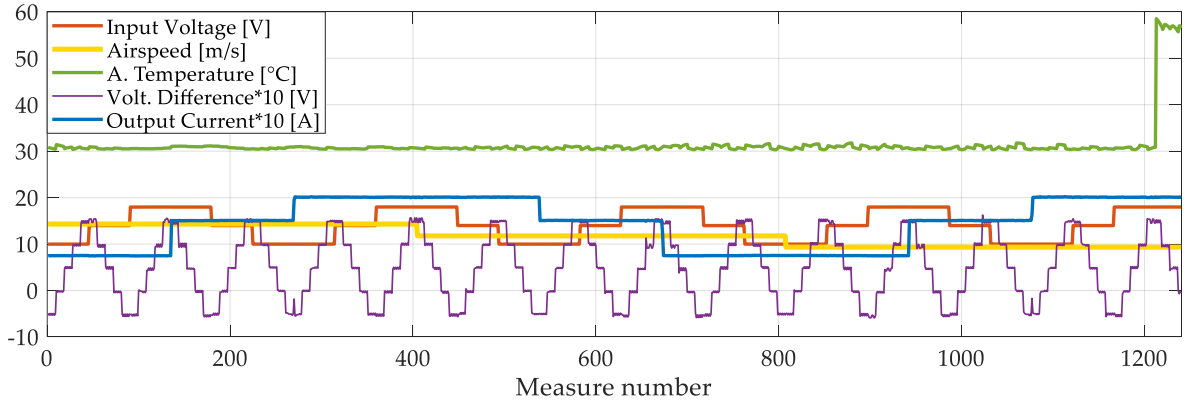

Figure 4.9 Mission profile in which the PCA 431110 was tested.

Figure 4.10 presents a plot of the efficiency of PCA 431110 as a function of voltage difference in 5 different operating conditions. Both SE and RQ kernels have predictions whose behaviours (or shapes) do not match those of the measurements. Both M52 and EX have behaviours (or shapes) that seem to fit well the predictions. This is coherent with the fact that

both are mathematically very similar. The EX also seems to have the lowest error of all the kernels at those 5 experimental points.

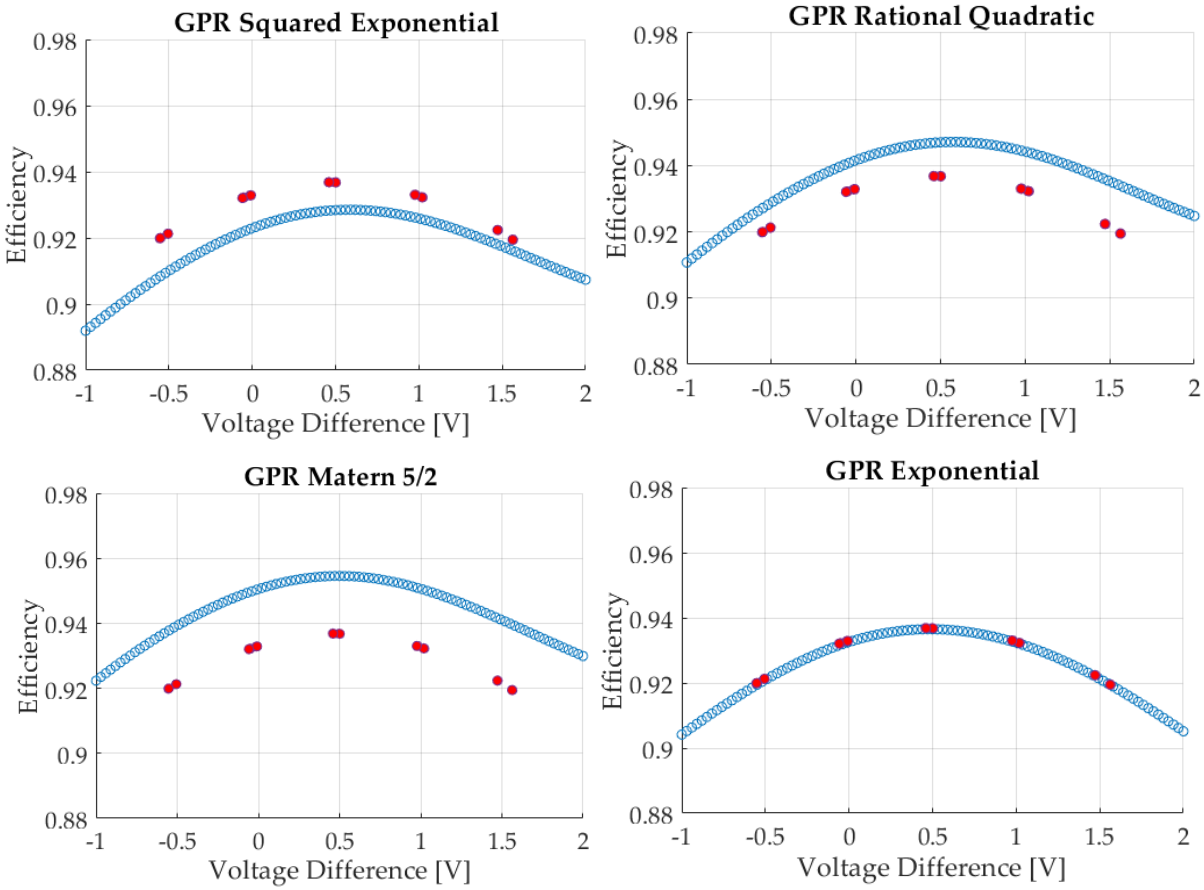

Figure 4.10 Blue circles: Predictions of the efficiency in function of the voltage difference. Red dots: Five real measurements obtained with the PCA 341110.

A more detailed analysis of the error is proposed in Figure 4.11. The prediction errors for each kernel (predicted value – real value) are displayed on the y-axis. The x-axis corresponds to the measurement number.

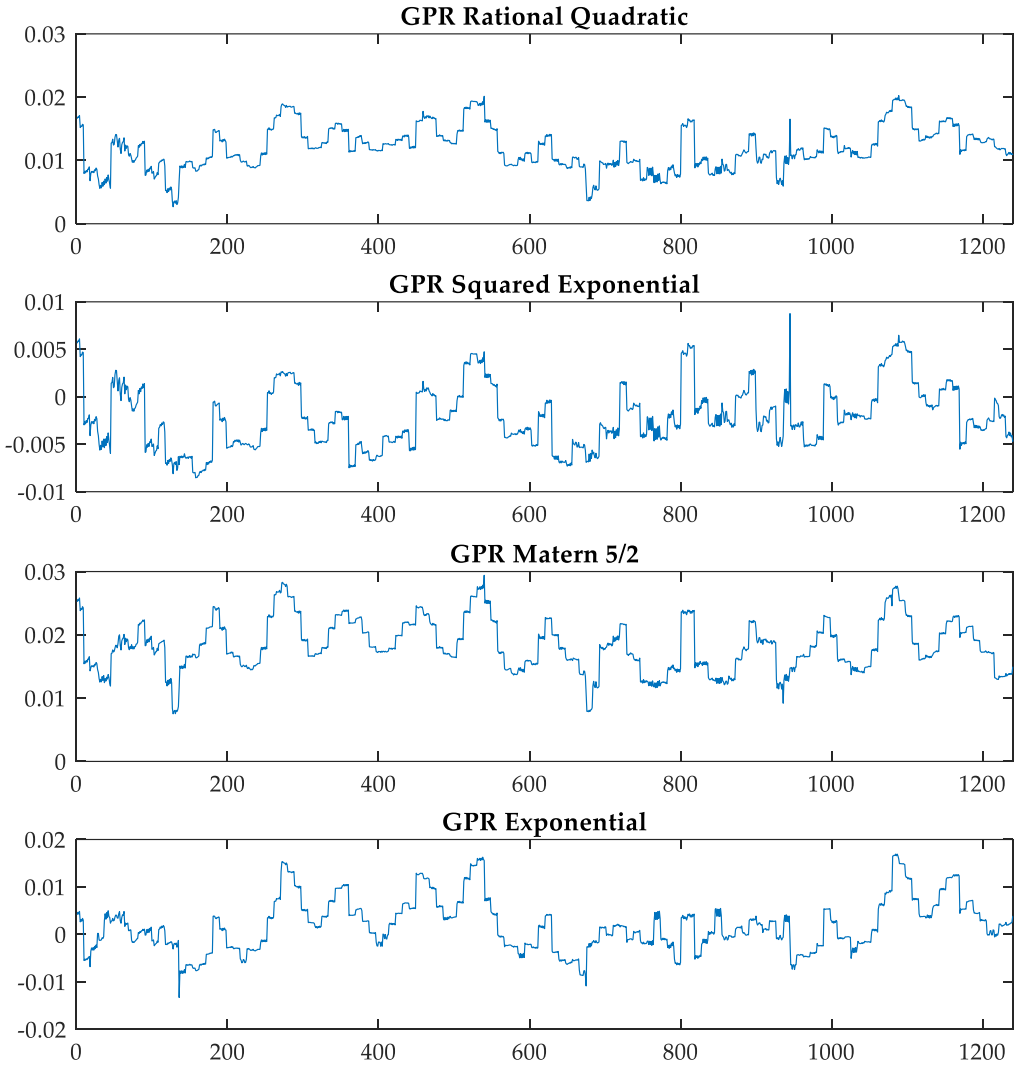

Figure 4.11 The efficiency error (predicted efficiency value – real efficiency value) that each model present for the 1240 experimental measurements performed with the prototype 431110. The y-axis units are points of efficiency.

With the results displayed in Figure 4.11, the SE kernel presents an excellent performance, predicting all the 139 different operating points with less than 0.01 point of efficiency (1%) from the actual measured value. The EX also presents a good performance. However, the M52 and RQ kernels overestimate the efficiency in all predictions.

The average prediction can be quantified by the root mean squared error (RMSE) presented in Table 4.4. As the SE presented the smallest RMSE, it is the kernel chosen to perform the interpolation predictions of efficiency. However, for the extrapolation predictions, it can be seen in Figure 4.7 that the EX kernel is the only one which have physical coherency.

Table 4.4 Performance details of each kernel for the efficiency model

Kernel (Σ_p)	RMSE [points of efficiency 10^{-3}]	Training time [min]
Exponential (EX)	5.8	28.9
Matern 5/2 (M52)	18.7	23.9
Rational quadratic (RQ)	12.4	22.1
Squared exponential (SE)	3.9	12.9

To verify that the extrapolations of the EX model look coherent with the physical properties of a power converter, it was performed predictions while extrapolating 6 different variables: voltage difference, output current, input voltage, ambient temperature, number of lines and number of columns. The extrapolations boundaries are made as defined in Table 4.2. These 6 predictions are presented in Figure 4.12.

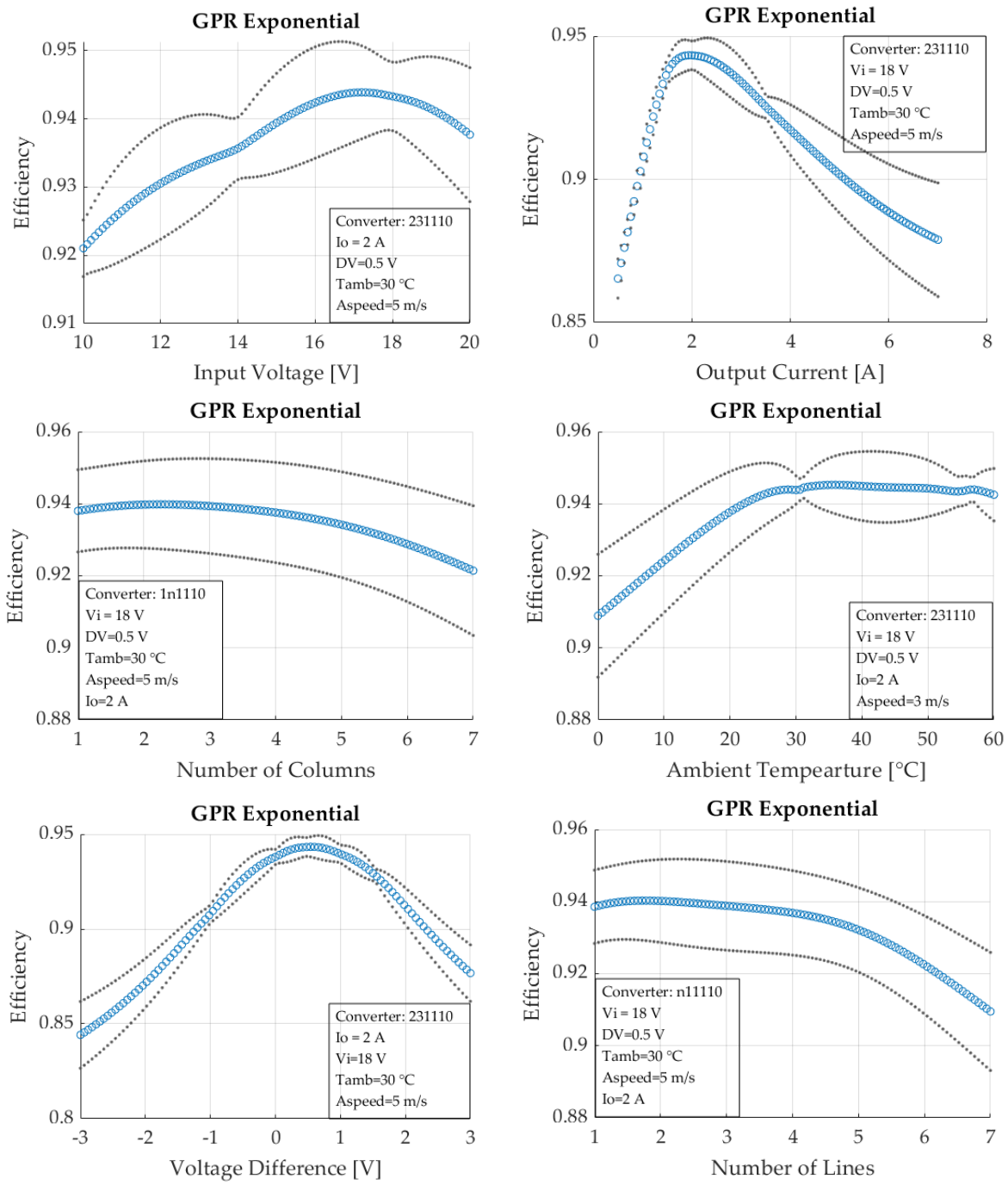

Figure 4.12 Predictions within the extrapolations boundaries. The input data for each plot is detailed inside the square.

In Figure 4.12, the input variables that are considered to present a physically consistent result for the whole range of extrapolation are: output current, voltage difference, number of columns and number of lines. However, it is impossible to know how precise these results are without an independent validation data set.

Regarding the impact of ambient temperature on predictions, it presents a strange behaviour for low temperatures. This strange behaviour must be caused due to the fact that mostly all dataset is concentrated just over 2 temperatures: 30 and 55 °C.

Another input variable that presents a strange behaviour is the input voltage. It is known, from past tests, not presented in this work, that the efficiency at 20 V is higher than at lower voltages. However, the model predicts that the peak efficiency peak is around 17 V.
In order to perform more reliable extrapolations, there are two alternatives. Either by obtaining some experimental data in the extreme points, thus creating a dataset with more information, or using alternative kernels with more complex equations capable of extracting more information from the dataset.

4.4.3 Converter Temperature GPR model

The second GPR model presented in this work focuses on predicting the operating temperature of the PCA as a function of all 11 input variables. This section will use the same four classic GPR kernels used in the first model: exponential (EX), Matern 5/2 (M52), rational quadratic (RQ) and squared exponential (SE). They all were fitted following a 5-fold cross-validation.
The training data used to fit the temperature GPR model using the four kernels listed above was the same one used for the efficiency model. Likewise, the same independent dataset from PCA 431110 was used for the final validation.
Evaluating the error of the predictions is the first validation step used for the kernels considered in the temperature model. Figure 4.13 presents prediction errors of each model for the 124 operating points (predicted value – real measured value). The right y-axis presents the percentage error. Table 4.5 presents the RMSE that each model had in this test.

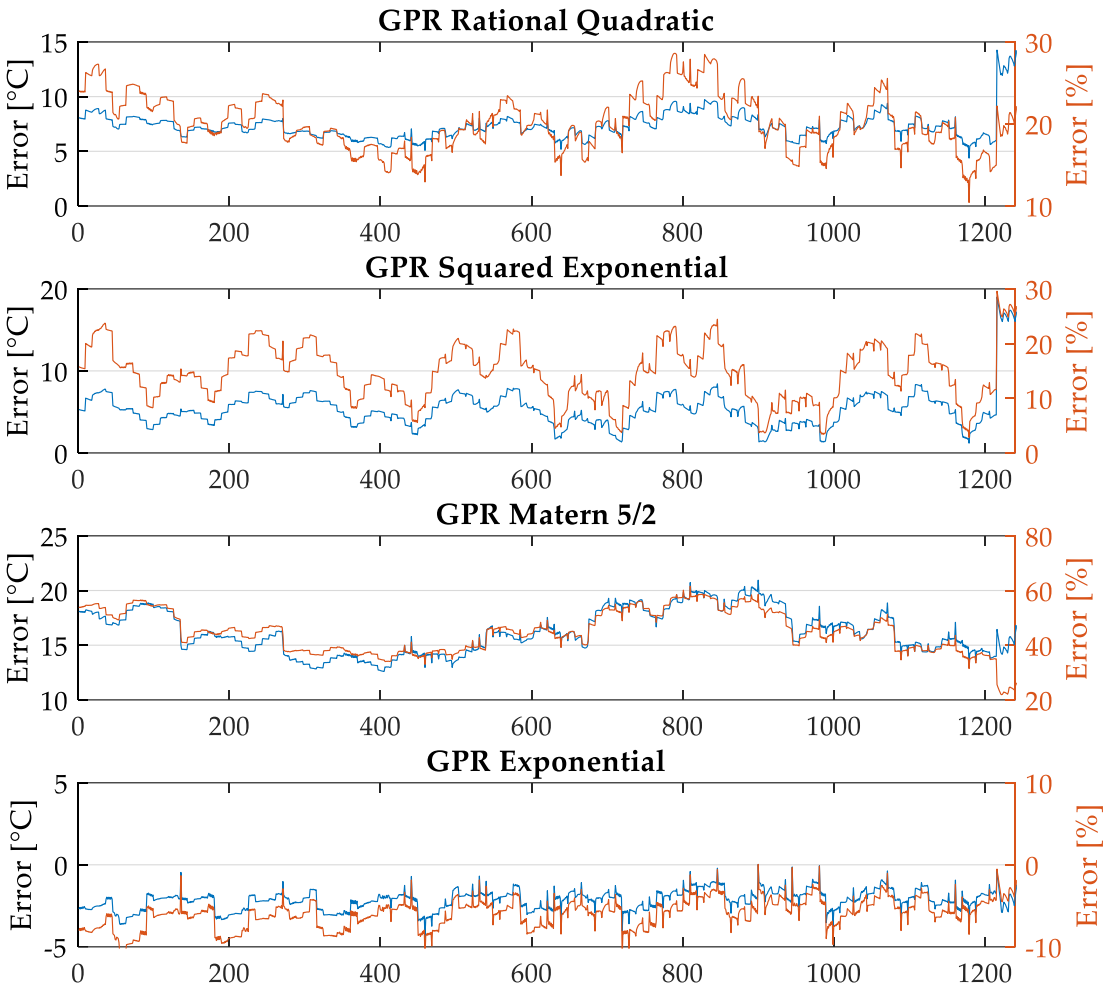

Figure 4.13 The converter temperature error (predicted efficiency value – real efficiency value) for each model.

Table 4.5 Performance details of each kernel for the temperature model

Kernel (Σ_p)	RMSE [°C]	Training time [min]
Exponential (EX)	2.22	7.6
Matern 5/2 (M52)	16.34	5.2
Rational quadratic (RQ)	7.46	12.4
Squared exponential (SQ)	5.96	4.7

The data presented in Table 4.5 confirms that the EX kernel outperforms all the others, with an RMSE of 2.2 °C.

The final verification of the GPR temperature model based on the EX kernel is an analysis of the physical coherence of predictions in extrapolated operating conditions. In this test, predictions of the four variables known to have an important impact in converter temperature were analysed: output current, number of lines, ambient temperature and airspeed. Results are shown in Figure 4.14.

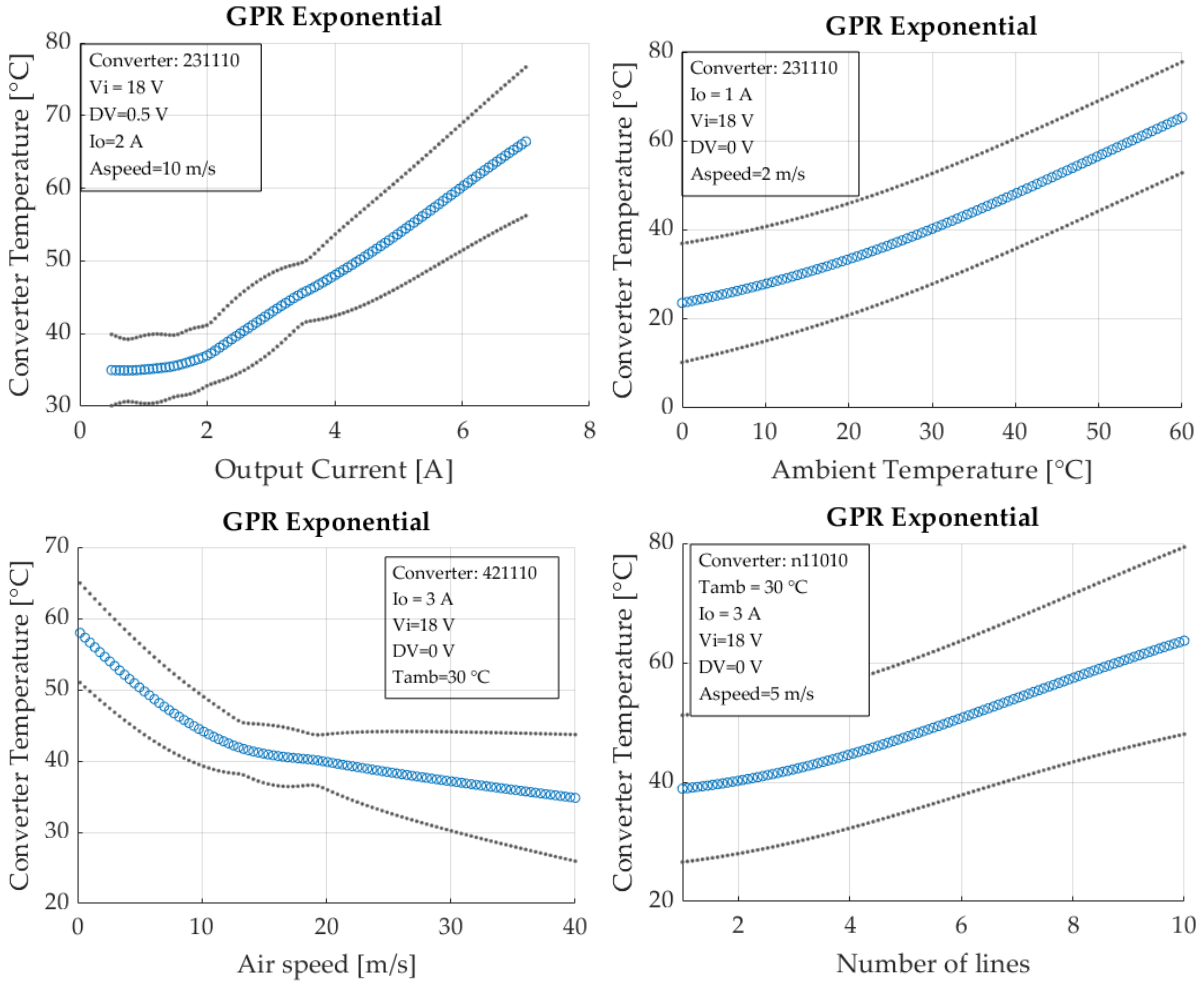

Figure 4.14 Predictions for the converter temperature within the extrapolations boundaries. The input data for each plot is detailed inside the squares.

The converter temperature rises for higher output currents and for higher ambient temperature, which is coherent with physical principles of operation, as it is shown in Figure 4.14. The rise in the temperature with the number of lines can be explained by the fact that the number of lines grows perpendicularly to the airflow direction, as described in chapter one. In consequence, the cooling performances are affected by the number of lines, in terms of pressure loss but also coolant temperature rise through the lines.

The only variable that lowers converter temperature is the airspeed. Higher air speeds lead to a lower temperature, as expected physically. However, it is interesting to notice in Figure 4.14d) that even at its highest value, the air speed does not drop the converter temperature below the ambient temperature, which is also coherent physically.

4.5 Conclusion

This chapter introduced some basic vocabulary of statistical modelling. Some simple example cases were presented to illustrate some of the key concepts that are required to understand how to create a statistical model and how to judge its quality. Based on these concepts,

discussions about the choice of the modelling technique was made. The qualities and drawbacks of parametric and non-parametric methods were presented. Finally, the Gaussian process regression was chosen as the modelling technique to deal with the problem of this thesis.

In order to create a Gaussian process regression model, it is required to choose a covariance matrix (kernel). This work tried out four different kernels that created four different GPR models for predicting the efficiency and four models for predicting the converter temperature. Their performances were compared either for interpolation predictions (values inside the boundaries of the training data) and for extrapolation predictions (outside the boundaries of the training data).

For the efficiency prediction, the squared exponential kernel presented the most satisfying performance for the interpolation predictions; it will be used to make the predictions inside the boundaries of the training data. For the extrapolation performance, the exponential kernel presented the most coherent results. Finally, both models are kept and will be used according to the region in which the desired prediction is awaited.

For the converter temperature prediction, the EX kernel performed better in both interpolation region and extrapolation. This model is then used to any prediction desired.

It is important to notice that in the future, more data can be added to the dataset, either with the PCAs already tested or with new PCAs. In this way, the models can be improved, either by increasing the interpolation region and by obtaining more restrict confidence interval boundaries.

The next chapter uses the models to give examples of how powerful this methodology can be in predicting the behaviour of converters before their existence, opening new ideas for power electronic designers to work with.

5 Design Rules and Performance Prediction

The Automated Design for Manufacture (ADFM) method for Power Converter Arrays (PCA) proposed in this work is largely inspired by the microelectronics industry approach for mass manufacturing. The main principles of this method were described in chapter 1, which justified the use of statistical modelling from data acquired through a careful Design of Experiments carried out via an automated experimental platform, all described in detail in chapters 2, 3 and 4.

In this last chapter, this work will focus on two applications of these statistical models:

- Illustrate how these statistical models can be used to define the safe operating area of any PCA
- Use the prediction capabilities of the statistical models to perform a comparison of PCAs in a real-case application of a battery charger converter

5.1 Introduction

This chapter will use the models fit in chapter 4 to predict the behaviour of converters created with the technology platform (TP) G2ELab-Maatel, using the CSC 20V5A family. To simplify the name of each PCA, this chapter adopts the six-digit code to define the architecture and configuration of a given PCA. The proposed code follows the (*xyzabc*) standard, where *x* is the number of lines, *y* the number of columns, *z* the number of boards, *a* is the configuration of columns, *b* the configuration of lines, and *c* the configuration of boards. A number is associated to each as follows: 1-IPOS, 2-ISOP, 0-Not connected. Table 5.1 presents some examples of how the code can be read.

These predictions will be used to identify the safe operation conditions of the technology platform associated with the CSC20V5A family and to study the behaviour of a group of PCAs corresponding to a set of specifications through virtual prototyping.

Table 5.1 PCAs that comply with the desired specifications

Converter number	Number of lines (*x*)	Number of columns (*y*)	Number of boards (*z*)	Configuration of lines (*a*)	Configuration of columns (*b*)	Configuration of boards (*c*)
421110	4	2	1	IPOS (1)	IPOS (1)	Not connected (0)
n21110	n	2	1	IPOS (1)	IPOS (1)	Not connected (0)
322211	3	2	2	ISOP (2)	IPOS (1)	IPOS (1)

5.2 Safe operating area of the Technology Platform

PCAs are only able to operate safely within their Safe Operating Area (SOA). The SOA is described as the boundaries within which the technology platform is guaranteed to work correctly. The notion of SOA is the same as the one used for electrical components, especially power switches, that have their boundaries limited by maximum voltage and current rating with respect to conduction time, as it can be seen in their datasheets, displayed in Figure 5.1 [70]. PCAs have their SOA limited by their maximum temperature versus their electrical, physical, mechanical and thermal variables. In this work, only steady state limitations are studied

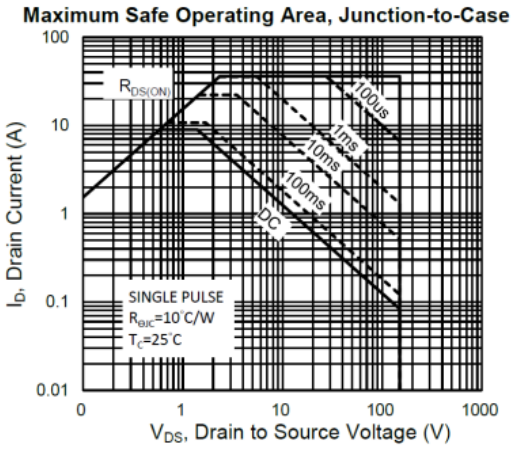

Figure 5.1 Safe operating area of a MOSFET, adapted from [70].

In order to illustrate the safe operating conditions of one PCA, Figure 5.2 brings representative curves of the behaviour of the PCA 421110. The two charts in Figure 5.2 present the temperature of the converter versus the output current. The dashed line represents the boundary of 90°C over which the PCA should not operate. This temperature limit, recommended by the PCB manufacturer, is important to maintain the converter board temperature below the maximum operating temperature of its components and soldering elements. The chart on the left presents several curves for various air speed conditions. It can be seen that, for example, while operating with an air speed of 1 m/s the converter cannot operate with an output current above 4 A/CSC, but with an airspeed of 5 m/s it can operate under the thermal limit up to 5.5 A/CSC. The chart on the right brings curves for various ambient temperatures. A similar analysis can be done, showing that depending on the ambient air temperature, the converter current rating at CSC level may be limited in order to stay below the PCB board below the limit. This 90°C temperature is a first steady state SOA limit that can be inserted in an abacus to help designers making the good choices.

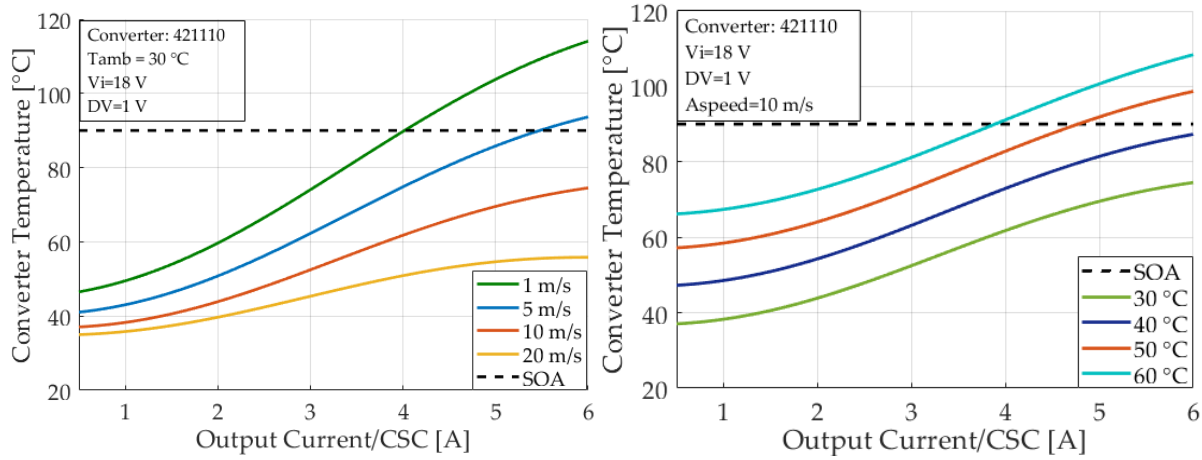

Figure 5.2 Safe operating area of a PCA versus the output current. Left: curves for several values of air speed. Right: curves for several ambient temperatures.

The SOA can be also analysed in terms of the architecture of the PCA. As introduced in chapter 1, page 29, there is a correlation between the maximum operating temperature of the converter and its architecture. Figure 5.3 presents two charts that show PCA operating temperature versus the number of lines. The numbers of columns and boards (y and z) have been fixed to 2 and 1, respectively. The chart in the left illustrates the behaviour of several PCAs while operating at different air speeds. The chart in the right presents how the ambient temperature affects the converter temperature.

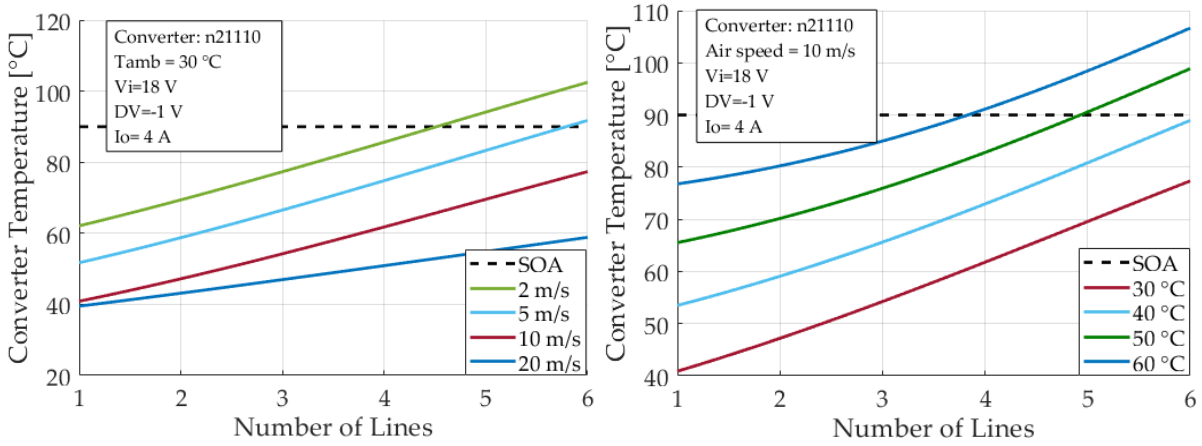

Figure 5.3 Safe operating area of a PCA versus the number of lines. Left: presents curves for various values of air speed. Right: presents curves for different ambient temperatures.

Figure 5.3 can be used by a designer to choose the number of lines of a PCA depending on the air speed of its cooler and the ambient temperature under which the PCA will work. The designer can be guided or required by the automated design environment to select only the architectures for which the numbers of lines are compliant with the PCA SOA. Having such insight is one of the strong points of the ADFM PCA methodology proposed in this work.

The last example shows how the converter SOA can be cross-checked with a combination of specification parameters.

Figure 5.4 presents a 3D surface of the temperature of the PCA 421110 versus its voltage difference and its air speed. The operating points outside the SOA are signalized with red circles. The figure shows that a converter may have different thermal behaviours even while operating at a similar power level but with different voltage conversion ratings.

The proposed ADFM PCA method is able to cross-check such complex and high-coupled behaviour and provide even to non-expert designers with warning signs. This ensures SOA compliance, guaranteeing performance, industrialization and mass production of the PCA under study.

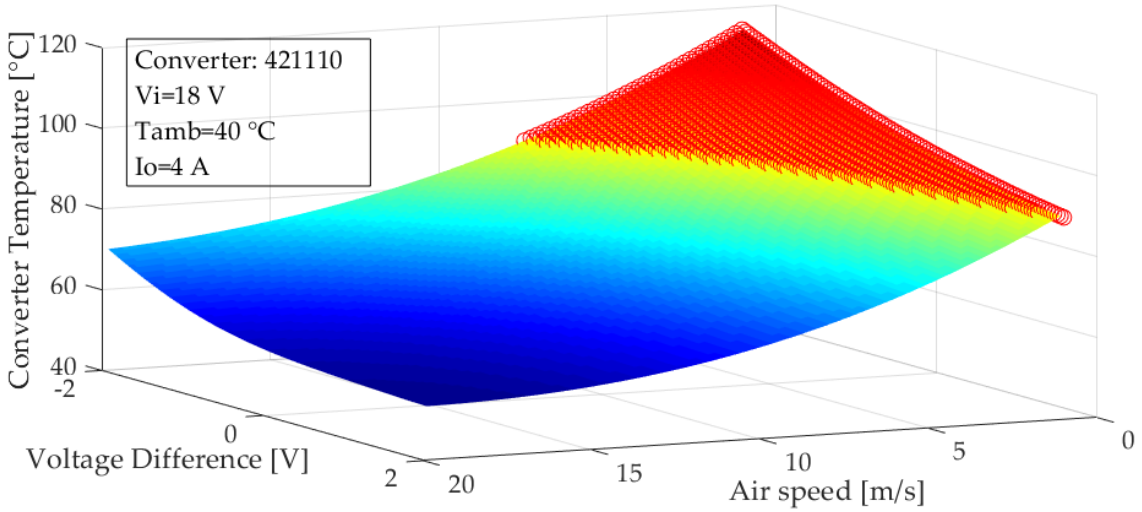

Figure 5.4 PCA 421110 temperature versus the voltage difference (input voltage-output voltage) per CSC and the air speed.

As Gaussian Process Regression was used to perform the predictions, it can be also presented the confidence interval, as presented in Figure 5.5. While some work is still needed to reduce the confidence intervals in Figure 5.5, the proposed statistical model provides a solid start in the support analysis needed by the proposed PCA ADFM method.

Next section shows how the proposed methodology in this work could be used to design and optimize a PCA from a set of expected values for efficiency, power density and behaviour for a full mission profile. Considering that the model is well representative of a real PCA, such an approach can be used to distinguish the best solution for all possible operating points of the PCA. Again, such profound insight is only possible using the PCA ADFM method.

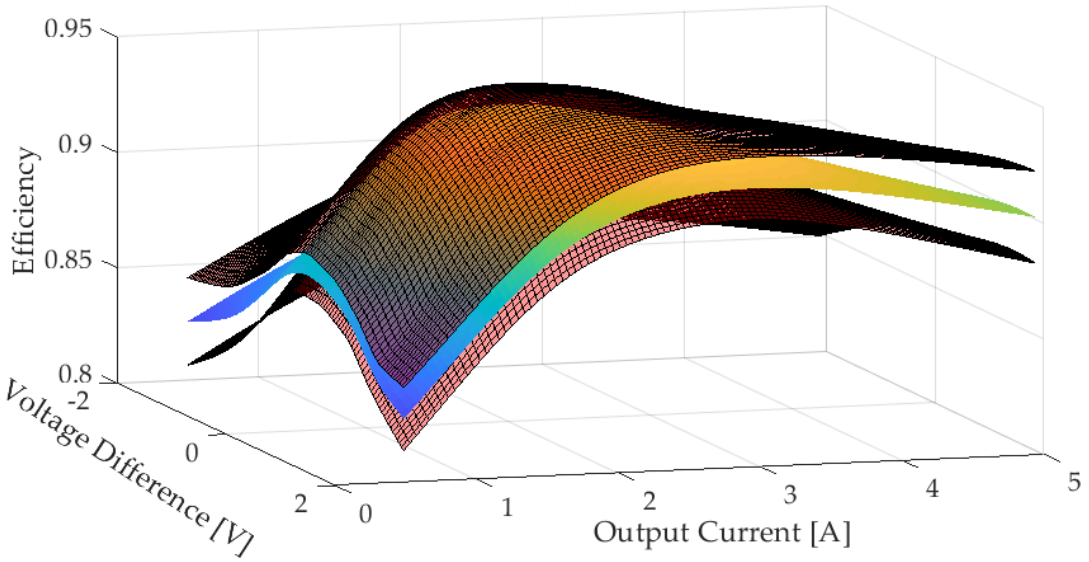

Figure 5.5 Prediction of the efficiency versus the output current and the voltage difference for the converter 421110 at: Vi= 18 V; Ambient temperature= 30 °C and air speed=5 m/s. Confidence intervals are also plotted with respect to model accuracy but also measurement tolerance.

5.3 PCA Selection - Virtual Prototyping

Virtual prototyping, in the context of this work, is the use of models to predict the performance of PCAs in order to compare solutions that perform a similar power conversion. This section will illustrate virtual prototyping by using the same example that was introduced in chapter 1, section 1.5, page 34. This example is composed of specifications for an isolated, bidirectional DC to DC converter that would interconnect a 120 V DC bus with a 36 V battery. The eight PACs that complied with all the initial specifications are recalled in Table 5.2.

Using the Gaussian Process Regression models developed in chapter 4, it is possible to compare all the solutions in Table 5.2 in more details. Figure 5.6 presents the efficiency of each PCA versus the battery voltage for a constant DC bus voltage of 120V. When charging the battery, the PCA operates in buck mode (from 120V to 36V) and while discharging the PCA operates in boost mode (from 36V to 120V). As the CSCs have a different efficiency when working in buck or in boost modes, the two charts present different results.

Table 5.2 PCAs that comply with the desired specifications

	#	Architecture	No. of CSCs	Configuration	Max. Power (W)	Max. Input voltage (V)	Max. Output voltage (V)	Code
GM5A-20V	1	2x6x1	12	PS-SP-0	1200	40	120	261120
	3	1x6x2	12	PS-0-SP	1200	40	120	162102
	4	2x3x2	12	PS-PS-SP	1200	40	120	232112
	6	3x2x2	12	SP-PS-PS	1200	40	120	322211
	9	2x7x1	14	PS-SP-0	1400	40	140	271120
	11	1x7x2	14	PS-0-SP	1400	40	140	172102
	12	2x4x2	16	PS-PS-SP	1600	40	160	242112
	13	4x2x2	16	PS-PS-SP	1600	40	160	422112

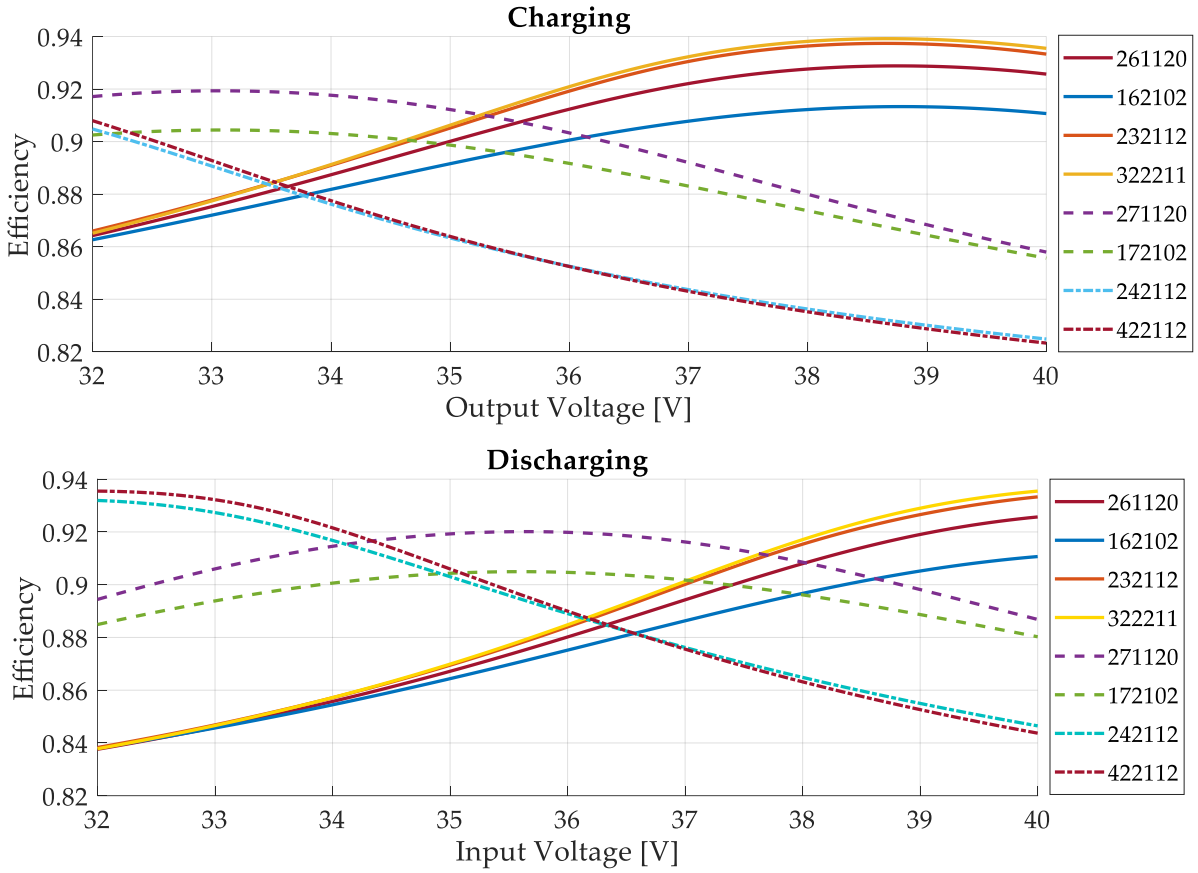

Figure 5.6 Efficiency versus the input voltage (charging sequence) and output voltage (discharging sequence) for all solutions that comply with the converter specifications presented in chapter 1. The other input variables are fixed at: Air speed = 5 m/s; Ambient temperature = 30 °C. In charging mode: Input voltage = 120 V, Input current = 6 A; In discharging mode: Output Voltage = 120 V Output current = 6 A.

Virtual prototyping is not limited to simply estimate a single point of operation for the PCAs. A more in-depth analysis of the performance of each PCA can be carried out by defining a mission profile. In the example above, the mission profile can be set by analysing the type of battery the converter will be connected to.

The battery cells used in the example above are the LIR18650 form the company EEMB [71]. In the battery cell datasheet, the charge and discharge curves are used to set up the mission profiles for the charge and the discharge sequences. The battery pack is made of 5 parallel connected groups of 9 cells connected in series. Its charge and discharge characteristic are shown in Figure 5.7.

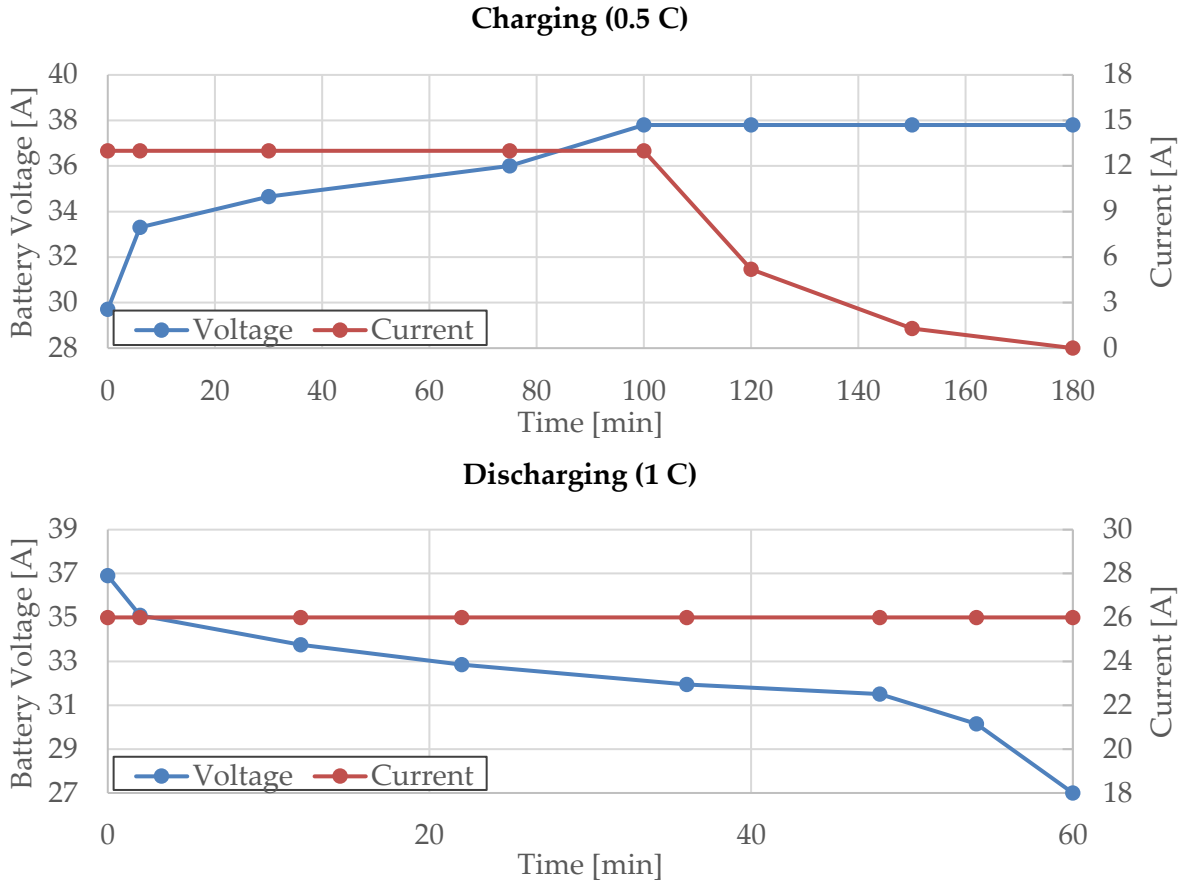

Figure 5.7 Mission profile of charging and discharging cycles of a battery pack containing 45 LIR18650 cells. The pack consists in 5 parallel connected groups of 9 cells connected in series.

Using the prediction models, it is possible to derive accurately the efficiency that each PCA has at each operating point (voltage and current) for the 180 minutes of the charging and the 60 minutes of the discharging sequences. Among the eight solutions, the three most efficient PCAs for different voltage levels were considered for comparison: 322211, 271120 and 422112. The instantaneous efficiency that each of these solutions presents during the charge and discharge cycles are presented in Figure 5.8.

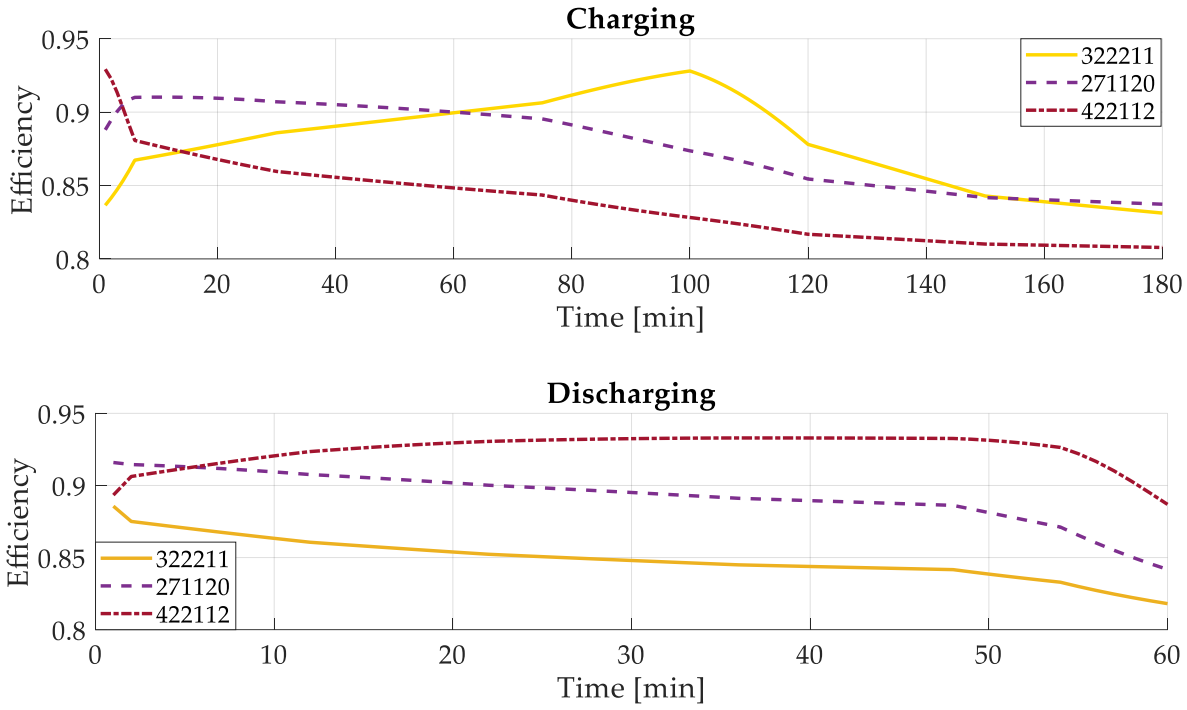

Figure 5.8 The instantaneous efficiency levels that each PCA presents during the 180 minutes of the charging sequence and the 60 minutes of the discharging sequence presented in Figure 5.6.

In charge mode, the battery passes most of the time between 34 V and 38 V. It can be seen in Figure 5.6 that the converters 322211 and 271120 present a better efficiency level in that output voltage range.

In discharge mode, the PCA 422112 outperforms the others. This can be explained by the fact that PCA 422112 is more efficient in boost mode compounded with the fact that it has 8 CSCs in parallel, lowering the overall current and thus allowing it to operate with the output voltage close to the input voltage.

In order to determine which PCA performs the best over an entire charge and discharge cycle, Figure 5.9 brings the instantaneous power losses each PCA dissipates over time for both cycles.

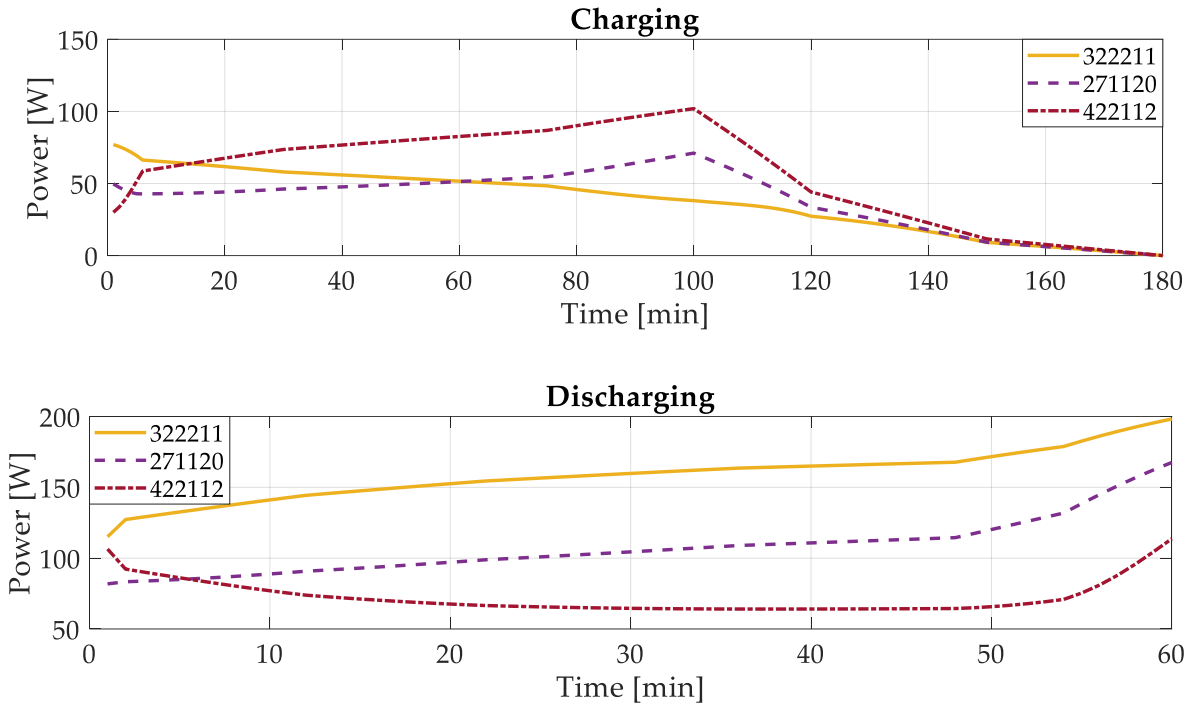

Figure 5.9 The instantaneous power losses that each PCA dissipates during the 180 minutes of the charging and the 60 minutes of discharge.

By integrating the instantaneous power losses, it is possible to calculate the total energy dissipated during each sequence and also during the whole 180+60 minutes charge discharge cycle for each PCA. The predictions are illustrated in Figure 5.10. Details are given in Table 5.3 for each PCA during charge, discharge and the whole mission profile. The table also brings the predictions made using the upper and lower boundaries of the 95% (indicated by U95% and L95%).

Table 5.3 Evaluation of the energy losses during the charging and discharging sequences and during the whole cycle for each tested PCA

Converter	Energy Loss while Charging [kJ]			Energy Loss while Discharging [kJ]			Total Energy Loss [kJ]		
	L95%	**Prediction**	U95%	L95%	**Prediction**	U95%	L95%	**Prediction**	U95%
322211	327	**401**	479	450	**585**	730	777	**986**	1209
271120	337	**424**	515	315	**401**	490	652	**825**	1005
422112	519	**635**	758	197	**237**	278	716	**872**	1036

The predictions show that a same PCA offers the best performance for each sequence. Figure 5.10 shows the predicted energy losses for each PCA for charge, discharge and the total mission profile. It shows that PCA 271120, which has an average performance in charging and discharging, ends up being the best option for the whole mission profile.

However, when the 95% confidence intervals are evaluated, it is not possible to draw a definitive conclusion on which converter is the best to perform the charge controller function. In order to better analyse the predictions and their associated boundaries data, three charts are

presented in Figure 5.10. It can be seen that for charging, PCA 322211 is certainly the best choice, and for discharging PCA 422112 is the best one. However, in total it is not possible to define the best one, as there is a significant amount of overlap among the predictions.

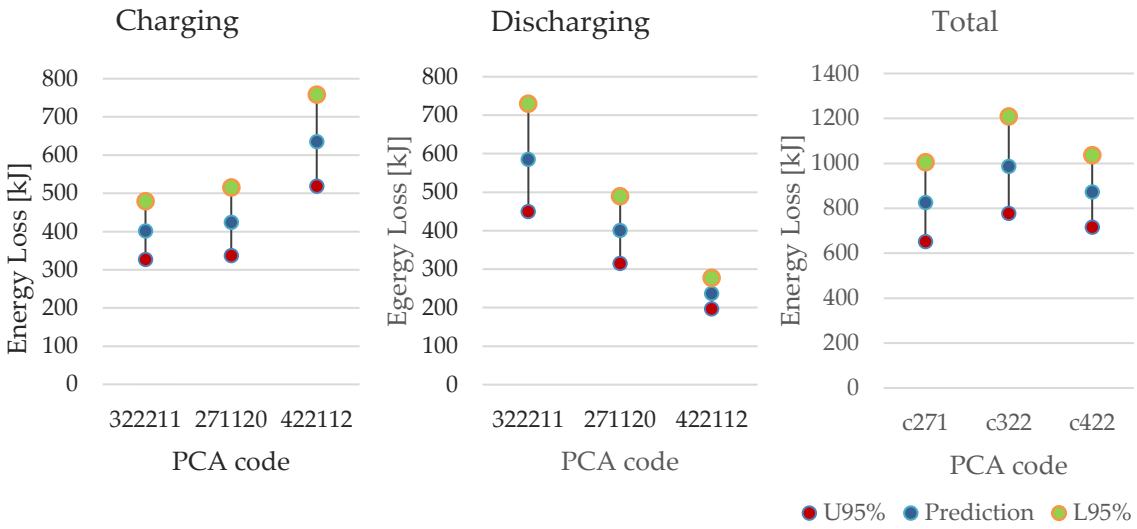

Figure 5.10 Energy loss prediction for each PCA and the upper and lower 95% confidence interval predictions

Model predictions outside the boundaries of the training data (extrapolation) have a very high level of incertitude. This is the case of this example, where several predictions were extrapolations. So it is safe to say that the incertitude of the proposed results of energy loss are quite large. Despite the inconclusive restults of this example, the method is coherent and efforts must be done in order to increase the precision of the predictions.

The same approach used to estimate and compare losses can be applied to PCA temperature. Table 5.4 lists the predicted maximum temperature that each PCA reach during the charging and discharging cycles. These predictions are made for a constant airspeed of 3 m/s. The results are shown in Table 5.4. It can be seen that, despite having less CSCs, and operating at higher currents, the 271120 present lower temperatures than the PCA 422122.

Table 5.4 Evaluation of the maximum temperature during the charging and discharging sequences for each tested PCA

Converter	Max temperature Charging [°C]	Max temperature Discharging [°C]
322211	51	63
271120	48	58
422112	56	59

Finally, the PCA ADFM also allows for a mechanical comparison of the different solutions. Figure 5.11 shows a 3D representation of the 3 PCAs. For example, PCA 271120 has a much

larger fan section due to its numerous columns. A next step would be to provide a more detailed pressure loss study in order to define which solution would require more power for cooling.

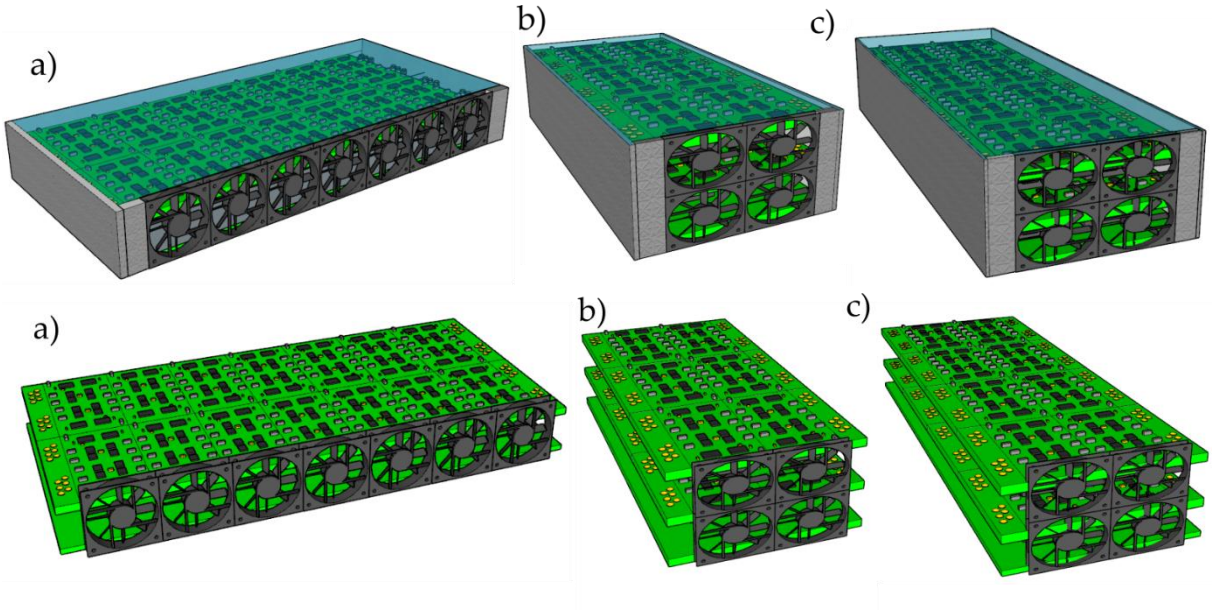

Figure 5.11 Artistic representation of the three PCAs compared: a) 271120, b) 322211, c) 422112

The example considered in this section is only a glimpse into the full design process using the APC ADFM method. More parameters still need to be studied and evaluated for the process of choosing the most suitable APC, such as EMI compliance, radiated and conducted, dynamic responses to voltage or load variations, hold time, overcharge capabilities to cite a few. This is a first step that needs to be completed with other studies as published in [72], [73].

5.4 Conclusion

This chapter on design rules and performance prediction presented how the statistical models developed in this work can be used to enhance the design and selection of Power Converter Array (PCA) solutions based on the G2Elab-Maatel Technology Platform.

These statistical models were shown to contribute to establish design rules based on the requirements for a PCA to operate inside its safe operating area. Thanks to the prediction models, it is possible to fine-tune the cooling conditions and design reliable PCA.

Virtual prototyping using these statistical models was also presented. As it was presented in chapter 1, page 35, several PCAs can be able to perform a same task. However, these PCAs naturally present different performances, physical and thermal characteristics. This chapter revisited three of these PCAs and presented a detailed comparison between them. The statistical models were used to predict the efficiency of the converters during a charge and

discharge cycle of a lithium-ion battery. From the results, energy loss was estimated for each PCA in order to help in selecting the best solution with respect to numerous criteria.

Losses prediction in power electronics is an important and yet very complex subject. The method used in this work, based on experimental data and statistical models, enables predictions with respect to electric, thermal and physical variables. The results presented in this chapter illustrate how compelling the PCA methodology can be when combined with accurate prediction models.

General Conclusion

Automated design methods in power electronics has been a topic of discussion in the scientific community for the past decades. While some methods have been proposed, mainly Power Electronics Building Blocks (PEBB) and Modular Multilevel Converters (MCC), the power electronics community failed to adopt these into a large scale or to trigger the equivalent of a Moore's Law in power electronics. This work has presented a new automated design method based on PEBB, MCC and the microelectronics industry design methods. This method was called Automated Design for Manufacturing (ADFM).

ADFM revisits the idea of what is a power converter and how to create it. A power converter is created from the interconnection of an array of conversion standard cells (CSC), thus creating a Power Converter Array (PCA). CSCs, together with other standard cells, compose a Technology Platform (TP). In theory, a designer using the ADFM goes from a set of specifications to the manufacturing files of the PCA through a fully automated process. This process includes virtual prototyping several PCAs and cross-comparing their performances. A thorough description of the ADFM is made in **chapter 1**.

The main objective of the thesis was to create statistical models that can predict the performance of any PCA built from a given technology platform. To achieve this goal, the work was divided into three parts: the design of experiments, the test bench setup and the statistical model selection.

The design of experiments was presented in **chapter 2**. The main idea behind selecting the quantity of experiments is to get the maximum amount of information while minimizing the number of experiments. In practice this meant choosing which prototypes to build, in order to save resources, and under which conditions should input and output variables be measured, to save time. A total of 15 prototypes where chosen to be built and a total of 360 operating points per converter to be measured. This chapter lists in details the methodology followed to achieve these results.

Chapter 3 presented the experimental test bench. Special attention was paid to controlling the thermal variables of the experiments, mainly the ambient temperature and the cooling condition of the converter. A set of experiments was detailed to validate the proper operation of the test bench and to determine the accuracy of the measurements. Overall accuracy was estimated at 0.36% for efficiency and 3 °C for temperature. Thanks to the automatic measurement procedure, eight converters were tested, 2548 measures were performed, totalizing over 210 hours of testing. The converters were built in the context of the Mamaatec project, financed by the Région Rhone Alpes.

All the data obtained was stored in a dataset, which is presented in details in **Chapter 4**. An introduction to statistical modelling and analysis of which modelling technique is most suited to perform the predictions was presented. The Gaussian process regression (GPR) was chosen, mainly due to three factors: it can easily handle many dimensions, it calculates the confidence interval of each prediction and it has a more physically coherent interpolation and extrapolation performances. GPR uses a covariance matrix (or kernel) to extract information

from its dataset. The chapter presented a comparison between four kernels, and their performances were tested for interpolation and extrapolation. Finally, the best kernel for predicting the efficiency was the squared exponential for interpolation and the exponential for extrapolation. The converter operating temperature results obtained using the exponential kernel for both interpolation and extrapolation.

Chapter 5 demonstrated how to use the models developed in chapter 4. The models were used to estimate the safe operating area for the PCAs built with the introduced TP. The models were also used to predict the thermal limit of PCAs for different operating scenarios. providing hindsight on the required cooling condition associated with each PCA for each scenario. Virtual prototyping was also emulated using the models. The result was a comparison of the efficiency rates of different PCAs under the same mission profile of charging and discharging a battery. The energy losses of the three most promising PCAs were cross compared. These results allowed a benchmark of the ADFM methodology proposed in this work.

The predictions made to compare the PCAs in the charge/discharge battery application presented a quite high level of incertitude. The main reason is that several operation points predicted by the model tried were extrapolations well beyond the boundaries of its dataset. For example, the voltage difference (DV) in the dataset is mainly concentrated in -1 V to +1.5 V, while in the battery predictions the DV varied from -5 V to 4 V. The decision of the tested range was made in chapter 2, in the definition of the DOE, if this range was increased, the predictions would have been more accurate.

Another field that can be investigated to improve the accuracy of the models is the kernels that compose the GPR. It is possible to test different methods to select the hyper parameters and even create hybrid kernels to extract more information on the data and represent more accurately the behaviour of the PCAs.

Perspectives

During the completion of this thesis, several ideas rose for applications either directly related to the ADFM-PCA method or related to other applications in power electronics.

- The same methodology used in this work (selection of experiments, realization of the experiments and fit of statistical models) can be applied to analyse other characteristics of PCAs. For example, dynamical response, electromagnetic compatibility, etc.
- Every new PCA created with the technology platform studied in this work can be tested in a set of operating points, this new data can be stored in the dataset, and new models can be fitted to enhance the accuracy that the model can bring about the TP.
- When the DOE was defined, there was no certainty that the measured points would be inside the safe operating area of the converter. Several tests resulted in converter failure, and then the DOE was updated by an interactive (destructive) process. Now, if it is desired to perform new experiments to enrich the model, it is possible to create a DOE and use the model created in this work in to predict if the selected experiences are inside the safe operating area or not.

- The test bench can be improved in order to be able to identify safely and automatically the SOA of the PCAs. For achieving this, the control of the converter must be significantly coupled with the test bench control, so the converter temperature can be used to set the operating points although it might be necessary to reach failure to identify the operation limit correctly.
- This work presented the base ideas to evaluate the thermal behaviour of the PCAs and correlate with the cooling implementation. However, many studies can emerge from this base. For example, if it is defined a relationship between the architecture of the PCA and the pressure loss of the forced air-cooling, it is possible to relate the power of the fan directly to the temperature of the PCA. These studies, coupled with the models presented in this thesis, can make automatically the cooling design and its implementation.
- The test bench developed in this thesis can be used to characterize any air-cooled PCB power converter. The automatic characterization process, considering electric and thermal variables can test the converter in several operating points, and the data can be used to generate a kind of "converter datasheet".

Résumé de la thèse

La conception et la fabrication des convertisseurs de puissance sont très coûteuses en termes de temps et argent. Plusieurs méthodes de conception ont été proposées par la communauté scientifique pour objectif à simplifier le processus. Parmi eux, les plus reconnus sont le « Power Electronics Building Blocks » (PEBB) et les « multicell converters » (MCC). Les deux proposent de simplifier et d'accélérer le design des convertisseurs en utilisant des blocks préconçus. Pourtant, les convertisseurs fabriqués en suivant ces méthodes ne représentent qu'un petit marché de la totalité de l'électronique de puissance.

Ce travail est une contribution au développement d'une nouvelle méthodologie de conception de convertisseurs inspirée des approches PEBB et MCC, mais aussi d'un formalisme à l'image de la micro-électronique digitale. Cette nouvelle méthodologie s'appelle « Automate Design for Manufacture » (ADFM) et conduit à la synthèse de réseaux de convertisseurs.

Via l'ADFM un convertisseur n'est plus une pièce issue d'une ingénierie multidisciplinaire, mais un assemblage simple d'éléments normalisés maîtrisés et fiables. De plus, l'ADFM introduit une forme de prototypage virtuel permettant d'estimer les caractéristiques de tous types d'assemblages de cellules standards (CSs). En quelques minutes, l'utilisateur peut générer des fichiers de fabrication. Le résultat est un réseau de convertisseurs aussi appelé « Power Converter Array » (PCA) en langue anglaise aux caractéristiques conformes au cahier des charges.

La clé pour le prototypage virtuel d'un PCA c'est l'utilisation d'une « Technology Platform » (TP) mature, pièce centrale de la démarche ADFM. La maturité d'une TP signifie la caractérisation et la description minutieuse de chaque cellule standard une fois qu'elles sont dans des versions stables et industrialisées.

La caractérisation d'une TP mature est traduite en données. Ces données sont utilisées pour la création de modèles capables d'interpoler les comportements électriques et thermiques de tout PCA réalisable par la technologie quelque(s) soit(ent) son (ses) points d'opération dans le l'espace de caractérisation. Les mêmes modèles peuvent aussi extrapoler, avec un certain niveau de certitude, le comportement des PCAs plus « exotiques » au-delà de l'espace de caractérisation de la TP. L'objectif de cette thèse est de faire l'acquisition des données nécessaires pour la création de ces modèles.

Pour répondre à cet objectif, cette thèse est focalisée sur l'étude de deux caractéristiques d'un convertisseur de puissance : son rendement et sa température de fonctionnement. Ces paramètres seront interpolés ou extrapolées par des modèles statistiques entrainées par une grande base de données acquise de façon expérimentale, en suivant un plan d'expérience et en utilisant un banc de caractérisation automatique.

Chapitre I

Ce chapitre apporte un résumé de l'état de l'art des convertisseurs modulaires/multicell. Les points en commun et les différences entre les méthodes de conception existantes et le méthode ADFM sont mis en évidence. La Figure R1 présente les principaux éléments de la méthode ADFM.

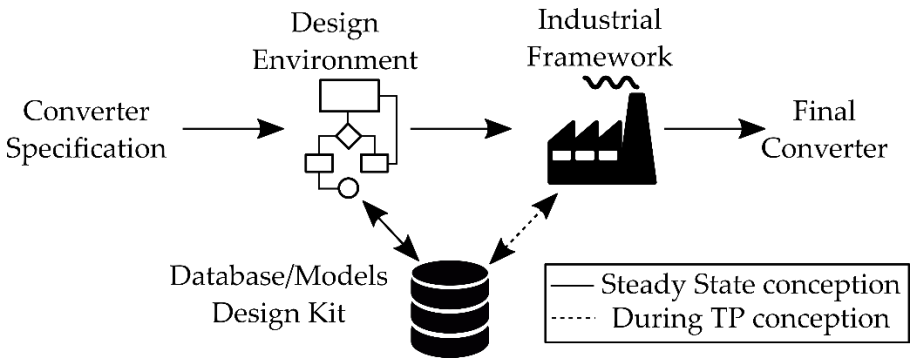

Figure R1. Les trois piliers de la démarche ADFM.

La méthode est divisée en trois piliers :

- L'environnement de conception, avec l'ensemble des outils pour la synthèse, le layout, les vérifications et extractions.
- La filière technologique et le procédé de fabrication ainsi que les familles de standard-cells déjà caractérisées, prêtes à être assemblées.
- Le design kit et les modèles relatifs à la filière technologique, lesquels seront utilisés pour décrire, concevoir et prédire tous les aspects des PCAs.

Le chapitre décrit comment un convertisseur peut être divisé en une famille de cellules standards et comment une filière technologique doit être structurée. Ensuite, est présentée la filière technologique avec laquelle la suite de la thèse est développée : la TP G2Elab-Maatel (GM). C'est dans le cadre du projet Mamaatec soutenu par la région Rhône Alpes Auvergne que ces travaux sont menés, sur une plateforme technologique, développée en partenariat avec la société Maatel.

La cellule standard de conversion CSC de la filière technologique GM est présentée à la Figure R2. Constituée d'un dual active bridge, cette CSC peut convertir un puissance allant jusqu'à 100 W.

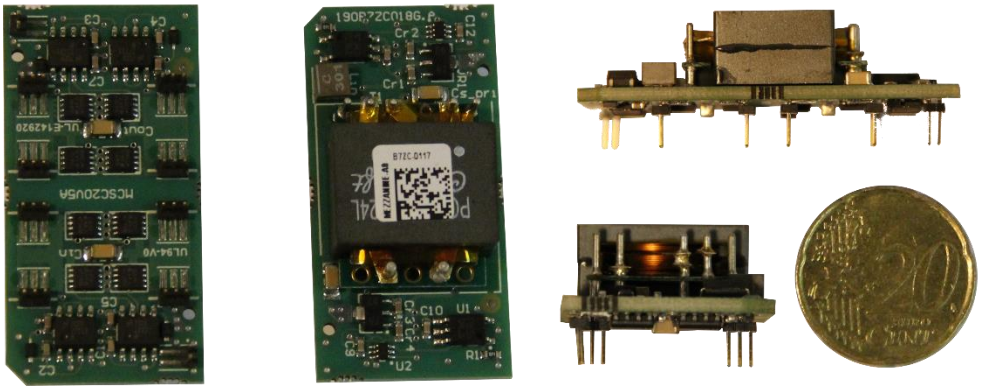

Figure R2. La cellule standard de conversion de la filière technologique G2ELab Maatel.

Pour illustrer la démarche complète d'un cahier des charges jusqu'à la synthèse d'un PCA, la suite du chapitre I développe un exemple d'un convertisseur conçu pour réaliser la connexion d'un BUS DC 120 V a un pack de batteries de 32 V à 40 V. L'environnement propose 20 solutions possibles avec des PCAs capables ou proches de répondre au besoin. Pour illustrer le fonctionnement d'un PCA, une solution est construite et testée à puissance nominale. Le PCA testé est présenté sur la Figure R3. Ce PCA a une architecture 4x2x2 (4 lignes, 2 colonnes, 2 cartes) et une configuration PS-SP-SP (colonnes connectées en parallèle-série, lignes reliés en série-parallèle, cartes reliées en série parallèle). Les tests à puissance nominale sont présentés en Figure R4a) en ventilation forcée, et Figure R4b) en convection naturelle.

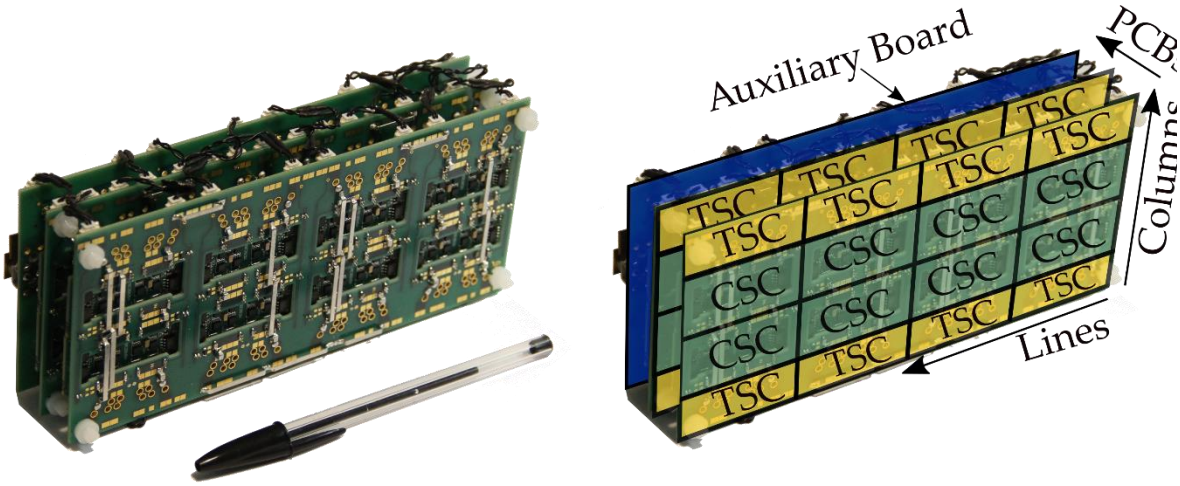

Figure R3. PCA construite pour réaliser la connexion DC/DC entre un bus 120 V à un pack de batteries 32 à 40 V.

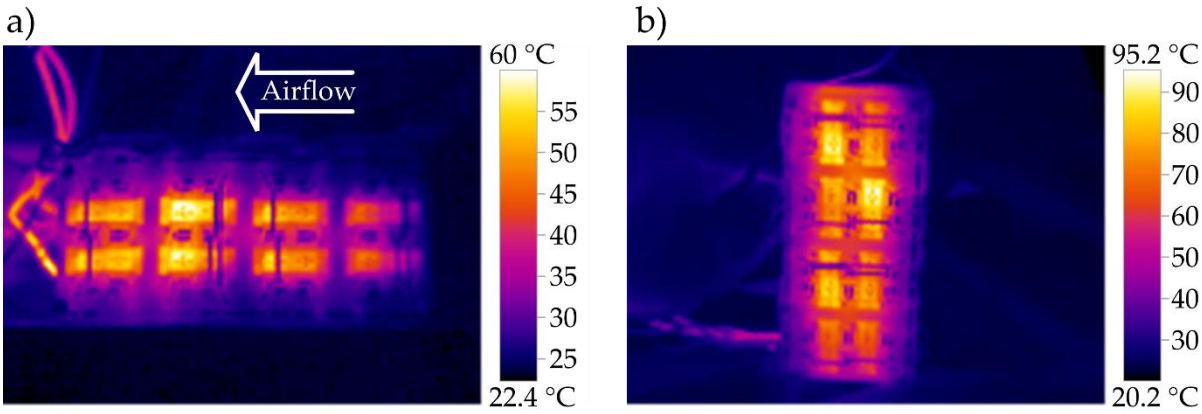

Figure R4. Tests réalisés avec le PCA conçu puis réalisé en a) puissance nominale avec ventilation forcée, b) convection naturelle.

Chapitre II

Ce chapitre présente la définition des variables d'entrée et de sortie qui seront prises en compte pour la caractérisation des PCAs. Onze variables d'entrée sont considérées, elles sont divisées en deux groupes:
Variables du point de fonctionnement du convertisseur: Tension d'entrée (Vi), tension de sortie (Vo), courant de sortie (Io), température ambiente (Ta) et vitesse d'écoulement du fluide de refroidissement (Aspeed)
Variables de construction: Architecture et configuration du PCA.
Le plan d'expérience doit choisir un nombre réduit de points pour minimiser la durée du test et la quantité des prototypes à caractériser. Pour choisir les points de fonctionnement, le travail suit une stratégie simple et robuste pour réaliser un ensemble de tests en modifiant une variable à la fois "one variable at a time". Les variables et leurs plages de variation sont présentées sur la table R1.

Table R.1 Plages de variation du test "One variable at a time".

	Variables d'entrée				
Setup	Io	Vi	DV	Ta	Aspeed
I	0.5 to 4.5 A	Fixed	Fixed	Fixed	Fixed
II	Fixed	10 to 19 V	Fixed	Fixed	Fixed
III	Fixed	Fixed	-2 to 2 V	Fixed	Fixed
IV	Fixed	Fixed	Fixed	20 to 70 °C	Fixed
V	Fixed	Fixed	Fixed	Fixed	2 to 12 m/s

Après une analyse des résultats avec trois prototypes différents, les points choisis par la méthode sont présentés sur la table R2.

Table R.2 Points choisis par la méthode.

Operation Point				
Vi [V]	**DV [V]**	**Io [A]**	**Air [m/s]**	**Tamb [°C]**
[10; 14; 18]	[-1; 0; 0.5; 1;1.5]	[0.75; 1.5;2;3.5]	[2; 4; 8]	[30; 55]

Chapitre III

Ce chapitre est consacré à définir les besoins expérimentaux pour réaliser tous les tests définis au plan d'expérience de façon précise, reproductible et automatique. La figure R5 présente un schémas global des tests, soulignant tous les équipements nécessaires.

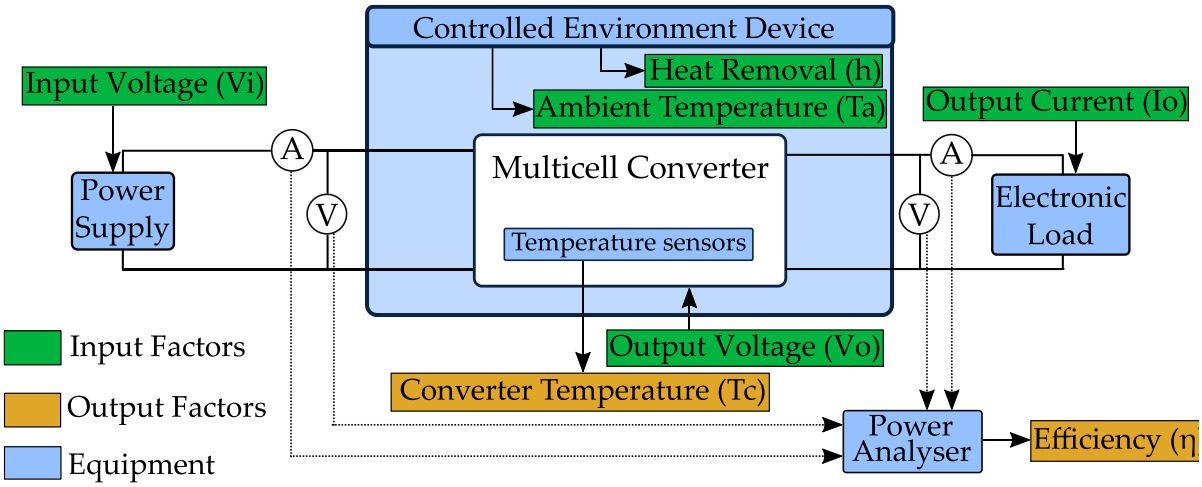

Figure R5. Vue globale des variables d'entrée et de sortie à contrôler et mesurer pour caractériser une plateforme technologique et ensemble des équipements nécessaires.

Une grande partie du chapitre détaille la construction d'une tuyère, utilisée pour mettre les PCA dans des conditions plus proches de la réalité. La tuyère est capable de régler la température ambiante, la vitesse du flux d'air qui traverse les dispositifs sous test. Les images de la tuyère complète sont présentées sur la figure R6.

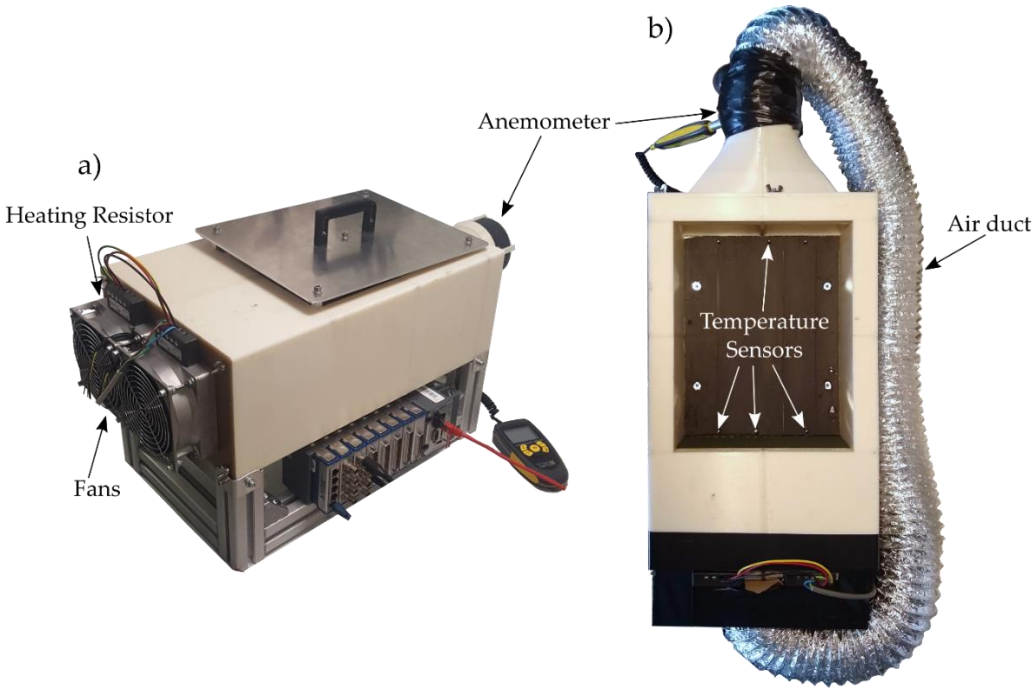

Figure R6. a) Tuyère. b) Vue de dessus de la tuyère ainsi que de son conduit de recyclage d'air chaud.

Le chapitre présente en détails la calibration et la validation du dispositif complet. Plusieurs tests permettant d'identifier la dynamique de changement des consignes sont réalisés. Pour finir toutes les mesures déterminées par le plan d'expérience sont réalisés.

Chapitre IV

Avec les 2500 mesures stockées dans une base de données, le chapitre présente la conception d'un modèle statistique capable de prédire le fonctionnement de tout un espace de PCAs multi dimensions. Initialement le chapitre présente plusieurs techniques de modèlisation statistiques. En fin de chapitre, la méthode "Gaussian Process Regression" est choisie. Cette méthode Meta-paramétrique, basée sur la probabilité Bayésienne, est capable de trouver la fonction la plus probable de représenter une base de données issue de la caractérisation multi dimensions.
Pour créer un GPR, il est nécessaire de choisir un 'kernel'. Différents kernels peuvent rendre le modèle plus ou moins flexible. Le chapitre présente une comparaison entre 4 kernels différents. les résultats de prédiction avec les 4 kernels du rendement versus le courant de sortie sont présentés sur la figure R7.

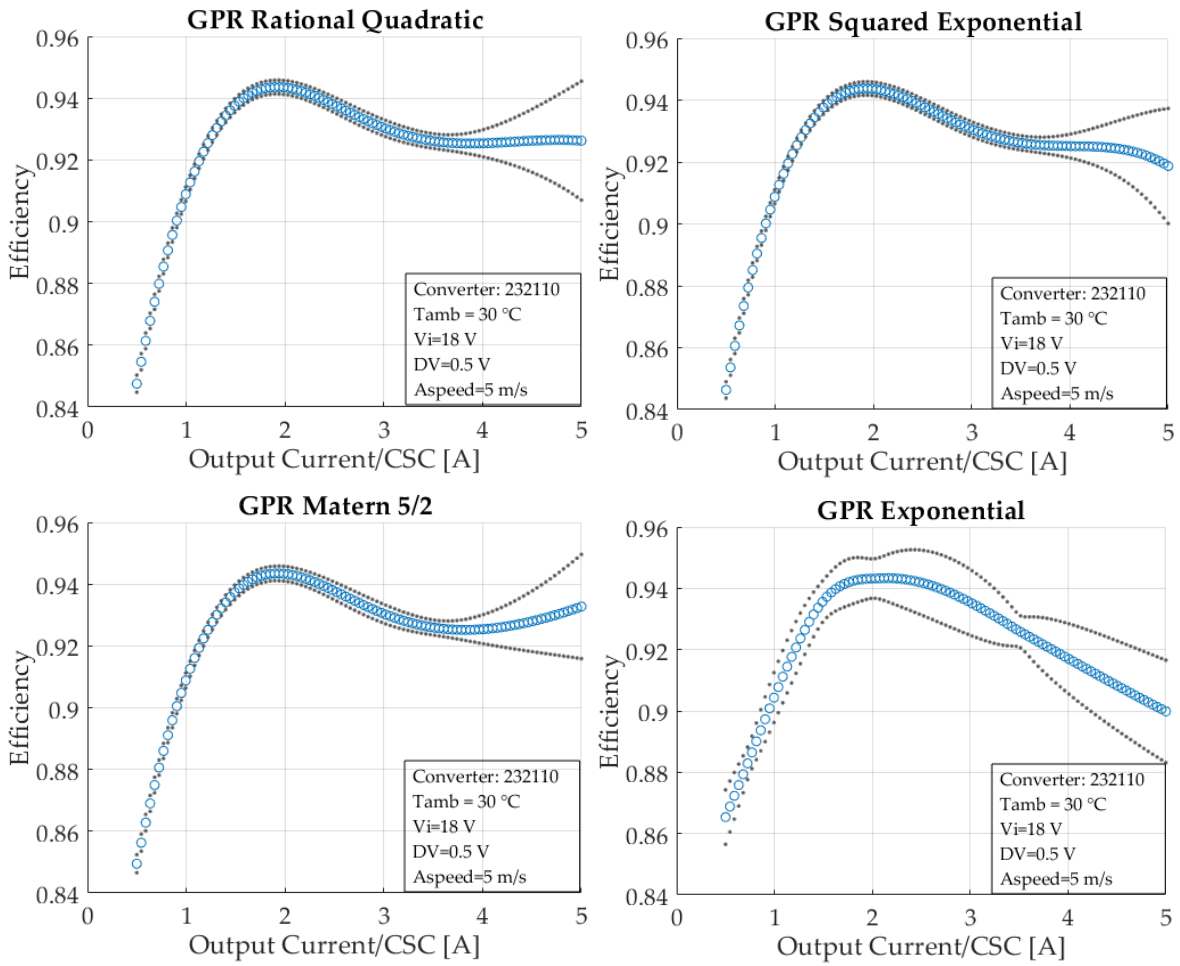

Figure R7. Prédictions du rendement versus le courant de sortie pour 4 kernels différentes. Cercles blues : valeurs de prédiction. Points gris : l'intervalle de confiance à 95 %. Le code 232110 veut dire: 2 lignes, 3 colonnes, 1 carte, 1D: IPOS, 2D: IPOS, 3D: NC.

Pour comparer la qualité des modèles et valider leur précision, un nouveau PCA est construit et caractérisé en 139 points de fonctionnement, en 9 itérations, totalisant 1240 mesures. Chaque mesure est comparée à la prédiction des modèles obtenues pour les 4 différents kernels. Le résultat de cette comparaison est présenté dans la figure R8.

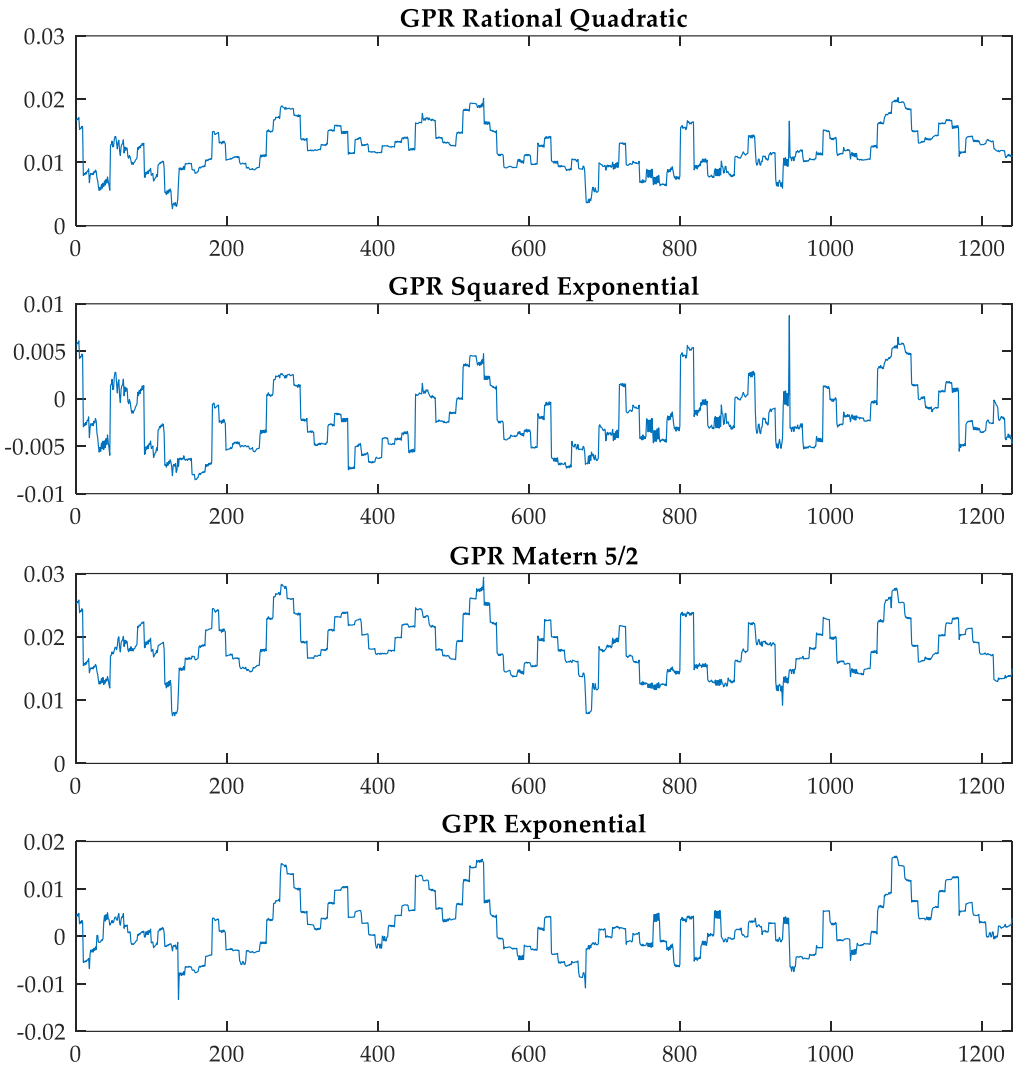

Figure R8. Erreur sur le rendement (Rendement prédit – rendement mesuré) que chaque modèle présente pour les 1240 points de mesure réalisés sur le prototype 431110. L'axe Y est un pourcentage de rendement.

Le modèle qui utilise le kernel « Squared Exponential » produit l'erreur efficace la plus faible. Ce modèle est donc sélectionné comme modèle de prédiction dans la zone d'interpolation. Les modèles ont ensuite été testés pour réaliser des prédictions dans la zone d'extrapolation et là c'est le modèle avec le kernel « exponential » qui a eu les meilleurs résultats. La figure R9 présente certaines extrapolations faites avec le modèle.

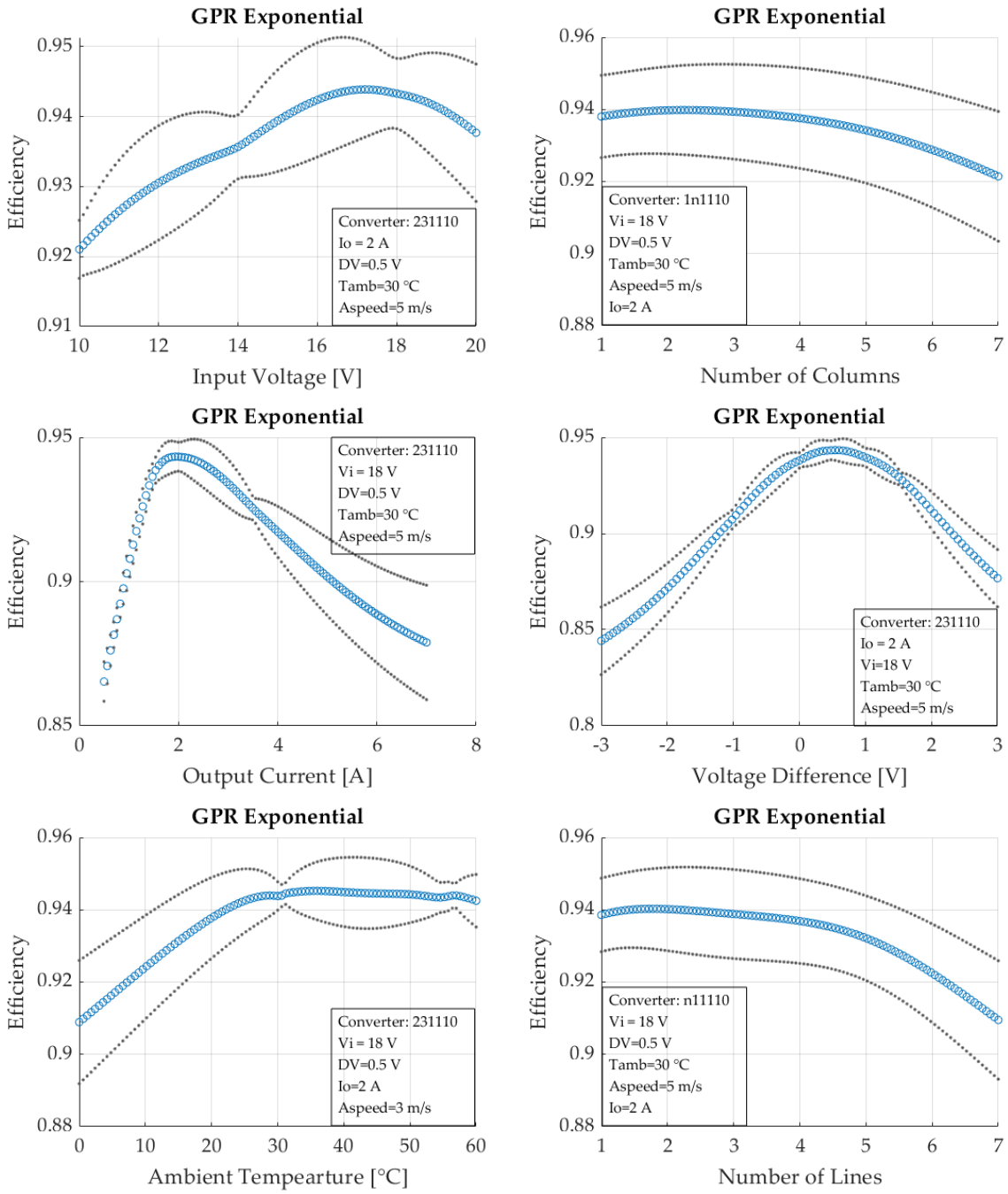

Figure R9. Prédictions dans les limites des extrapolations. Les données d'entrée pour chaque test sont détaillées à l'intérieur du rectangle.

Chapitre V

Une fois les modèles de prédiction définis, le chapitre 5 les met en application pour réaliser du prototypage virtuel. La figure R10 présente des prédictions de la température d'un PCA en fonction du courant de sortie, soumis à différentes vitesses d'écoulement d'air et à différentes températures ambiantes. Les graphiques illustrent aussi la « Safe operating area », définie, dans ces cas, au-dessous de 90 °C.

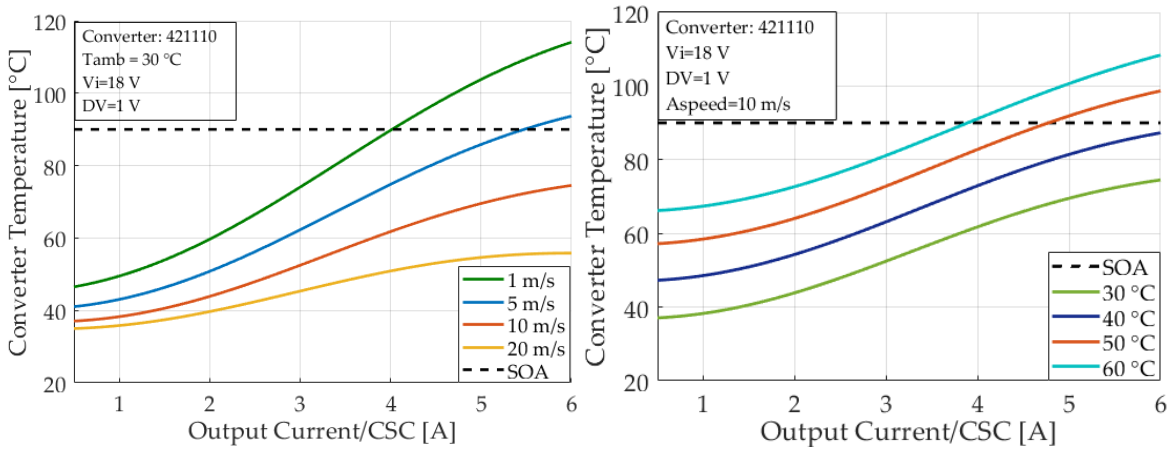

Figure R10.Safe operating area d'un ACP en fonction du courant de sortie. A gauche : courbes pour plusieurs valeurs de la vitesse de l'air. A droite : courbes pour plusieurs températures ambiantes.

La figure R11 apporte des informations concernant l'impact de l'architecture (nombre de lignes) sur la température d'un PCA. Également, les graphiques montrent la zone d'opération sécurisée dans laquelle le PCA est censé travailler sans risque.

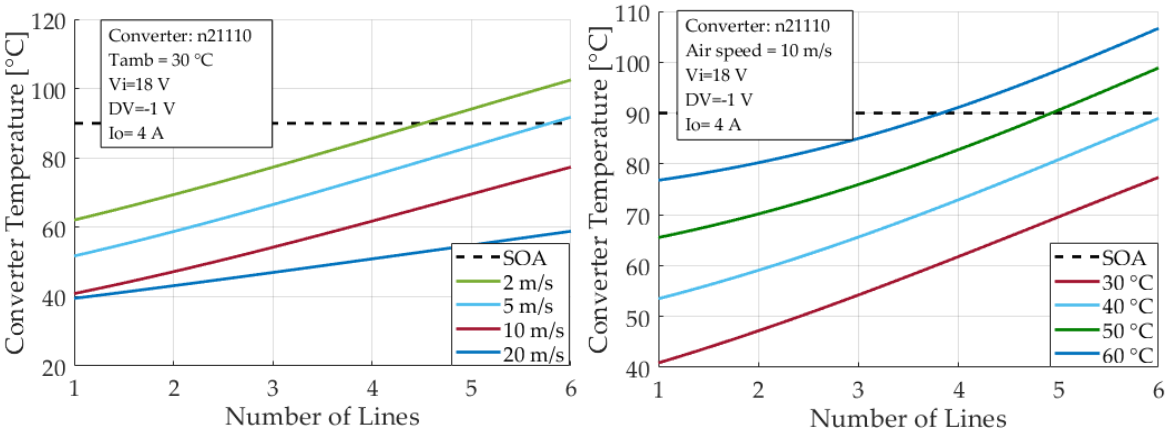

Figure R11.Safe operating area d'un PCA par rapport au nombre de lignes. A gauche : courbes pour différentes valeurs de la vitesse de l'air. A droite : courbes pour différentes températures ambiantes.

Enfin, le chapitre reprend l'exemple du chargeur de batterie présenté au chapitre 1. Cette fois, avec l'aide des modèles, il est possible à prédire les performances que chaque PCAs va avoir pour les points de fonctionnements correspondant au profil de mission de recharge un pack de batteries.

Conclusion

Cette thèse a présenté une nouvelle méthode de conception des convertisseurs de puissance appelée « Automatic design for manufacturing » (ADFM) en électronique de puissance. Le principal objectif de la thèse est de créer des modèles statistiques permettant de prédire les performances de n'importe quel PCA conçu à partir d'une plateforme technologique G2ELab/Maatel, dans le cadre du projet région Mamaatec. Pour atteindre cet objectif, les travaux ont été divisés en trois étapes : la construction d'un plan d'expérience, la construction d'une plateforme expérimentale et la création des modèles statistiques.
Les principales contributions de ce travail sont :

- La structuration et la formalisation de la démarche « Automatic design for manufaturing »
- La validation expérimentale du fonctionnement des convertisseurs (PCAs) conçus de façon automatique
- La proposition d'une méthodologie pour définir un plan d'expérience avec plusieurs variables d'entrée et sortie pour la caractérisation de convertisseurs de puissance
- La construction d'un dispositif de tests de convertisseurs de puissance refroidis par air recréant les conditions de fonctionnement d'une application réelle.
- L'utilisation d'algorithmes d'apprentissage automatique pour la modélisation en électronique de puissance
- La génération d'un ensemble de modèles statistiques pour la plateforme technologique G2Elab/Maatel.

References

[1] C. C. Harskind and M. M. Morack, “A History of Mercury-Arc Rectifiers in North America,” *IEEE Ind. Appl. Soc. Piscataway NJ Publ. TH*, pp. 201–207, 1987.

[2] B. Bose, “The past, present, and future of power electronics [Guest Introduction],” *IEEE Ind. Electron. Mag.*, vol. 3, no. 2, pp. 7–11, 14, Jun. 2009.

[3] B. K. Bose, “Power Electronics, Smart Grid, and Renewable Energy Systems,” *Proc. IEEE*, vol. 105, no. 11, pp. 2011–2018, Nov. 2017.

[4] N. Holonyak, “The silicon pnpn switch and controlled rectifier (thyristor),” *IEEE Trans. Power Electron.*, vol. 16, no. 1, pp. 8–16, 2001.

[5] P. Friedrichs *et al.*, “ECPE Position Paper on Next Generation Power Electronics based on Wide Bandgap Devices.” Jul-2016.

[6] D. Boroyevich, R. Burgos, L. Arnedo, and F. Wang, “Synthesis and Integration of Future Electronic Power Distribution Systems,” in *2007 Power Conversion Conference - Nagoya*, 2007, p. K-1.

[7] D.-B. Nguyen, “Intégration fonctionnelle autour des composants quatre quadrants Avec l’application à la conversion AC/AC,” Université Grenoble Alpes, Doctoral dissertation, 2008.

[8] T. Ericsen and A. Tucker, “Power Electronics Building Blocks and potential power modulator applications,” in *Conference Record of the Twenty-Third International Power Modulator Symposium (Cat. No. 98CH36133)*, 1998, pp. 12–15.

[9] T. Ericsen, “Power Electronic Building Blocks-a systematic approach to power electronics,” in *2000 Power Engineering Society Summer Meeting (Cat. No.00CH37134)*, 2000, vol. 2, pp. 1216–1218 vol. 2.

[10] F. C. Lee, “Power electronics building block and system integration,” in *Proceedings IPEMC 2000. Third International Power Electronics and Motion Control Conference (IEEE Cat. No.00EX435)*, 2000, vol. 1, pp. 1–8 vol.1.

[11] F. Wang, S. Rosado, T. Thacker, and D. Boroyevich, “Power electronics building blocks for utility power system applications,” *Power Electron. Motion Control Conf. 2004 IPEMC 2004 4th Int.*, vol. 1, pp. 354--359 Vol.1, 2004.

[12] F. Mariut, S. Rosu, and R. B. A. Tenconi, “Multiphase modular power converter using the PEBB concept and FPGA-based direct high speed voltage measurement,” in *2015 17th European Conference on Power Electronics and Applications (EPE’15 ECCE-Europe)*, 2015, pp. 1–10.

[13] A. R. Iyer, R. P. Kandula, R. Moghe, J. E. Hernandez, F. C. Lambert, and D. Divan, “Validation of the Plug-and-Play AC/AC Power Electronics Building Block (AC-PEBB) for Medium-Voltage Grid Control Applications,” *IEEE Trans. Ind. Appl.*, vol. 50, no. 5, pp. 3549–3557, Sep. 2014.

[14] F. Wang, Z. Zhang, T. Ericsen, R. Raju, R. Burgos, and D. Boroyevich, “Advances in Power Conversion and Drives for Shipboard Systems,” *Proc. IEEE*, vol. 103, no. 12, pp. 2285–2311, 2015.

[15] M. S. Ortmann, W. Hoffmann, S. A. Mussa, and M. L. Heldwein, “Multilevel multistate switching cells PEBBs as the basis for the implementation of advanced rectifiers,” in *2013 Twenty-Eighth Annual IEEE Applied Power Electronics Conference and Exposition (APEC)*, 2013, pp. 1871–1877.

[16] C. Klumpner, F. Blaabjerg, and P. Nielsen, “Speeding-up the maturation process of the matrix converter technology,” in *2001 IEEE 32nd Annual Power Electronics Specialists Conference (IEEE Cat. No.01CH37230)*, 2001, vol. 2, pp. 1083–1088 vol.2.

[17] M. Liserre, T. Sauter, and J. Hung, “Future Energy Systems: Integrating Renewable Energy Sources into the Smart Power Grid Through Industrial Electronics,” *IEEE Ind. Electron. Mag.*, vol. 4, no. 1, pp. 18–37, Mar. 2010.

[18] J. Chivite-Zabalza, I. Larrazabal, I. Zubimendi, S. Aurtenetxea, and M. Zabaleta, "Multi-megawatt wind turbine converter configurations suitable for off-shore applications, combining 3-L NPC PEBBs," in *2013 IEEE Energy Conversion Congress and Exposition*, 2013, pp. 2635–2640.
[19] I. Cvetkovic *et al.*, "Modular scalable medium-voltage impedance measurement unit using 10 kV SiC MOSFET PEBBs," in *2015 IEEE Electric Ship Technologies Symposium (ESTS)*, 2015, pp. 326–331.
[20] P. K. Steimer, B. Oedegard, O. Apeldoorn, S. Bernet, and T. Brückner, "Very high power IGCT PEBB technology," in *2005 IEEE 36th Power Electronics Specialists Conference*, 2005, pp. 1–7.
[21] D. Boroyevich, "Building block integration in power electronics," in *2010 IEEE International Symposium on Industrial Electronics*, 2010, pp. 3673–3678.
[22] D. Boroyevich *et al.*, "IPEM-based power electronics system integration," in *5th International Conference on Integrated Power Electronics Systems*, 2008, pp. 1–10.
[23] R. Chen, F. Canales, B. Yang, and J. D. vanWyk, "Volumetric Optimal Design of Passive Integrated Power Electronics Module (IPEM) for Distributed Power System (DPS) Front-End DC/DC Converter," *IEEE Trans. Ind. Appl.*, vol. 41, no. 1, pp. 9–17, Jan. 2005.
[24] ABB, "ACS 6000 datasheet." ABB, 2008.
[25] P. Steimer, O. Apeldoorn, and E. Carroll, "IGCT devices-applications and future opportunities," in *2000 Power Engineering Society Summer Meeting (Cat. No. 00CH37134)*, 2000, vol. 2, pp. 1223–1228.
[26] T. A. Meynard and H. Foch, "Multi-level conversion: high voltage choppers and voltage-source inverters," in *PESC '92 Record. 23rd Annual IEEE Power Electronics Specialists Conference*, 1992, pp. 397–403 vol.1.
[27] G. Gateau, P. Maussion, and T. Meynard, "Fuzzy phase control of series multicell converters," in *Proceedings of 6th International Fuzzy Systems Conference*, 1997, vol. 3, pp. 1627–1633.
[28] T. A. Meynard, H. Foch, P. Thomas, J. Courault, R. Jakob, and M. Nahrstaedt, "Multicell converters: basic concepts and industry applications," *IEEE Trans. Ind. Electron.*, vol. 49, no. 5, pp. 955–964, Oct. 2002.
[29] Y. Lei *et al.*, "A 2 kW, single-phase, 7-level, GaN inverter with an active energy buffer achieving 216 W/in3 power density and 97.6% peak efficiency," in *2016 IEEE Applied Power Electronics Conference and Exposition (APEC)*, 2016, pp. 1512–1519.
[30] Z. Liao, Y. Lei, and R. C. N. Pilawa-Podgurski, "Analysis and Design of a High Power Density Flying-Capacitor Multilevel Boost Converter for High Step-Up Conversion," *IEEE Trans. Power Electron.*, vol. 34, no. 5, pp. 4087–4099, May 2019.
[31] H. Ertl, J. W. Kolar, and F. C. Zach, "A novel multicell DC-AC converter for applications in renewable energy systems," *IEEE Trans. Ind. Electron.*, vol. 49, no. 5, pp. 1048–1057, Oct. 2002.
[32] M. Kasper, D. Bortis, and J. W. Kolar, "Scaling and balancing of multi-cell converters," in *2014 International Power Electronics Conference (IPEC-Hiroshima 2014 - ECCE ASIA)*, 2014, pp. 2079–2086.
[33] S. Busquets-Monge and L. Caballero, "Switching-Cell Arrays—An Alternative Design Approach in Power Conversion," *IEEE Trans. Ind. Electron.*, vol. 66, no. 1, pp. 25–36, Jan. 2019.
[34] M. Kasper, D. Bortis, G. Deboy, and J. W. Kolar, "Design of a Highly Efficient (97.7%) and Very Compact (2.2 kW/dm3) Isolated AC–DC Telecom Power Supply Module Based on the Multicell ISOP Converter Approach," *IEEE Trans. Power Electron.*, vol. 32, no. 10, pp. 7750–7769, Oct. 2017.
[35] U. Badstuebner, J. Miniboeck, and J. W. Kolar, "Experimental verification of the efficiency/power-density (η-ρ) Pareto Front of single-phase double-boost and TCM PFC

rectifier systems," in *2013 Twenty-Eighth Annual IEEE Applied Power Electronics Conference and Exposition (APEC)*, 2013, pp. 1050–1057.
[36] M. Moosavi and H. A. Toliyat, "A Multicell Cascaded High-Frequency Link Inverter With Soft Switching and Isolation," *IEEE Trans. Ind. Electron.*, vol. 66, no. 4, pp. 2518–2528, Apr. 2019.
[37] A. Bindra and A. Mantooth, "Modern Tool Limitations in Design Automation: Advancing Automation in Design Tools is Gathering Momentum," *IEEE Power Electron. Mag.*, vol. 6, no. 1, pp. 28–33, Mar. 2019.
[38] M. Delhommais, J. Schanen, F. Wurtz, C. Rigaud, and S. Chardon, "First order design by optimization method: Application to an interleaved buck converter and validation," in *2018 IEEE Applied Power Electronics Conference and Exposition (APEC)*, 2018, pp. 944–951.
[39] "POWERFORGE, Multi-level by design," *[Acessed Jul. 2019]*. [Online]. Available: https://powerdesign.tech/product/.
[40] T. M. Evans *et al.*, "PowerSynth: A Power Module Layout Generation Tool," *IEEE Trans. Power Electron.*, vol. 34, no. 6, pp. 5063–5078, Jun. 2019.
[41] H. Dang Thai, "Reseaux de micro-convertisseurs," Institut National Polytechnique de Grenoble - INPG, Doctoral dissertation, 2009.
[42] O. Deleage, "Conception, réalisation et mise en oeuvre d'un micro-convertisseur intégré pour la conversion DC/DC," Sciences de l'ingénieur [physics], Université Joseph-Fourier - Grenoble I, Doctoral dissertation, 2009.
[43] T. Hieu Trinh, "Réeseaux de micro convertisseurs, les premiers pas vers le circuit de puissance programmable," Energie electrique, Université de Grenoble, Doctoral dissertation, 2013.
[44] L. Kerachev, "Technologies de mise en oeuvre et stratégies de configuration de réseaux de micro-convertisseurs - Application au photovoltaique," Autre, Université Grenoble Alpes, Doctoral dissertation, 2013.
[45] T. Hai Phung, "Conception d'un équilibreur de charge de batterie à base du réseau de micro-convertisseurs," Autre, Université Grenoble Alpes, Doctoral dissertation, 2013.
[46] T. Lamorelle, A. Andreta, Y. Lembeye, J.-C. Crébier, and J.-C. Podvin, "Design level power electronics building block: Industrial framework for DC-DC conversion," in *2018 IEEE International Conference on Industrial Technology (ICIT)*, 2018, pp. 670–675.
[47] J. Wang, V. Veliadis, J. Zhang, Y. Alsmadi, P. R. Wilson, and M. J. Scott, "IEEE ITRW Working Group Position Paper-System Integration and Application: Silicon Carbide: A Roadmap for Silicon Carbide Adoption in Power Conversion Applications," *IEEE Power Electron. Mag.*, vol. 5, no. 2, pp. 40–44, Jun. 2018.
[48] H. Amano, "The 2018 GaN power electronics roadmap," *J. Phys. Appl. Phys.*, vol. 51, 2018.
[49] D. Bortis, D. Neumayr, and J. W. Kolar, "ηρ-Pareto optimization and comparative evaluation of inverter concepts considered for the GOOGLE Little Box Challenge," in *2016 IEEE 17th Workshop on Control and Modeling for Power Electronics (COMPEL)*, 2016, pp. 1–5.
[50] R. Ghosh *et al.*, "Industrial Approach to Design a 2-kVa Inverter for Google Little Box Challenge," *IEEE Trans. Ind. Electron.*, vol. 65, no. 7, pp. 5539–5549, Jul. 2018.
[51] L. Zhang, R. Born, X. Zhao, and J. Lai, "A high efficiency inverter design for Google little box challenge," in *2015 IEEE 3rd Workshop on Wide Bandgap Power Devices and Applications (WiPDA)*, 2015, pp. 319–322.
[52] C. W. Halsted and M. D. Manjrekar, "A Critique of Little Box Challenge Inverter Designs: Breaking from Traditional Design Tradeoffs," *IEEE Power Electron. Mag.*, vol. 5, no. 4, pp. 52–60, Dec. 2018.
[53] S. Rosado, F. Wang, and D. Boroyevich, "Design of PEBB based power electronics systems," in *2006 IEEE Power Engineering Society General Meeting*, 2006, pp. 5 pp.-.

[54] R. Giri, V. Choudhary, R. Ayyanar, and N. Mohan, “Common-duty-ratio control of input-series connected modular DC-DC converters with active input voltage and load-current sharing,” *IEEE Trans. Ind. Appl.*, vol. 42, no. 4, pp. 1101–1111, Jul. 2006.
[55] Wikipedia contributors, “Manufacturing readiness level,” *Wikipedia, The Free Encyclopedia*. Retrieved 17:49, September 19, 2019, from https://en.wikipedia.org/w/index.php?title=Manufacturing_readiness_level&oldid=907751405.
[56] L. Kerachev, “Technologies de mise en oeuvre et stratégies de configuration de réseaux de micro-convertisseurs - Application au photovoltaique,” Autre, Université Grenoble Alpes, Doctoral dissertation, 2013.
[57] F. Krismer and J. W. Kolar, “Efficiency-optimized high-current dual active bridge converter for automotive applications,” *IEEE Trans. Ind. Electron.*, vol. 59, no. 7, pp. 2745–2760, 2011.
[58] M. Blanc, “Optimisation d’une structure de conversion DC/DC réversible pour application aéronautique de forte puissance,” Grenoble Alpes, Doctoral dissertation, 2017.
[59] NIST/SEMATECH, *e-Handbook of Statistical Methods*, E., vol. c, d vols. [Online] Available: http://www.itl.nist.gov/div898/handbook/. [Acessed: 10/03/2019].
[60] P. Schimmerling, J. C. Sisson, and A. Zaïdi, *Pratique des plans d’expériences*. Tec & Doc Lavoisier, Paris, 1998.
[61] A. M. Dean and D. Voss, *Design and Analysis of Experiments*. Springer New York, 2000.
[62] D. Coleman, G. Bert. *A DOE Handbook: A Simple Approach to Basic Statistical Design of Experiments*. Verlag nicht ermittelbar, 2014.
[63] W. J. Diamond, *Practical Experiment Designs: for Engineers and Scientists*. Wiley, 2001.
[64] R. W. De Doncker, D. M. Divan, and M. H. Kheraluwala, “A three-phase soft-switched high-power-density DC/DC converter for high-power applications,” *IEEE Trans. Ind. Appl.*, vol. 27, no. 1, pp. 63–73, 1991.
[65] G. James, D. Witten, T. Hastie, and R. Tibshirani, *An Introduction to Statistical Learning*, vol. 103. New York, NY: Springer New York, 2013.
[66] C. E. Rasmussen and C. K. I. Williams, *Gaussian processes for machine learning*, 3. print. Cambridge, Mass.: MIT Press, 2008.
[67] R. R. Richardson, M. A. Osborne, and D. A. Howey, “Battery health prediction under generalized conditions using a Gaussian process transition model,” *J. Energy Storage*, vol. 23, pp. 320–328, Jun. 2019.
[68] S. H. Ali, M. Heydarzadeh, S. Dusmez, X. Li, A. S. Kamath, and B. Akin, “Lifetime Estimation of Discrete IGBT Devices Based on Gaussian Process,” *IEEE Trans. Ind. Appl.*, vol. 54, no. 1, pp. 395–403, Jan. 2018.
[69] A. Andreta, Y. Lembeye, L. L. Villa, and J.-C. Crebier, “Statistical Modelling Method for Active Power Components Based on Datasheet Information,” in *PCIM Europe 2018; International Exhibition and Conference for Power Electronics, Intelligent Motion, Renewable Energy and Energy Management*, 2018, pp. 1–7.
[70] Taiwan Semiconductor, “N-Channel Power MOSFET.” TSM650N15CS datasheet.
[71] EEMB, “Lithium-ion Battery datasheet - LIR18650 2600mAh.” 2010.
[72] T. Lamorelle, Y. Lembeye, and J.-C. Crébier, “Handling differential mode conducted EMC in modular converters,” in *2018 20th European Conference on Power Electronics and Applications (EPE’18 ECCE Europe)*, 2018, p. P–1.
[73] T. Lamorelle, V.-S. Nguyen, J.-C. Crebier, Y. Lembeye, D. Rubio, and J. C. Podvin, “Multi-cell DC-DC converters - Input differential mode filtering generic design rules and implementation,” presented at the PCIM Europe 2019, Nuremberg, Germany, 2019.